NBS MONOGRAPH 96

Electrical Parameters of Precision, Coaxial, Air-Dielectric Transmission Lines

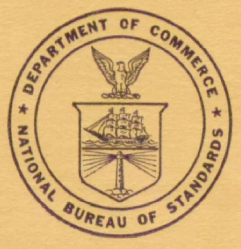

U.S. DEPARTMENT OF COMMERCE

NATIONAL BUREAU OF STANDARDS

UNITED STATES DEPARTMENT OF COMMERCE ● John T. Connor, *Secretary*
NATIONAL BUREAU OF STANDARDS ● A. V. Astin, *Director*

Electrical Parameters of Precision, Coaxial, Air-Dielectric Transmission Lines

Robert E. Nelson and Marlene R. Coryell

Institute for Basic Standards
National Bureau of Standards
Boulder, Colorado

National Bureau of Standards Monograph 96

Issued June 30, 1966

For sale by the Superintendent of Documents, U.S. Government Printing Office
Washington, D.C. 20402 - Price $1.25

Library of Congress Catalog Card Number: 66-60053

Contents

List of illustrations

* See last page of text

Electrical Parameters of Precision, Coaxial, Air-Dielectric Transmission Lines

Robert E. Nelson and Marlene R. Coryell

Since precision coaxial connectors have become commercially available, precision, coaxial, air-dielectric transmission lines are being widely used as radio frequency immittance standards. The evaluation of seven electrical parameters for four different line sizes, which are commonly used as standards, are presented in graphic form. The seven parameters, evaluated as functions of frequency, are inductance per inch, resistance per inch, characteristic impedance magnitude, characteristic impedance phase angle, attenuation per inch, phase-shift per inch, and wavelength. Also included are graphs showing how these parameters vary with changes in the resistivity of the conductors, the relative dielectric constant of air, and the diameters of the conductors.

Key words: Air-dielectric, coaxial transmission lines, electrical parameters, evaluation, functions of frequency, graphic presentation, and precision.

1. Introduction

For several years, the High Frequency Impedance Section of the National Bureau of Standards has maintained a set of fixed lengths of coaxial air lines which are used as the reference standards for high frequency immittance measurements [Powell, Jickling, and Hess, 1958; Jones and Nelson, 1962]. However, before these standards, or any standards, may be used to calibrate a measuring instrument with any degree of accuracy, a precision connector is needed to establish a definable reference plane between the standard and the instrument being tested. Recognizing a need to establish guidelines for commercial development of precision coaxial connectors, a committee was formed (later becoming the Institute of Electrical and Electronics Engineers, Inc., Instrumentation and Measurement Group, Technical Subcommittee on Precision Coaxial Connectors) to determine realistic limits on the mechanical and electrical parameters of precision coaxial connectors.

Following the guidelines established by this committee, several commercially developed precision connectors have appeared on the market which have led to the wide use of precision coaxial lines as immittance standards. However, before these lines can be used as standards, the electrical parameters of the lines must be known to a high degree of accuracy. This has required rather tedious calculations using long and involved formulas. This paper has been prepared to alleviate this situation by providing graphs from which the electrical parameters of the lines may be determined rapidly and accurately.

The graphs were constructed using the formulas derived by Stratton [1941]. These results were then compared with results obtained by using the more exact equations derived by Russell [1909].

An additional benefit was obtained from the evaluation of Russell's equations. A computer program was constructed to evaluate the Bessel functions *ber*, *bei*, *ker*, *kei*, and their first derivatives for order zero for large arguments since tables of these values were not available in the literature.

2. Description of the Air Lines

There are three basic dimensions used in the calculations of the electrical parameters of coaxial transmission lines. These are the diameter of the center conductor (dimension a), the inner diameter of the outer conductor (dimension b), and the outer diameter of the outer conductor (dimension c). For the purpose of this paper, the authors chose the four lines sizes which the committee used for connector studies. Line sizes are usually specified according to the inner diameter of the outer conductor (dimension b). Using this convention, the four line sizes are identified in this paper as:

- line size #1 (dimension $b=0.275591$ in.) (figs 1 to 19) (commonly referred to as 7 mm size)
- line size #2 (dimension $b=0.562500$ in.) (figs 20 to 38) (commonly referred to as 14 mm size)
- line size #3 (dimension $b=0.750000$ in.) (figs 39 to 57) (commonly referred to as 19 mm or 3/4 inch size)
- line size #4 (dimension $b=0.826772$ in.) (figs 58 to 76) (commonly referred to as 21 mm size).

In the calculations, both conductors were assumed to exhibit the same electrical properties with the center conductor being a solid rod. The annular space between conductors contains only air as the dielectric.

With the inner diameter of the outer conductor specified, the diameter of the center conductor (dimension a) was chosen so that the characteristic impedance of the line

is 50 Ω at a temperature of 23 degrees Celsius, an atmospheric pressure of 760 mm of mercury, 50 percent relative humidity, and infinite conductor conductivity. These were the conditions chosen by the Subcommittee on Precision Coaxial Connectors for the purpose of establishing uniformity of line sizes. Under these conditions, the equation for the characteristic impedance of the lines reduces to the form

$$Z_0 = \sqrt{\frac{L}{C}},$$

where

$$L = (0.0254)\frac{\mu_d}{2\pi}\ln\left(\frac{b}{a}\right),$$

$$C = \frac{(0.0254)(2\pi\epsilon_0)}{\ln\left(\frac{b}{a}\right)}\left(\frac{\epsilon}{\epsilon_0}\right)$$

which allows dimension a to be easily calculated. Actually, of course, the characteristic impedances of the lines under the above conditions are never 50 Ω since the ideal of infinite conductor conductivity can not be achieved. However, the characteristic impedance approaches 50 Ω asymptotically as frequency increases. The outer diameter of the outer conductor (dimension c) is of relatively minor importance except at very low frequencies.

In performing the calculations for the graphs, it was assumed that only the TEM wave is propagated in the lines.

3. Computational Methods

The resistance and inductance per unit length of a coaxial transmission line as a function of frequency and the physical and electrical properties of the line were calculated by means of a computer program using the mathematical development of Russell. Russell's equations were derived using a circuit theory approach with the assumptions that the line is infinitely long and Faraday's law of magnetic induction is valid.

Russell's equations, converted from absolute units to MKS units, are:

$$R = \frac{\rho m}{2\pi r_1 Y(mr_1)}(ber\ mr_1\ bei'\ mr_1 - bei\ mr_1\ ber'\ mr_1)$$

$$+\frac{\rho m\ bei'\ mr_1}{2\pi r_1\ Y(mr_1)}(M\ ber\ mr_2 + N\ bei\ mr_2 + O\ ker\ mr_2 + P\ kei\ mr_2)$$

$$-\frac{\rho m\ ber'\ mr_1}{2\pi r_1\ Y(mr_1)}(M\ bei\ mr_2 - N\ ber\ mr_2 + O\ kei\ mr_2 - P\ ker\ mr_2),$$

$$L = \frac{\mu_0}{2\pi}\log_e\left(\frac{r_2}{r_1}\right) + \frac{\rho m}{2\pi\omega r_1\ Y(mr_1)}(ber\ mr_1\ ber'\ mr_1 + bei\ mr_1\ bei'\ mr_1) + \frac{\rho m\ ber'\ mr_1}{2\pi\omega r_1\ Y(mr_1)}(M\ ber\ mr_2 + N\ bei\ mr_2 + O\ ker\ mr_2 + P\ kei\ mr_2) + \frac{\rho m\ bei'\ mr_1}{2\pi\omega r_1 Y(mr_1)}(M\ bei\ mr_2 - N\ ber\ mr_2 + O\ kei\ mr_2 - P\ ker\ mr_2),$$

where

$$m = \left[\frac{\mu_0\,\omega}{\rho}\right]^{1/2},$$

$$S(mx) = ber'\ mx\ ker'\ mx + bei'\ mx\ kei'\ mx,$$

$$T(mx) = bei'\ mx\ ker'\ mx - ber'\ mx\ kei'\ mx,$$

$$Y(mx) = ber'^2\ mx + bei'^2\ mx,$$

with $x = r_1$, r_2, or r_3,

$$M = \frac{-O\,S(mr_3) + P\,T(mr_3)}{Y(mr_3)},$$

$$N = \frac{-O\,T(mr_3) - P\,S(mr_3)}{Y(mr_3)},$$

$$O = \frac{-\frac{r_1}{r_2}Y(mr_3)(Y(mr_3)S(mr_2) - Y(mr_2)S(mr_3))}{(Y(mr_3)S(mr_2) - Y(mr_2)S(mr_3))^2 + (Y(mr_2)T(mr_3) - Y(mr_3)T(mr_2))^2}(bei'\ mr_1\ bei'\ mr_2 + ber'\ mr_1\ ber'\ mr_2)$$

$$+\frac{\frac{r_1}{r_2}Y(mr_3)(Y(mr_2)T(mr_3) - Y(mr_3)T(mr_2))}{(Y(mr_3)S(mr_2) - Y(mr_2)S(mr_3))^2 + (Y(mr_2)T(mr_3) - Y(mr_3)T(mr_2))^2}(ber'\ mr_1\ bei'\ mr_2 - bei'\ mr_1\ ber'\ mr_2)$$

$$P = \frac{-\frac{r_1}{r_2}Y(mr_3)(Y(mr_2)T(mr_3) - Y(mr_3)T(mr_2))}{(Y(mr_3)S(mr_2) - Y(mr_2)S(mr_3))^2 + (Y(mr_2)T(mr_3) - Y(mr_3)T(mr_2))^2}(ber'mr_1 ber'mr_2 + bei'mr_1 bei'mr_2)$$

$$-\frac{\frac{r_1}{r_2}Y(mr_3)(Y(mr_3)S(mr_2) - Y(mr_2)S(mr_3))}{(Y(mr_3)S(mr_2) - Y(mr_2)S(mr_3))^2 + (Y(mr_2)T(mr_3) - Y(mr_3)T(mr_2))^2}(ber'\ mr_1\ bei'\ mr_2 - bei'\ mr_1\ ber'\ mr_2).$$

The Bessel functions *ber*, *bei*, and allied functions appear in Russell's equations and it was found that presently available tables of values for these functions do not extend to large arguments. Consequently, computer programs had to be written to compute the eight functions *ber*, *bei*, *ker*, *kei*, and their first derivatives for order zero before Russell's equations could be programmed and values calculated.

Asymptotic expansion formulas were employed to compute these functions, since the numerical values computed were not adaptable to normal series expansions. The expansion formulas are:

$$ber_\nu z \sim \frac{e^{z/\sqrt{2}}}{\sqrt{(2\pi z)}}\left\{\lambda_\nu(z)\cos\left(\frac{z}{\sqrt{2}}-\frac{1}{8}\pi+\frac{1}{2}\nu\pi\right)\right.$$
$$\left.-\chi_\nu(z)\sin\left(\frac{z}{\sqrt{2}}-\frac{1}{8}\pi+\frac{1}{2}\nu\pi\right)\right\},$$

$$bei_\nu z \sim \frac{e^{z/\sqrt{2}}}{\sqrt{(2\pi z)}}\left\{\chi_\nu(z)\cos\left(\frac{z}{\sqrt{2}}-\frac{1}{8}\pi+\frac{1}{2}\nu\pi\right)\right.$$
$$\left.+\lambda_\nu(z)\sin\left(\frac{z}{\sqrt{2}}-\frac{1}{8}\pi+\frac{1}{2}\nu\pi\right)\right\},$$

where

$$\lambda_\nu(z) \sim 1-\frac{(4\nu^2-1^2)}{1!8z}\cos\frac{1}{4}\pi+\cdots$$
$$+\frac{(-1)^r(4\nu^2-1^2)(4\nu^2-3^2)\cdots\{4\nu^2-(2r-1)^2\}}{r!(8z)^r}$$
$$\left(\cos\frac{1}{4}r\pi+\cdots\right),$$

the number of the term being $r+1$; and

$$\chi_\nu(z) \sim \frac{(4\nu^2-1^2)}{1!8z}\sin\frac{1}{4}\pi-\cdots$$
$$+\frac{(-1)^{r+1}(4\nu^2-1^2)(4\nu^2-3^2)\cdots\{4\nu^2-(2r-1)^2\}}{r!(8z)^r}$$
$$\left(\sin\frac{1}{4}r\pi+\cdots\right),$$

the number of the term being r.

$$ber'_\nu z \sim \frac{e^{z/\sqrt{2}}}{\sqrt{(2\pi z)}}\left\{\psi_\nu(z)\cos\left(\frac{z}{\sqrt{2}}+\frac{1}{8}\pi+\frac{1}{2}\nu\pi\right)\right.$$
$$\left.-\Omega_\nu(z)\sin\left(\frac{z}{\sqrt{2}}+\frac{1}{8}\pi+\frac{1}{2}\nu\pi\right)\right\},$$

$$bei'_\nu z \sim \frac{e^{z/\sqrt{2}}}{\sqrt{(2\pi z)}}\left\{\Omega_\nu(z)\cos\left(\frac{z}{\sqrt{2}}+\frac{1}{8}\pi+\frac{1}{2}\nu\pi\right)\right.$$
$$\left.+\psi_\nu(z)\sin\left(\frac{z}{\sqrt{2}}+\frac{1}{8}\pi+\frac{1}{2}\nu\pi\right)\right\},$$

---

where

$$\psi_\nu(z)=\frac{1}{2}\{\lambda_{\nu+1}(z)+\lambda_{\nu-1}(z)\}=1-\frac{(4\nu^2+1\cdot 3)}{1!8z}\cos\frac{1}{4}\pi+\ldots$$
$$+\frac{(-1)^r(4\nu^2-1^2)(4\nu^2-3^2)\ldots\{4\nu^2-(2r-3)^2\}\{4\nu^2+(2r-1)(2r+1)\}}{r!(8z)^r}$$
$$\left(\cos\frac{1}{4}r\pi+\ldots\right),$$

the number of the term being $r+1$; and

$$\Omega_\nu(z)=\frac{1}{2}\{\chi_{\nu+1}(z)+\chi_{\nu-1}(z)\}=\frac{(4\nu^2+1\cdot 3)}{1!8z}\sin\frac{1}{4}\pi-\ldots$$
$$+\frac{(-1)^{r+1}(4\nu^2-1^2)(4\nu^2-3^2)\ldots\{4\nu^2-(2r-3)^2\}\{4\nu^2+(2r-1)(2r+1)\}}{r!(8z)^r}$$
$$\left(\sin\frac{1}{4}r\pi+\ldots\right),$$

the number of the term being r.

* See last page of text.

$$ker_\nu z \sim \sqrt{\left(\frac{\pi}{2z}\right) e^{-z/\sqrt{2}}} \left\{\lambda_\nu(-z) \cos\left(\frac{z}{\sqrt{2}}+\frac{1}{8}\pi+\frac{1}{2}\nu\pi\right)\right.$$

$$\left. +\chi_\nu(-z) \sin\left(\frac{z}{\sqrt{2}}+\frac{1}{8}\pi+\frac{1}{2}\nu\pi\right)\right\},$$

$$kei_\nu z \sim \sqrt{\left(\frac{\pi}{2z}\right) e^{-z/\sqrt{2}}}$$

$$\left\{\chi_\nu(-z) \cos\left(\frac{z}{\sqrt{2}}+\frac{1}{8}\pi+\frac{1}{2}\nu\pi\right)-\lambda_\nu(-z)\right.$$

$$\left.\sin\left(\frac{z}{\sqrt{2}}+\frac{1}{8}\pi+\frac{1}{2}\nu\pi\right)\right\},$$

$$ker'_\nu z \sim -\sqrt{\left(\frac{\pi}{2z}\right) e^{-z/\sqrt{2}}}$$

$$\left\{\psi_\nu(-z) \cos\left(\frac{z}{\sqrt{2}}-\frac{1}{8}\pi+\frac{1}{2}\nu\pi\right)+\Omega_\nu(-z)\right.$$

$$\left.\sin\left(\frac{z}{\sqrt{2}}-\frac{1}{8}\pi+\frac{1}{2}\nu\pi\right)\right\},$$

$$kei'_\nu z \sim -\sqrt{\left(\frac{\pi}{2z}\right) e^{-z/\sqrt{2}}}$$

$$\left\{\Omega_\nu(-z) \cos\left(\frac{z}{\sqrt{2}}-\frac{1}{8}\pi+\frac{1}{2}\nu\pi\right)-\psi_\nu(-z)\right.$$

$$\left.\sin\left(\frac{z}{\sqrt{2}}-\frac{1}{8}\pi+\frac{1}{2}\nu\pi\right)\right\},$$

where $\lambda_\nu(-z)$, $\chi_\nu(-z)$, $\psi_\nu(-z)$, and $\Omega_\nu(-z)$ are obtained by writing $-z$ for z in the forumlas given for $\lambda_\nu(z)$, $\chi_\nu(z)$, $\psi_\nu(z)$, and $\Omega_\nu(z)$ [McLachlan, 1961]. The terms of these asymptotic expansions decrease in magnitude until some minimum value is reached and then increase without limit. The error in the expansion does not exceed the first term neglected, provided the series is truncated before the minimum term. A discussion of asymptotic expansions is found in Watson [1944]. It has been determined that the number of usable terms is approximately equal to twice the value of the argument for an argument of 15. As the value of the argument increases, the smallest term in the series appears progressively farther out in the series. Since the accuracy of the expansion is limited by the magnitude of the smallest term, each term in the series was individually tested until the point was reached where the next term in the series was less than or equal to 1×10^{-23}. The series was then truncated at this point. For an argument of 35, only 20 terms were needed to reach this point. Thus, 20 terms, the maximum number of terms which were used in the program, were sufficient for the size of the arguments which were used. In fact, if the argument is large, the series can be calculated accurately to several decimal places by using only a few terms of the series.

The relationships among the Bessel functions reveal two equations used as check sums for each argument. The equations are

$$ber(x)\ ker'(x)+bei'(x)\ kei(x)$$

$$-ber'(x)\ ker(x)-bei(x)\ kei'(x)+\frac{1}{x}=0$$

and

$$ber(x)\ kei'(x)+bei(x)\ ker'(x)$$

$$-ber'(x)\ kei(x)-bei'(x)\ ker(x)=0 \qquad \text{[Lowell, 1959].}$$

These equations provided a means to aid in the determination of the number of significant figures computed for the different series for each argument. The check sums were of the order of 1×10^{-21} to 1×10^{-23} for all values with many of the check sums exactly zero.

The eight Bessel function programs were then incorporated into a larger program which calculated the resistance and inductance per unit length of a coaxial air line using Russell's equations. This program was written in 22 digit, double precision, floating point mode for maximum accuracy.

Another computer program, using 16 digits, was written to compute the resistance and inductance using the approximate formulas derived by Stratton. These formulas are

$$R \cong \left[\frac{f}{\pi}\right]^{1/2}\left[(\rho_i\mu_{ci})^{1/2}\left(\frac{1}{a}\right)+(\rho_0\mu_{c0})^{1/2}\left(\frac{1}{b}\right)\right] \text{ ohm/inch,}$$

$$L \cong (0.0254)\frac{\mu_d}{2\pi}\ln\left(\frac{b}{a}\right)+\frac{1}{(16\pi^3 f)^{1/2}}$$

$$\left[(\rho_i\mu_{ci})^{1/2}\left(\frac{2}{a}\right)+(\rho_0\mu_{c0})^{1/2}\left(\frac{2}{b}\right)\right] \text{ henry/inch.}$$

These formulas were derived using the theory of electromagnetic fields and waves. Stratton's formulas neglect those terms which are of concern only at the lower frequencies. It is interesting to note that Russell obtains these same formulas as approximations for very high frequency currents.

The results of the two programs were then compared to determine the magnitude of the differences obtained using the two different sets of formulas. At frequencies above 1 MHz, the differences were small enough to be insignificant when plotted on the graphs. For example, at a frequency of 1 MHz under standard conditions for line size #3, the difference in resistance per inch is less than $2\times10^{-6}\ \Omega$ when calculated by both equations. The difference in inductance per inch is less than 1×10^{-14} H under the same conditions. This being the case, the formulas derived by Stratton were used to compute the resistance and inductance in the final program.

* See last page of book.

The final computer program was written to calculate the values of the electrical parameters which were used to construct the curves on the graphs. This program was written in 16 digit, double precision, floating point mode. The equations used in the program to calculate the desired electrical parameters are given below: (These equations are variations of the usual equations which may be found in any good textbook on transmission line theory with the exception of the equations for R and L which are those derived by Stratton as described above.)

$$R=\left[\frac{f}{\pi}\right]^{1/2}\left[(\rho_i\mu_{ci})^{1/2}\left(\frac{1}{a}\right)+(\rho_0\mu_{c0})^{1/2}\left(\frac{1}{b}\right)\right]\ \Omega/\text{in.},$$

$$L=(0.0254)\frac{\mu_d}{2\pi}\ln\left(\frac{b}{a}\right)+\frac{1}{(16\pi^3 f)^{1/2}}\cdot\left[(\rho_i\mu_{ci})^{1/2}\left(\frac{2}{a}\right)+(\rho_0\mu_{c0})^{1/2}\left(\frac{2}{b}\right)\right]\ \text{H/in.},$$

$$C=\frac{(0.0254)(2\pi\epsilon_0)}{\ln\left(\frac{b}{a}\right)}\left(\frac{\epsilon}{\epsilon_0}\right)\ \text{F/in.},$$

$G\cong 0$ (for air dielectric),

$$|Z_0|=\left[\frac{L^2}{C^2}+\frac{R^2}{(\omega C)^2}\right]^{1/4}\Omega,$$

$$\theta=\frac{1}{2}\tan^{-1}\left(\frac{-R}{\omega L}\right)\ \text{rad.},$$

$$\beta=\left\{\frac{1}{2}\left[([R^2+\omega^2L^2]\,[G^2+\omega^2C^2])^{1/2}-RG+\omega^2LC\right]\right\}^{1/2}\ \text{rad./in.},$$

$$\alpha=\left\{\frac{1}{2}\left[([R^2+\omega^2L^2]\,[G^2+\omega^2C^2])^{1/2}+RG-\omega^2LC\right]\right\}^{1/2}\ \text{Np/in.},$$

$$\lambda=\frac{2\pi}{\beta}\ \text{inch},$$

where:

a = outer diameter of inner conductor in inches,
b = inner diameter of outer conductor in inches,
f = frequency in hertz,
ω = $2\pi f$,
ρ_i = resistivity of inner conductor in ohm-meters,
ρ_0 = resistivity of outer conductor in ohm-meters,
μ_d = magnetic permeability of the dielectric (air) between conductors in henry/meter,
μ_{ci} = magnetic permeability of inner conductor in henry/meter,
μ_{c0} = magnetic permeability of outer conductor in henry/meter,
ϵ_0 = dielectric constant of free space in farad/meter,
$\frac{\epsilon}{\epsilon_0}$ = relative dielectric constant of dielectric (air),

and the parameters calculated were:

R = resistance in ohms/inch,
L = inductance in henrys/inch,
C = capacitance in farads/inch,
G = conductance in mhos/inch ($\cong$ zero for air dielectric),
$|Z_0|$ = characteristic impedance magnitude in ohms,
θ = characteristic impedance phase angle in radians,
β = phase-shift constant in radians/inch,
α = attenuation in nepers/inch,
λ = wavelength in inches.

The graphs for C and G are not included since C is easily calculable and not a function of frequency and G is essentially zero for air dielectric. Since $|Z_0|$ is one of the more important parameters, curves were drawn as deviations from 50 Ω (i.e., $\Delta Z=(|Z_0|-50.000)\times 10^3\ \Omega$) to allow more precise values to be obtained from the graphs. The curves for β and λ were drawn as percent deviations from free space values $\left(\text{i.e., } \Delta\beta=\left(\frac{\beta-\beta_0}{\beta_0}\right)\times 10^2 \text{ and } \Delta\lambda=\left(\frac{\lambda-\lambda_0}{\lambda_0}\right)\times 10^2\right)$ for the same reason. The free space values were calculated using the formulas

$$\beta_0=\frac{\omega}{\nu_0},$$

$$\lambda_0=\frac{\nu_0}{f},$$

where,

$$\nu_0=1.180285\times 10^{10}\ \text{in./sec.},$$

which is the velocity of propagation of electromagnetic waves in free space.

The output of the computer program described above was printed in the form of tables and the final graphs were drawn using the values from these tables.

4. Graphs

The graphs are divided into four main groups corresponding to the four different line sizes.

The scales for the graphs were chosen to allow maximum practical accuracy in obtaining values directly from the curves and still keep the graphs of reasonable physical size for publication purposes. These considerations also restricted the frequency range to a certain degree. The upper frequency limit for each line size was chosen to be

that frequency below which only the TEM wave can be propagated. This frequency was determined by the approximate relationship

$$f_c \cong \frac{2\nu}{\pi(a+b)} \qquad \text{[Johnson, 1950]},$$

where ν is the velocity of propagation of electromagnetic waves in the line. The lower frequency limit was determined primarily by the physical size of the graphs and resulted in values of 10 MHz for line size #1 and 1 MHz for line sizes #2, #3, and #4.

After the graphs were reduced to publication size, it was determined that values could be read directly from the curves to within one-half the smallest scale division. In most cases, the uncertainty in reading the curves is much less than the uncertainties in the original constants (e.g., uncertainties in determining resistivity, ρ) so that the graphs are more than adequate considering the present state of the art in constructing coaxial line immittance standards.

Each line size is subdivided into four general categories which are discussed below. These subdivisions are (1) standard conditions, (2) variations with resistivity, ρ, (3) variations with relative dielectric constant, $\frac{\epsilon}{\epsilon_0}$, and (4) variations with diameters a and b.

4.1. Standard Conditions

The first seven graphs for each line size were drawn using values obtained from a set of "standard" conditions. These conditions are that the conductors be made of copper with an air dielectric, and that the lines be used under ambient conditions of 23 °C, 50 percent relative humidity and an atmospheric pressure of 760 mm of mercury. With the basic constants of the line determined by the above conditions, seven parameters were calculated and plotted as functions of frequency. The seven parameters are (1) resistance per inch, (2) inductance per inch, (3) characteristic impedance magnitude, (4) characteristic impedance phase angle, (5) attenuation per inch, (6) phase-shift constant, and (7) wavelength in the line.

4.2. Variations with Resistivity, ρ

The second set of graphs for each line size shows how the seven parameters listed in section 4.1 vary with changes in resistivity. Each graph is a family of curves with each curve representing a different value of resistivity. The resistivity was varied from a value of 0.1×10^{-7} Ω-m to a value of 0.1×10^{-6} Ω-m with several values between for purposes of interpolation.

4.3. Variations with Relative Dielectric Constant, $\frac{\epsilon}{\epsilon_0}$

The third set of graphs for each line size shows how three of the seven parameters vary with changes in relative dielectric constant. The three parameters which vary with relative dielectric constant are characteristic impedance magnitude, phase-shift constant, and wavelength. The other four parameters do not vary significantly with changes in relative dielectric constant, and consequently were not included in the graphs. The relative dielectric constant was varied from 1.000400 to 1.000800 with an occasional value in between when necessary for more accurate interpolation.

4.4. Variations with Diameters a and b

The fourth and final set of graphs for each line size shows how inductance per inch and characteristic impedance magnitude vary with changes in the diameters a and b. The rest of the seven parameters showed no significant variations with changes in the diameters. The diameter, b, was allowed to vary ± 0.0002 in. and the diameter, a, was allowed to vary ± 0.0001 in. from nominal. Only the two curves showing maximum variations on either side of nominal for the parameters were drawn since interpolation is not feasible between curves. Consequently, the graphs indicating variations with changes in a and b are more qualitative than quantitative and indicate only maximum possible variations from the nominal values of the parameters.

5. Summary

In conclusion, then, the authors have tried to provide the user with a rapid and accurate means of determining the electrical parameters of precision, air-dielectric, coaxial transmission lines. In addition, graphs have been provided showing how the electrical parameters of the lines are affected by variations in the resistivity of the conductors, the relative dielectric constant of air, and the diameters of the conductors.

The evaluation of the Bessel functions *ber, bei, ker, kei,* and their first derivatives for large arguments may be of considerable value. To the best of the authors' knowledge, these values are not available in the literature at this time. If there is a need for these values, the results of the computer program may be published either in tabular or graphic form at some future time.

The evaluation of resistance and inductance per unit length by two different methods showed no significant differences at frequencies above 1 MHz considering the present state of the art in constructing precision lines. At lower frequencies, however, the differences become greater and Russell's equations must be used to obtain the necessary accuracies in the calculated values.

6. References

Johnson, W. C. (1950), Transmission lines and networks, p. 89 (McGraw-Hill Book Co., Inc., New York, N.Y.).

Jones, R. N., and R. E. Nelson (1962), The role of capacitance in the national reference standards for high frequency impedance. Proceedings of the 17th Annual I.S.A. Conference and Exhibit, Paper No. 18.1.62.

Lowell, H. H. (1959), Tables of the Bessel-Kelvin functions *ber, bei, ker, kei*, and their derivatives for the argument range 0(0.01)107.50, National Aeronautics and Space Administration, Technical Report R–32, pp. 6, 7.

McLachlan, N. W. (1961), Bessel Functions for engineers, second ed., corrected printing, pp. 137–152, 209–210, 213 (Oxford University Press, London).

Powell, R. C., R. M. Jickling, and A. E. Hess (1958), High-frequency impedance standards at the National Bureau of Standards, IRE Trans. Instr., **I–7**, Numbers 3 and 4, 270–274.

Russell, A. (1909), The effective resistance and inductance of a concentric main, and methods of computing the *ber* and *bei* and allied functions, Philosophical Magazine **17**, 524–552.

Stratton, J. A. (1941), Electromagnetic theory, p. 553 (McGraw-Hill Book Co., Inc., New York, N.Y.).

Watson, G. N. (1944), A treatise on the theory of Bessel Functions, second ed., pp. 194–225 (Cambridge University Press, London).

Supplemental References

Gray, A., G. B. Mathews, and T. M. Mac Robert (1922), A treatise on Bessel Functions and their applications to physics (MacMillan and Co., Ltd., London).

Harris, I. A., and R. E. Spinney (1964), The realization of high-frequency impedance standards using air-spaced coaxial lines, IEEE Trans. Instr. Meas. **IM–13**, No. 4, 265–272.

Post, E. J. (1963), Phase, attenuation, and impedance characteristics of coaxial transmission lines with thin tubular conductors, IEEE Trans. Microwave Theory and Techniques **MTT–11**, No. 2, 129–136.

Schelkunoff, S. A. (1942), Electromagnetic Waves (D. Van Nostrand Co., Inc., New York).

Line size #1
Standard conditions

Constants used in calculations:

$a = 0.119670$ inch

$b = 0.275591$ inch

$\rho_i = \rho_0 = 0.17241 \times 10^{-7}$ ohm-meters

$\mu_{ci} = \mu_{co} = \mu_d = 4\pi \times 10^{-7}$ henry/meter

$\frac{\epsilon}{\epsilon_0} = 1.000649$

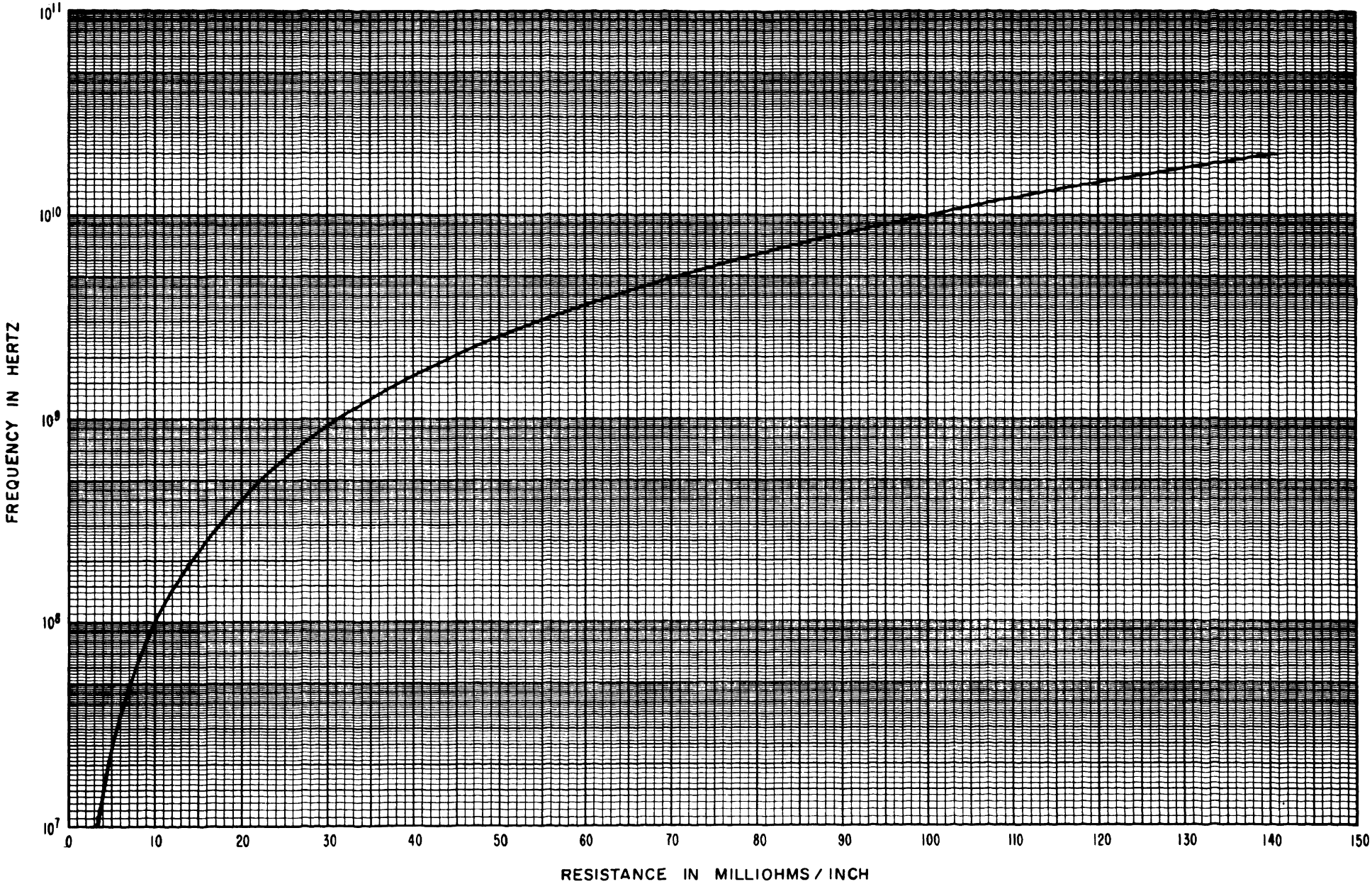

FIGURE 1. *Resistance per inch as a function of frequency under standard conditions for line size #1.*

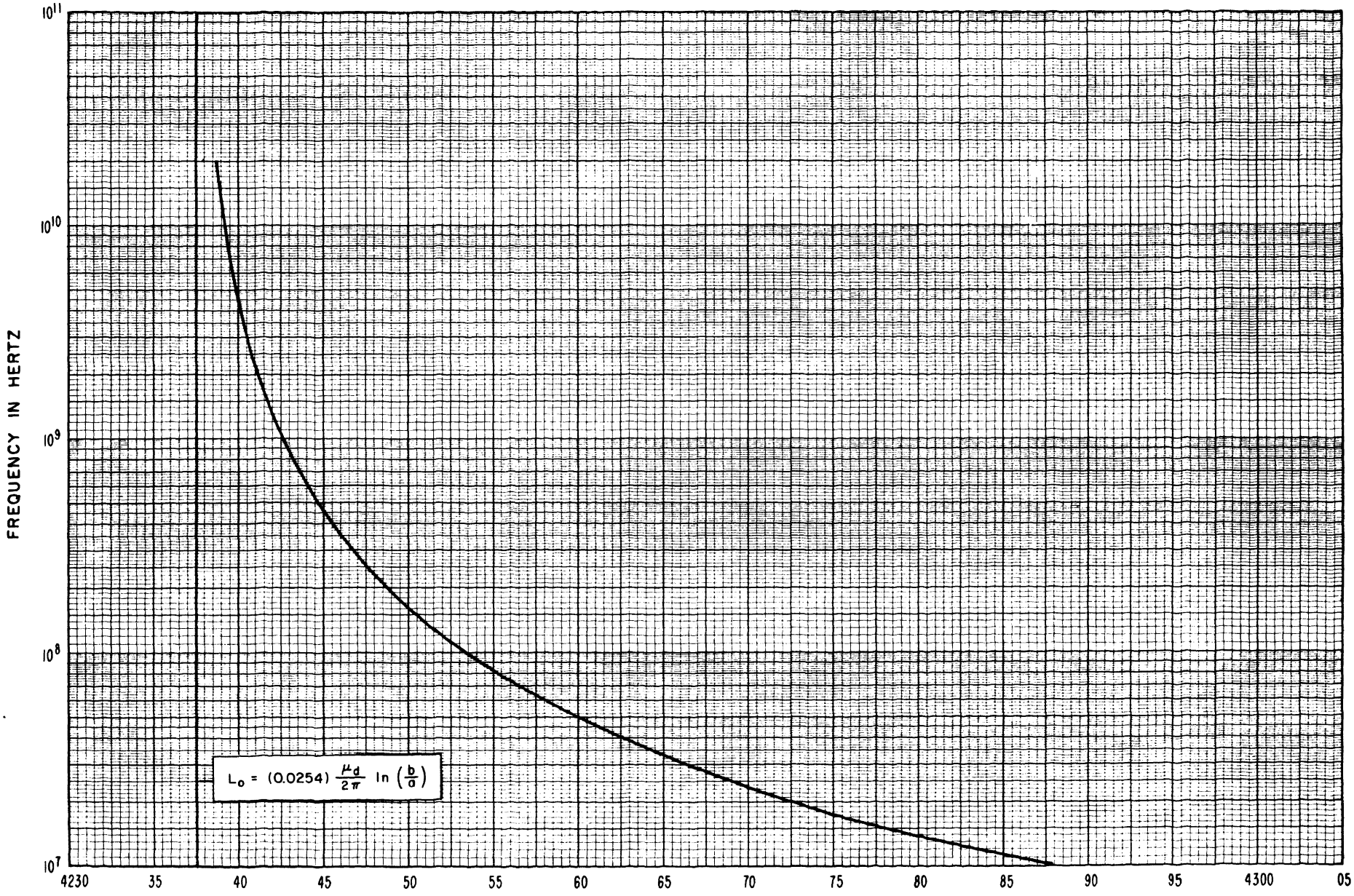

FIGURE 2. *Inductance per inch as a function of frequency under standard conditions for line size #1.*

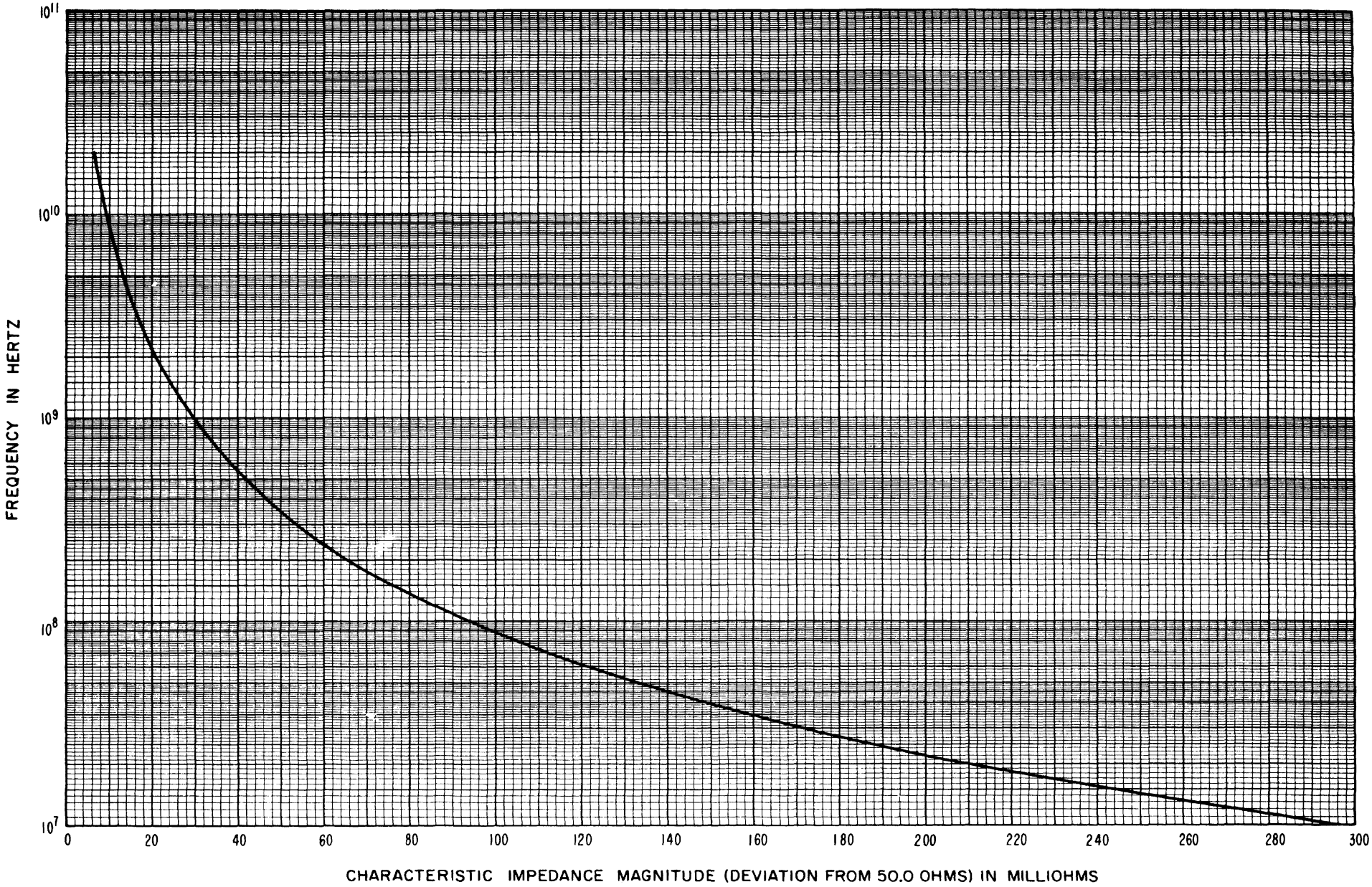

FIGURE 3. *Characteristic impedance magnitude (plotted as a deviation from 50.0 Ω) as a function of frequency under standard conditions for line size #1.*

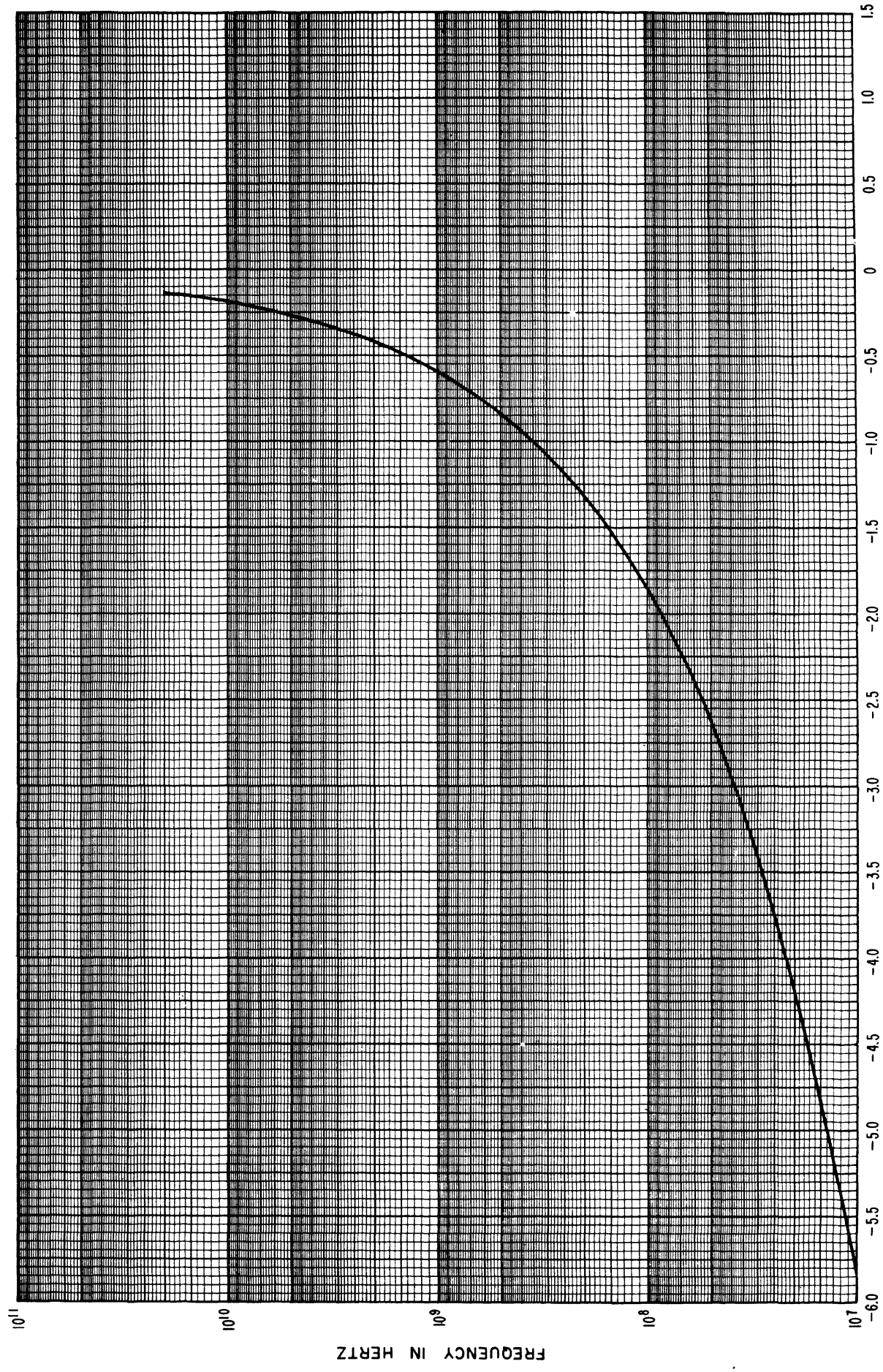

FIGURE 4. *Characteristic impedance phase angle as a function of frequency under standard conditions for line size #1.*

218-445 O-66—2

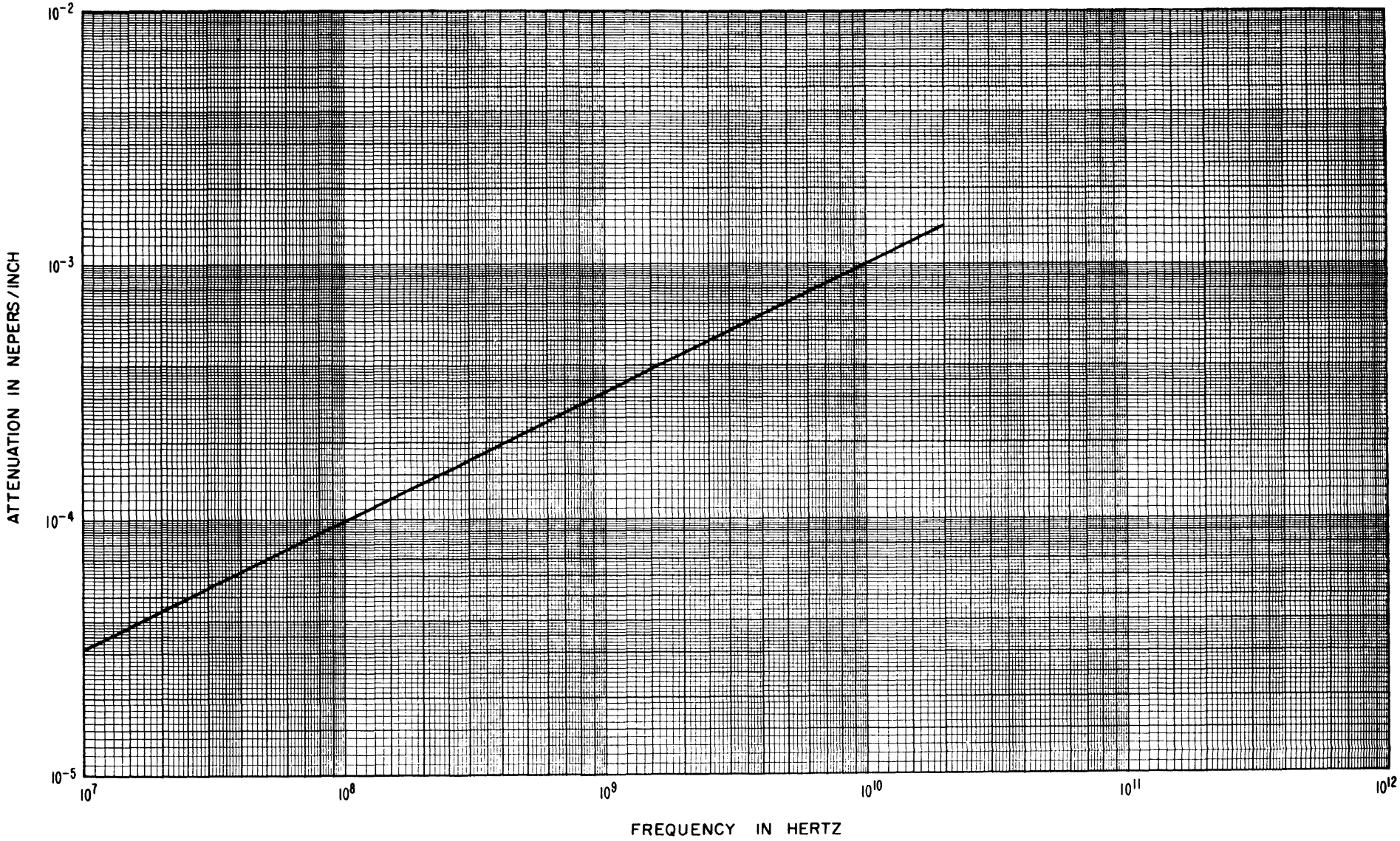

FIGURE 5. *Attenuation per inch as a function of frequency under standard conditions for line size #1.*

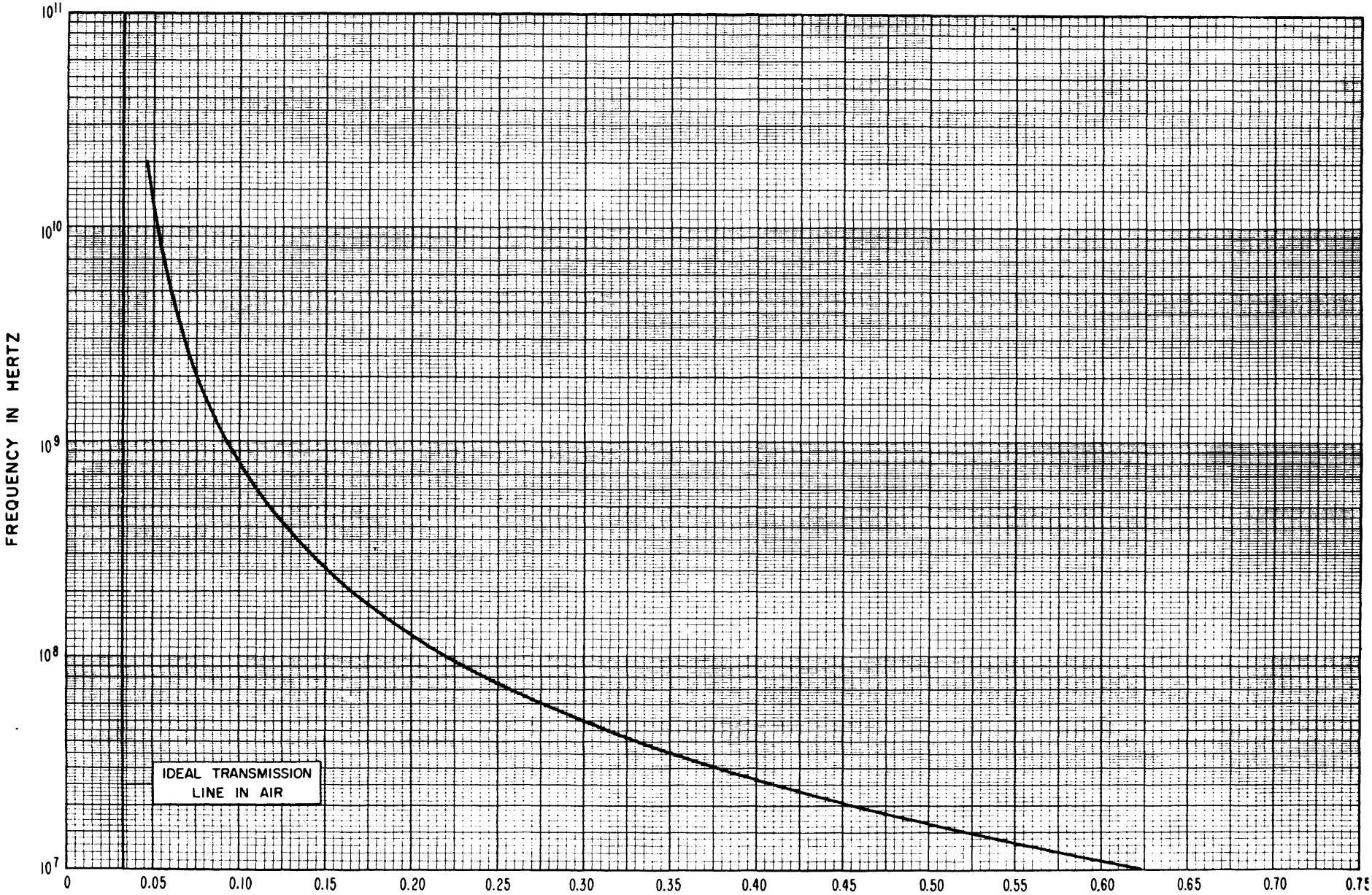

FIGURE 6. *Phase-shift per inch (plotted as a percent deviation from the free space value) as a function of frequency under standard conditions for line size #1.*

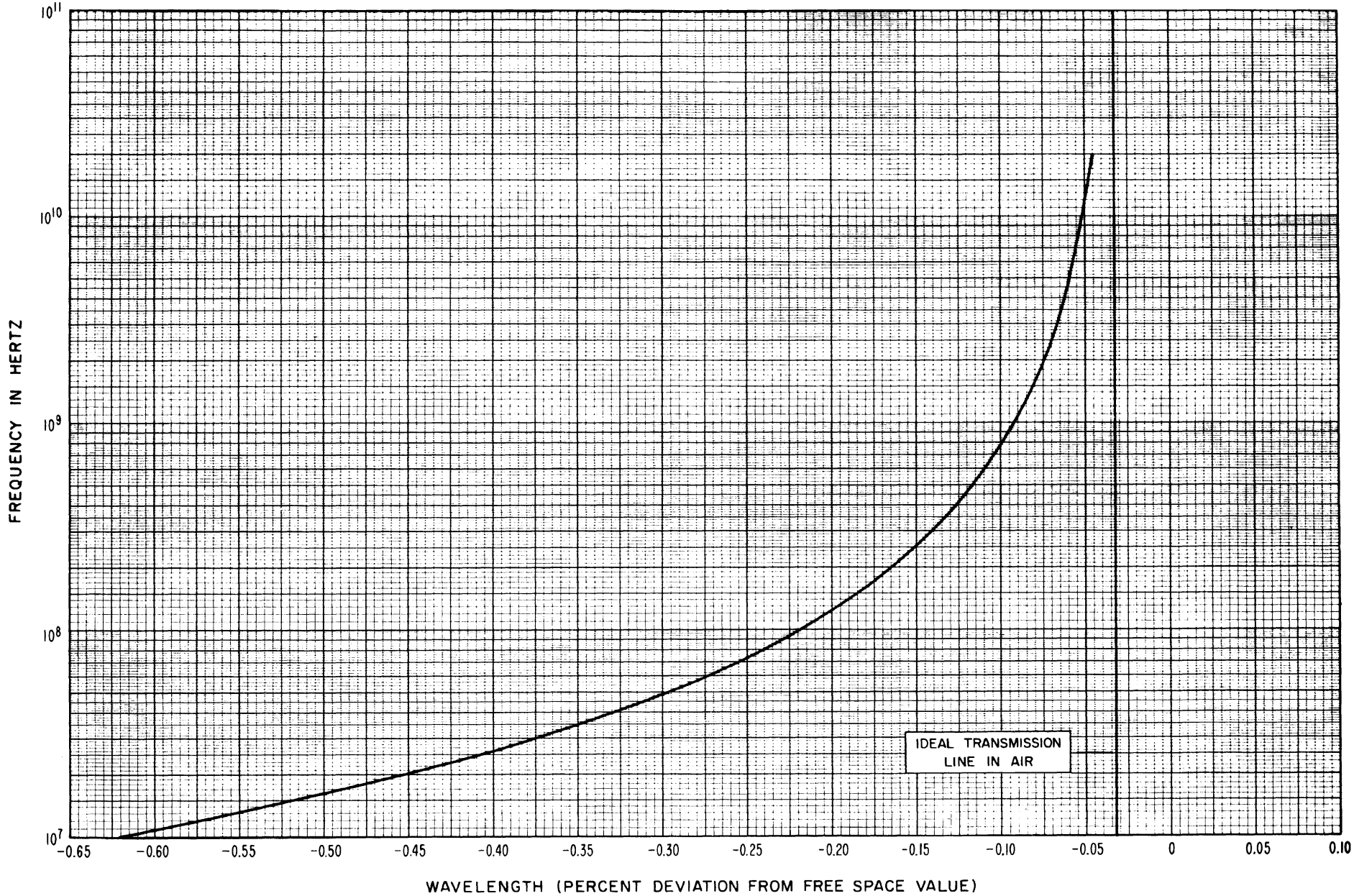

FIGURE 7. *Wavelength (plotted as a percent deviation from the free space value) as a function of frequency under standard conditions for line size #1.*

Line size #1
Variations with resistivity, ρ

Constants used in calculations are the same as those used under standard conditions except that ρ_i ($=\rho_0$) varies from 0.1×10^{-7} to 0.1×10^{-6} ohm-meters.

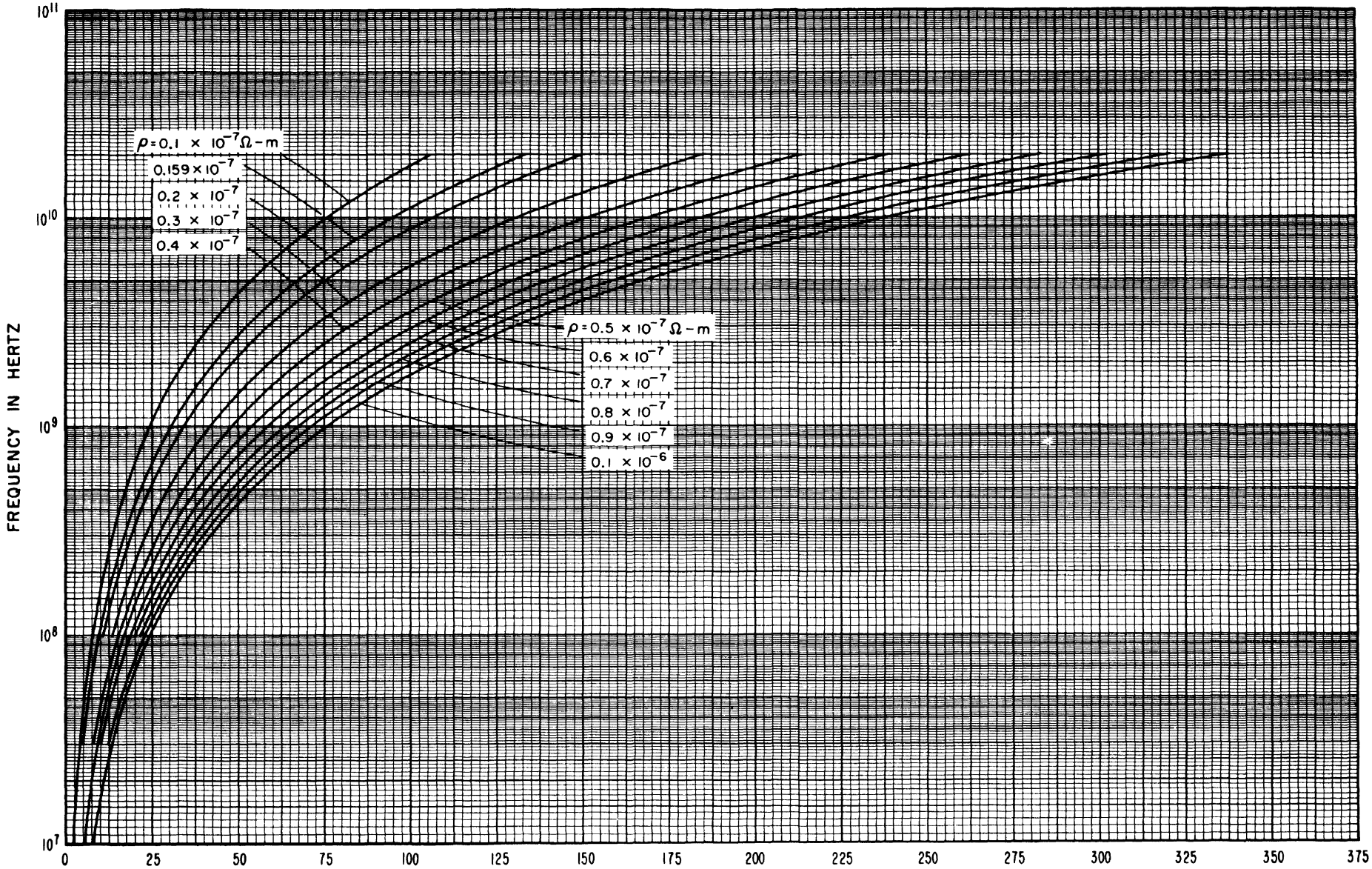

FIGURE 8. *Resistance per inch as a function of frequency for various values of ρ for line size #1.*

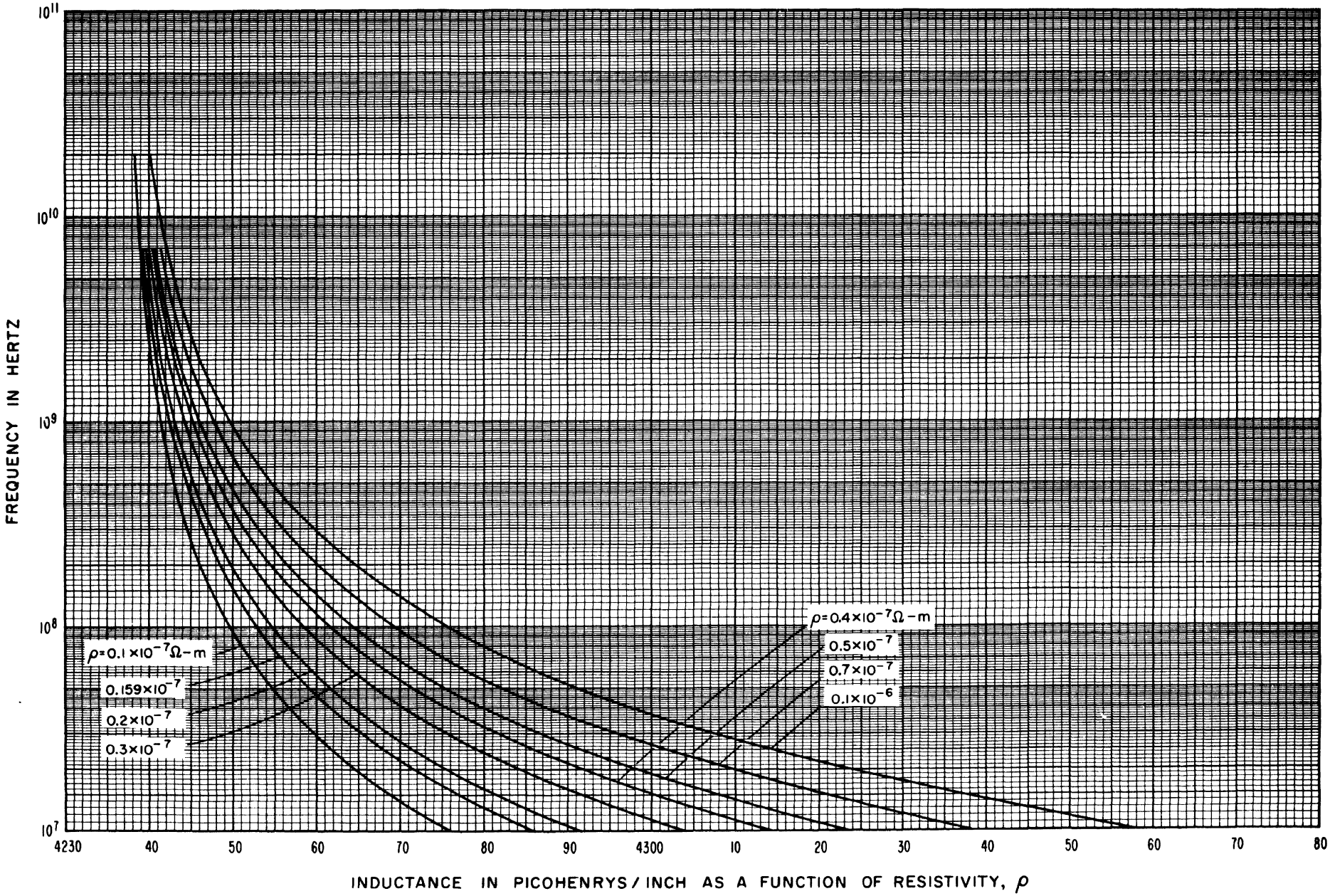

FIGURE 9. *Inductance per inch as a function of frequency for various values of ρ for line size #1.*

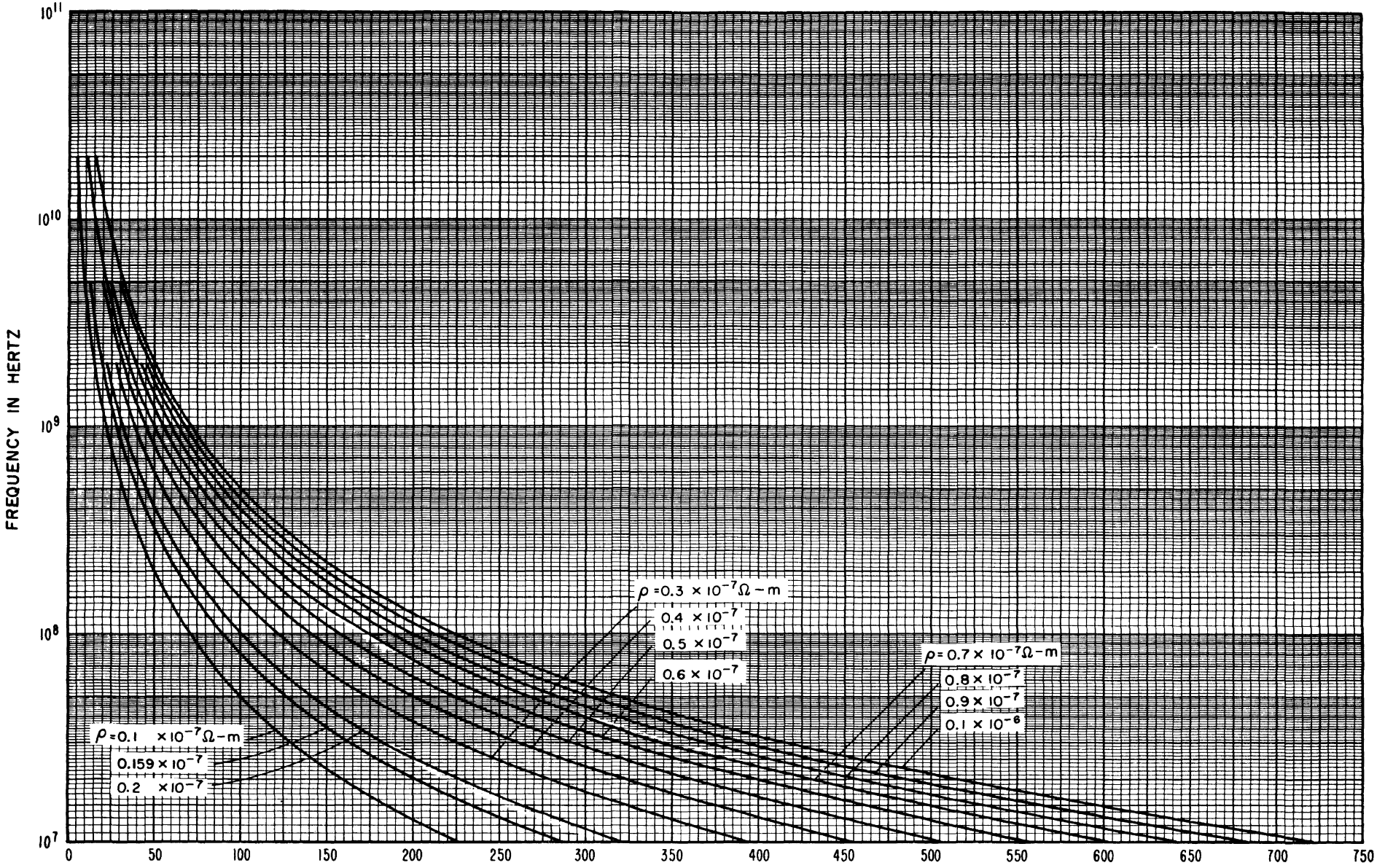

FIGURE 10. *Characteristic impedance magnitude (plotted as a deviation from 50.0 Ω) as a function of frequency for various values of ρ for line size #1.*

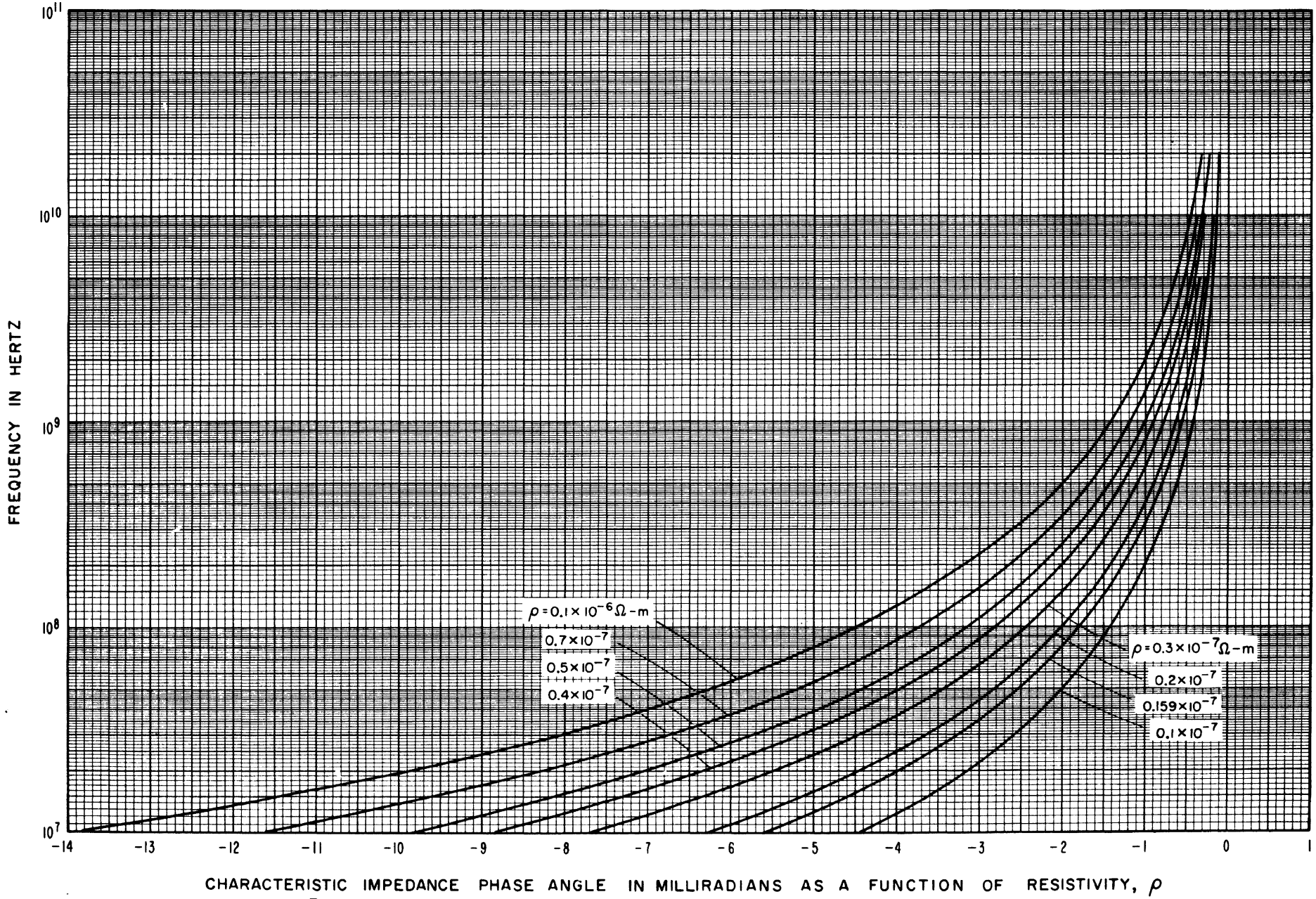

FIGURE 11. *Characteristic impedance phase angle as a function of frequency for various values of ρ for line size #1.*

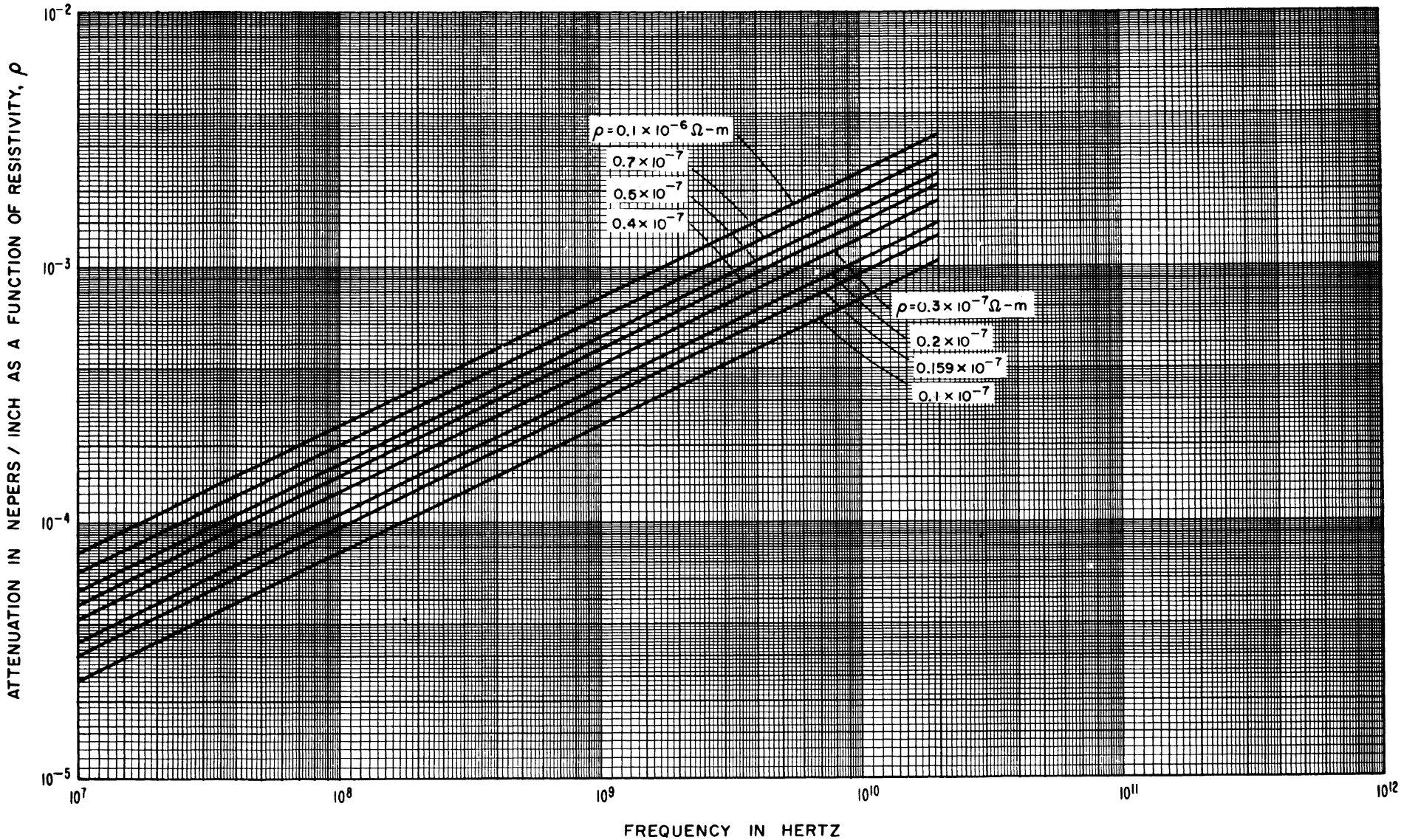

FIGURE 12. *Attenuation per inch as a function of frequency for various values of ρ for line size #1.*

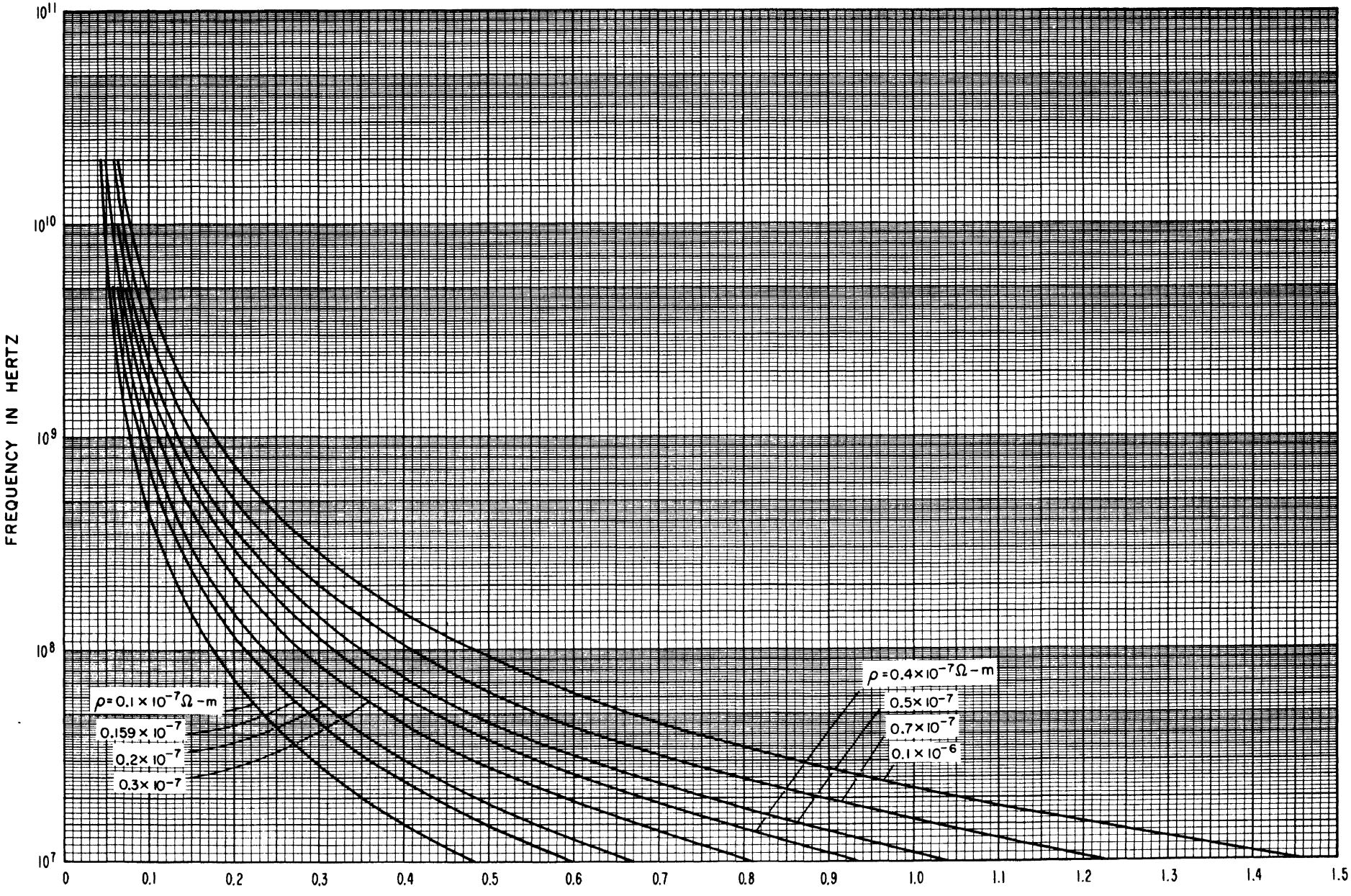

FIGURE 13. *Phase-shift per inch (plotted as a percent deviation from the free space value) as a function of frequency for various values of ρ for line size #1.*

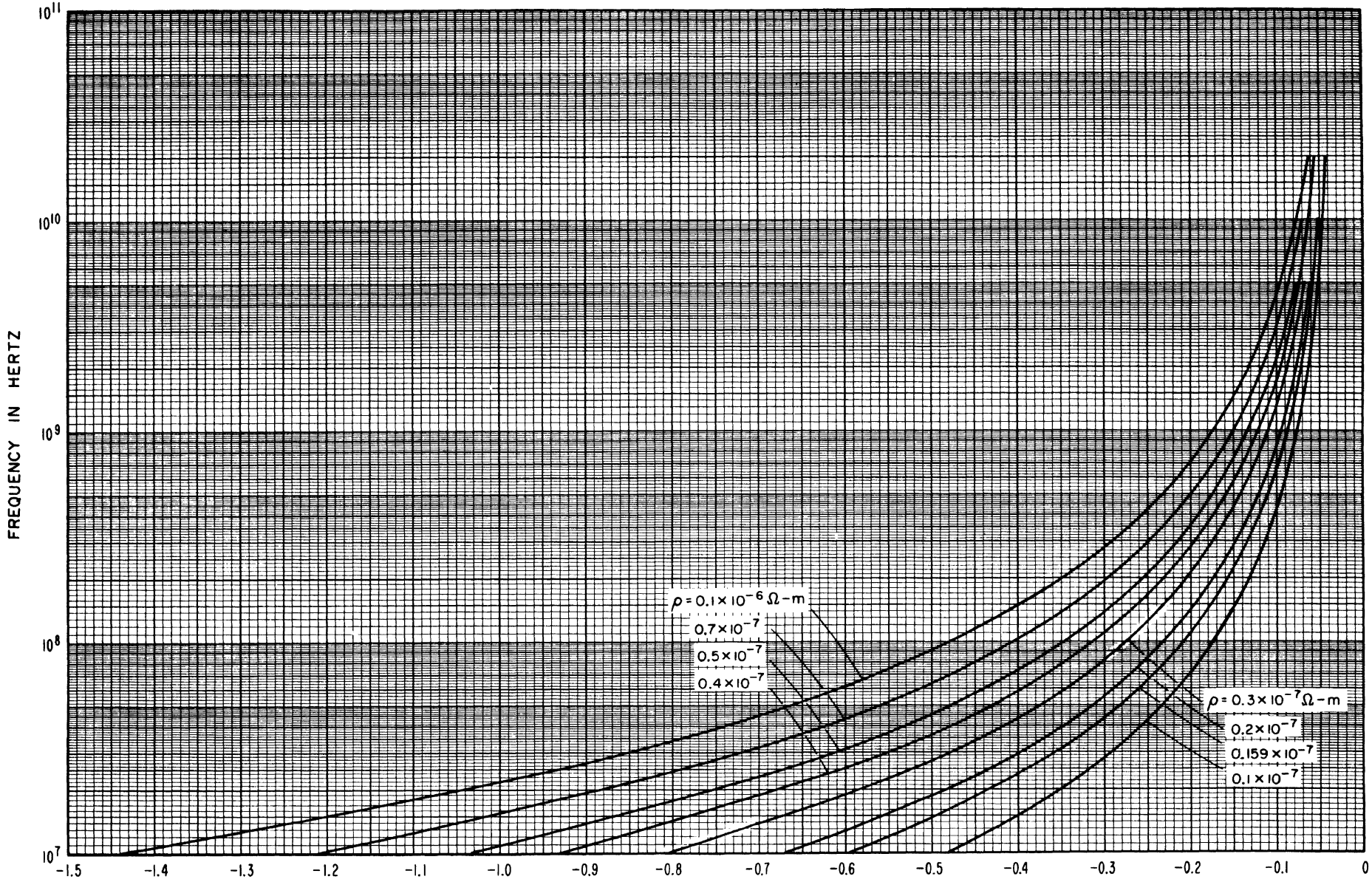

FIGURE 14. *Wavelength (plotted as a percent deviation from the free space value) as a function of frequency for various values of ρ for line size #1.*

Line size #1
Variations with relative dielectric constant, $\frac{\epsilon}{\epsilon_0}$

Constants used in calculations are the same as those used under standard conditions except that $\frac{\epsilon}{\epsilon_0}$ varies from 1.000400 to 1.000800.

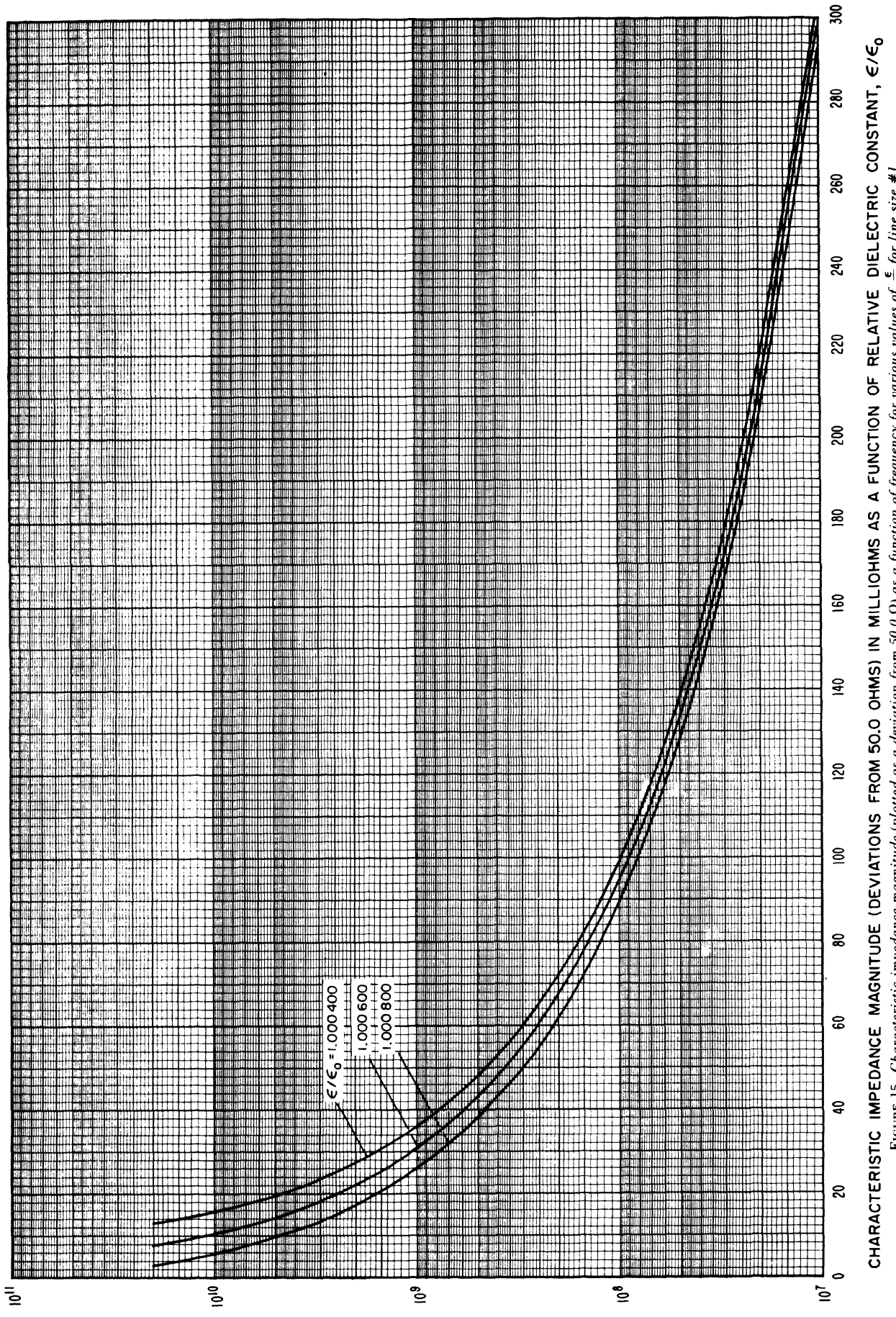

FIGURE 15. *Characteristic impedance magnitude (plotted as a deviation from 50.0 Ω) as a function of frequency for various values of* $\frac{\epsilon}{\epsilon_0}$ *for line size #1.*

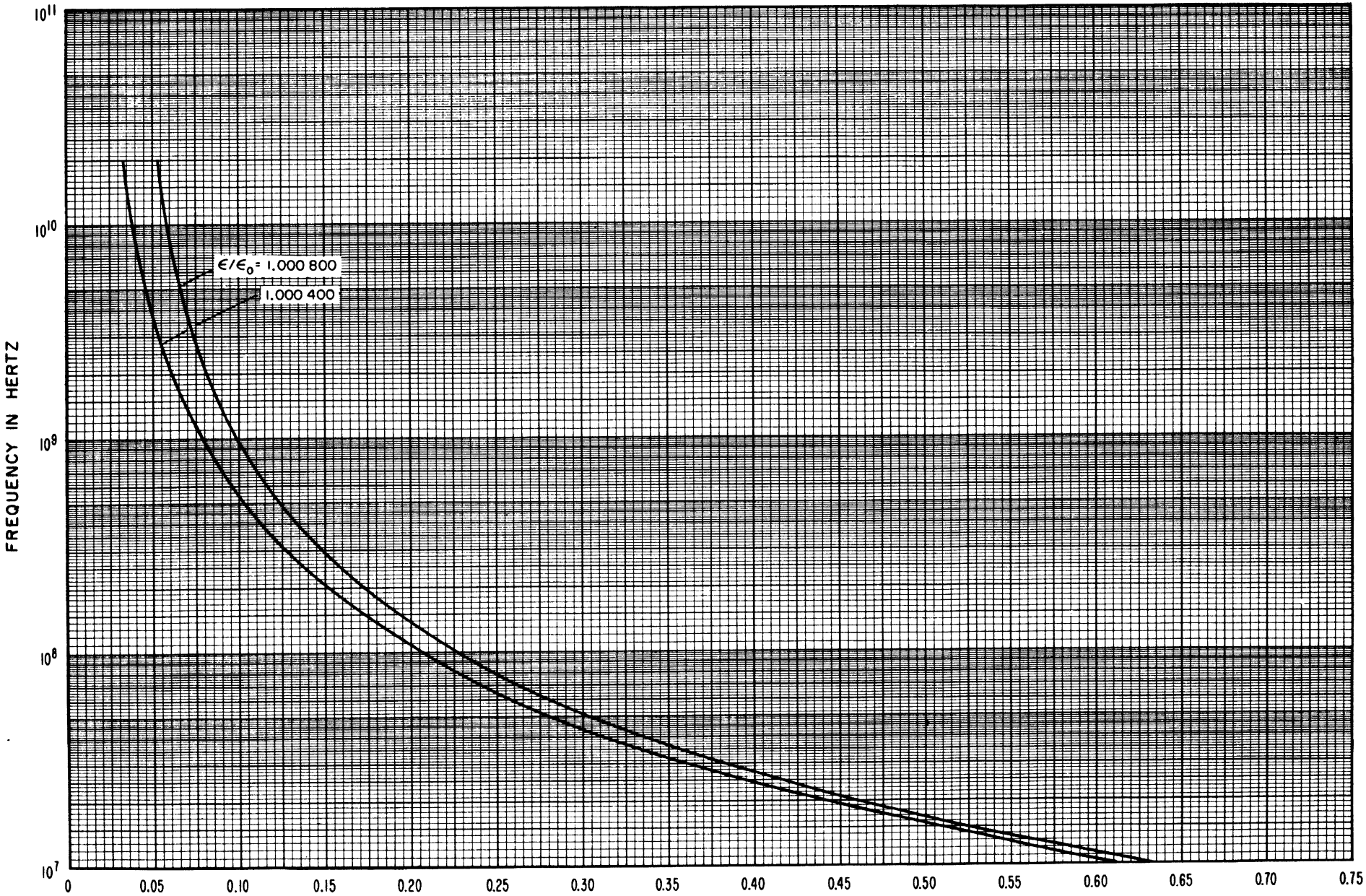

FIGURE 16. *Phase-shift per inch (plotted as a percent deviation from the free space value) as a function of frequency for various values of* $\frac{\epsilon}{\epsilon_0}$ *for line size #1.*

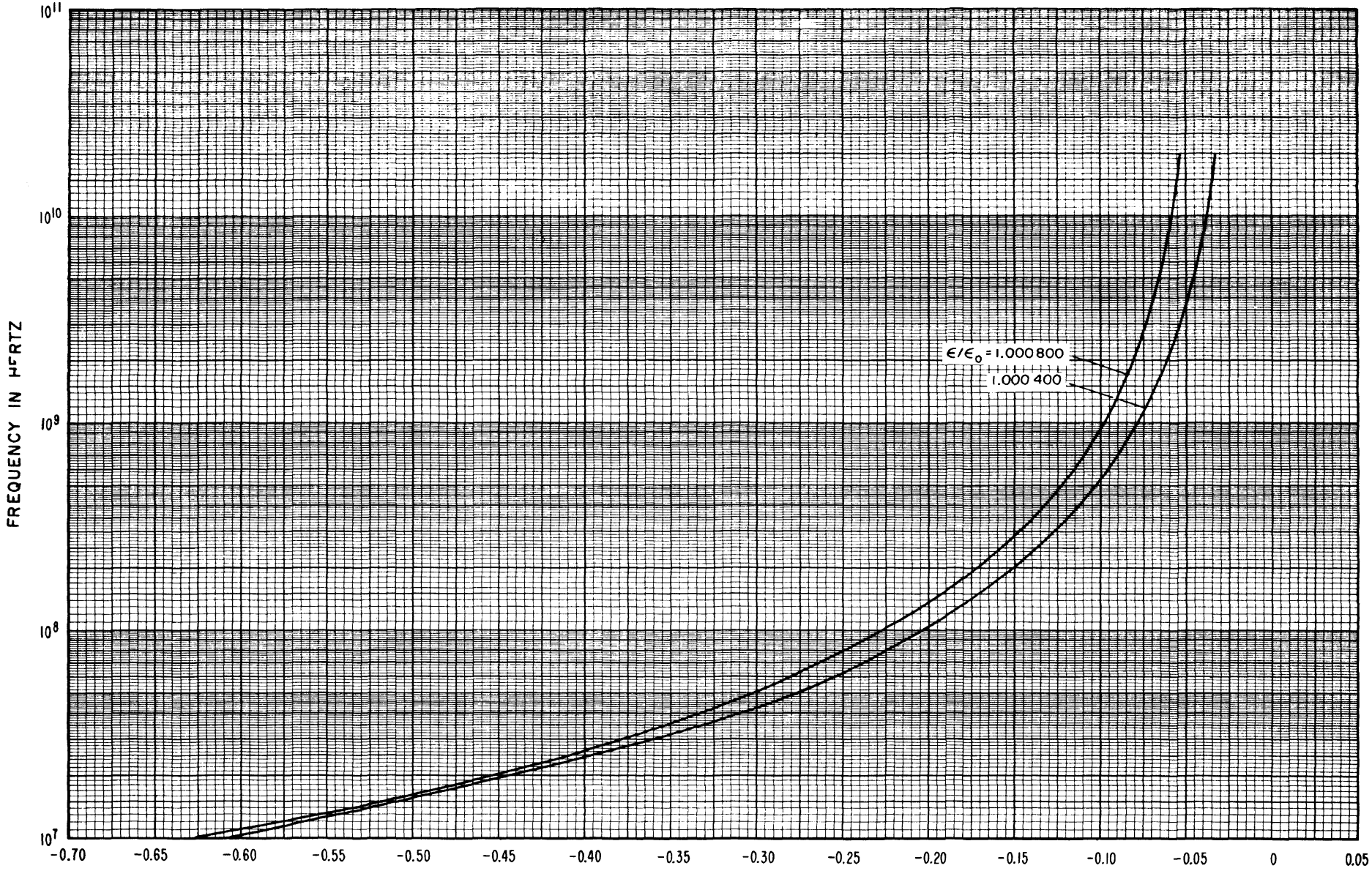

FIGURE 17. *Wavelength (plotted as a percent deviation from the free space value) as a function of frequency for various values of* $\frac{\epsilon}{\epsilon_0}$ *for line size #1.*

Line size #1
Variations with diameters a and b

Constants used in calculations are the same as those used under standard conditions except that a varies ± 0.0001 inch from standard conditions, and b varies ± 0.0002 inch from standard conditions.

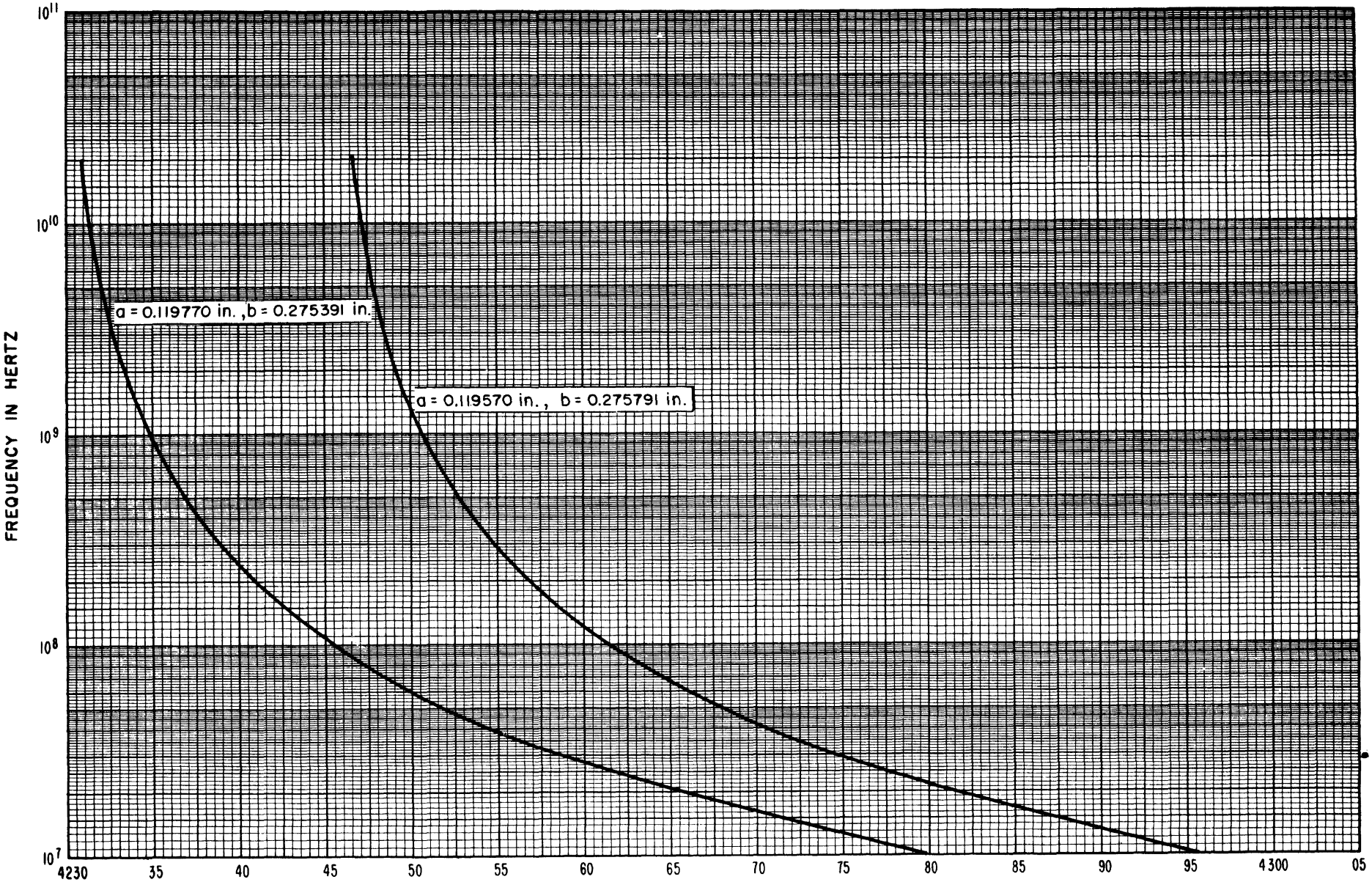

FIGURE 18. *Inductance per inch as a function of frequency for various values of diameters* a *and* b *for line size #1.*

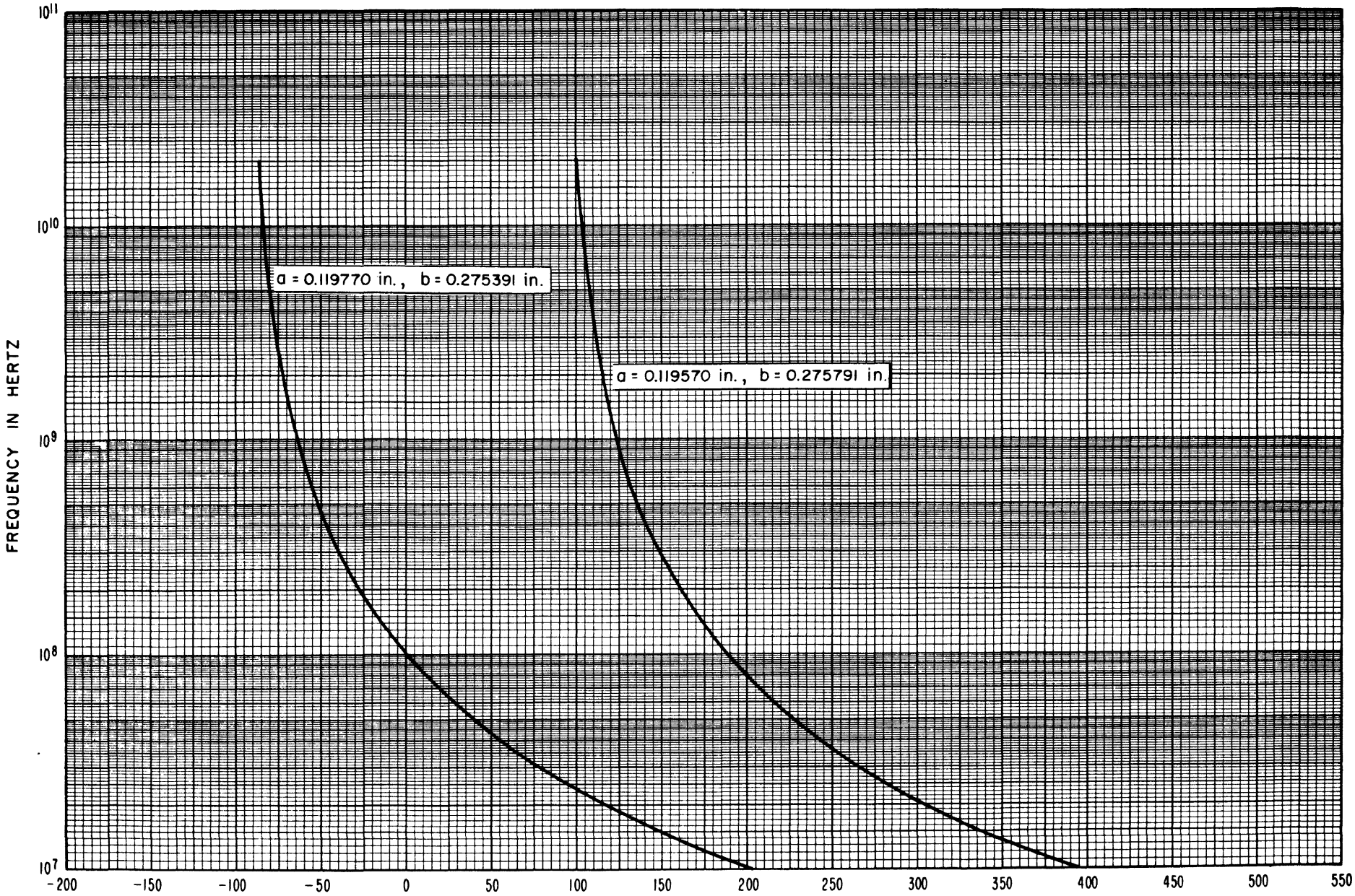

FIGURE 19. *Characteristic impedance magnitude (plotted as a deviation from 50.0 Ω) as a function of frequency for various values of diameters* a *and* b *for line size #1.*

14 mm
air line

Line size #2
Standard conditions

Constants used in calculations:

$a = 0.244255$ inch 0, 6 2 0 4 0 8 cm

$b = 0.562500$ inch 1, 4 2 8 7 5

$\rho_i = \rho_0 = 0.17241 \times 10^{-7}$ ohm-meters

$\mu_{ci} = \mu_{co} = \mu_d = 4\pi \times 10^{-7}$ henry/meter

$\frac{\epsilon}{\epsilon_0} = 1.000649$

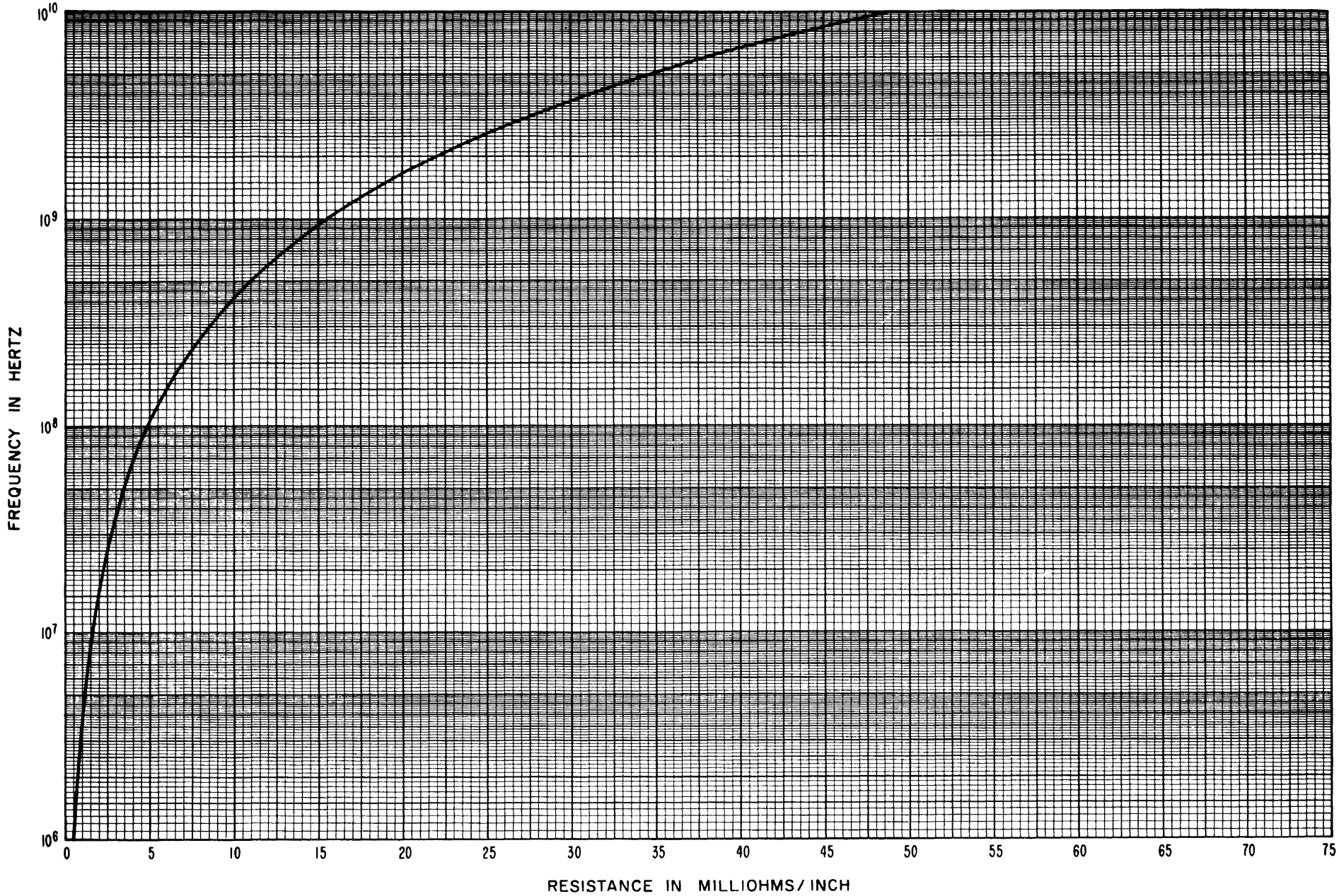

FIGURE 20. *Resistance per inch as a function of frequency under standard conditions for line size #2.*

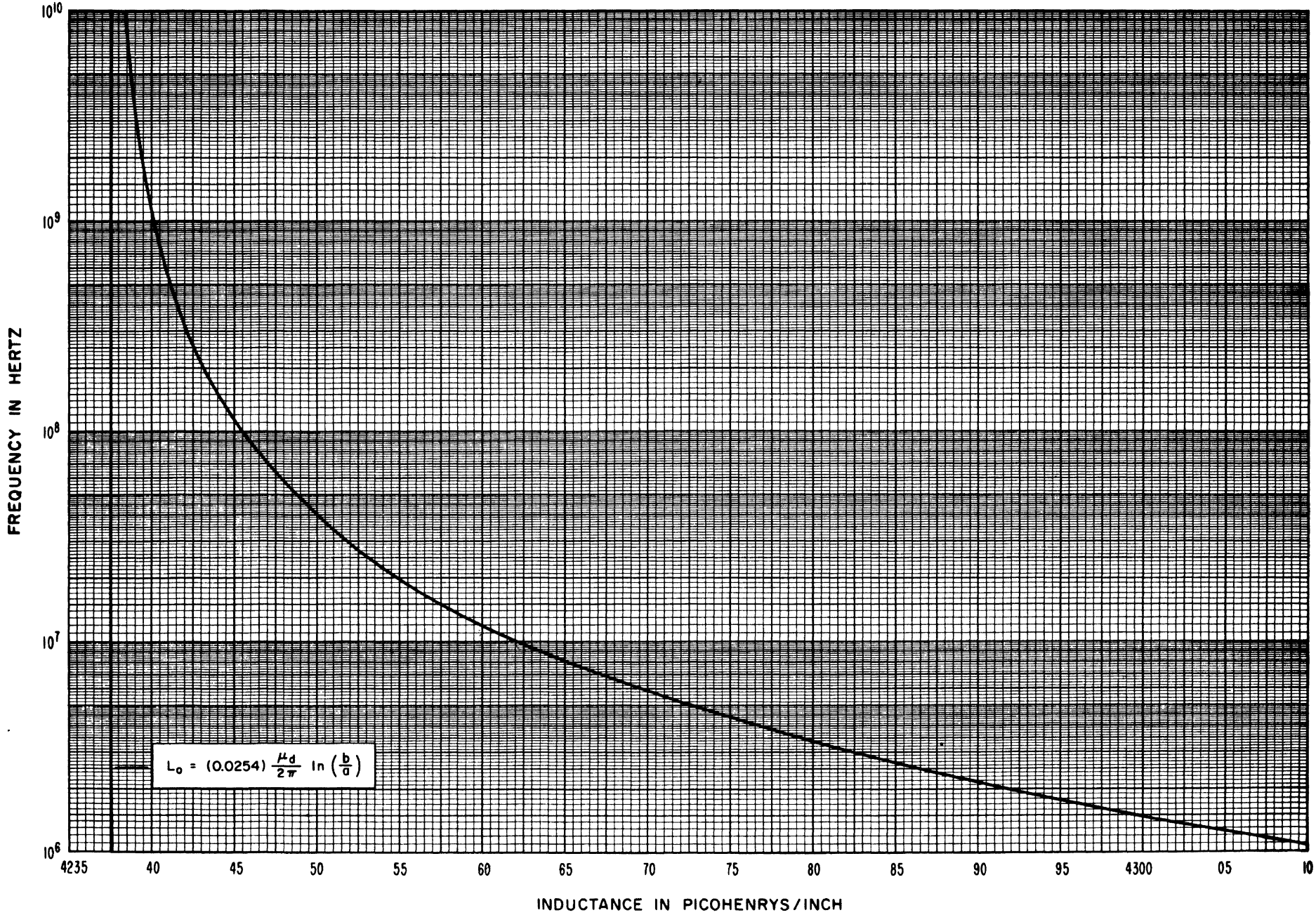

FIGURE 21. *Inductance per inch as a function of frequency under standard conditions for line size #2.*

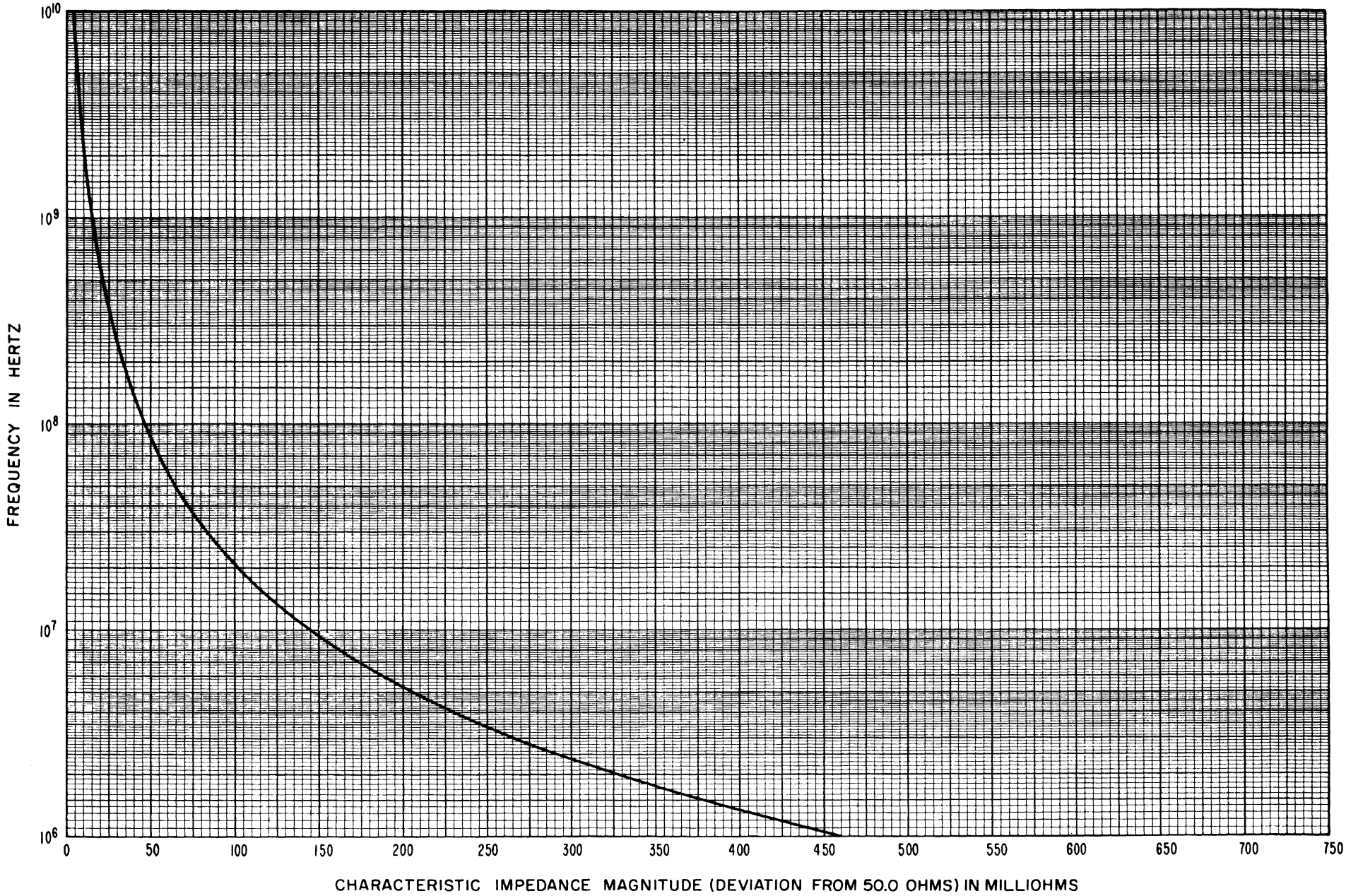

FIGURE 22. *Characteristic impedance magnitude (plotted as a deviation from 50.0 Ω) as a function of frequency under standard conditions for line size #2.*

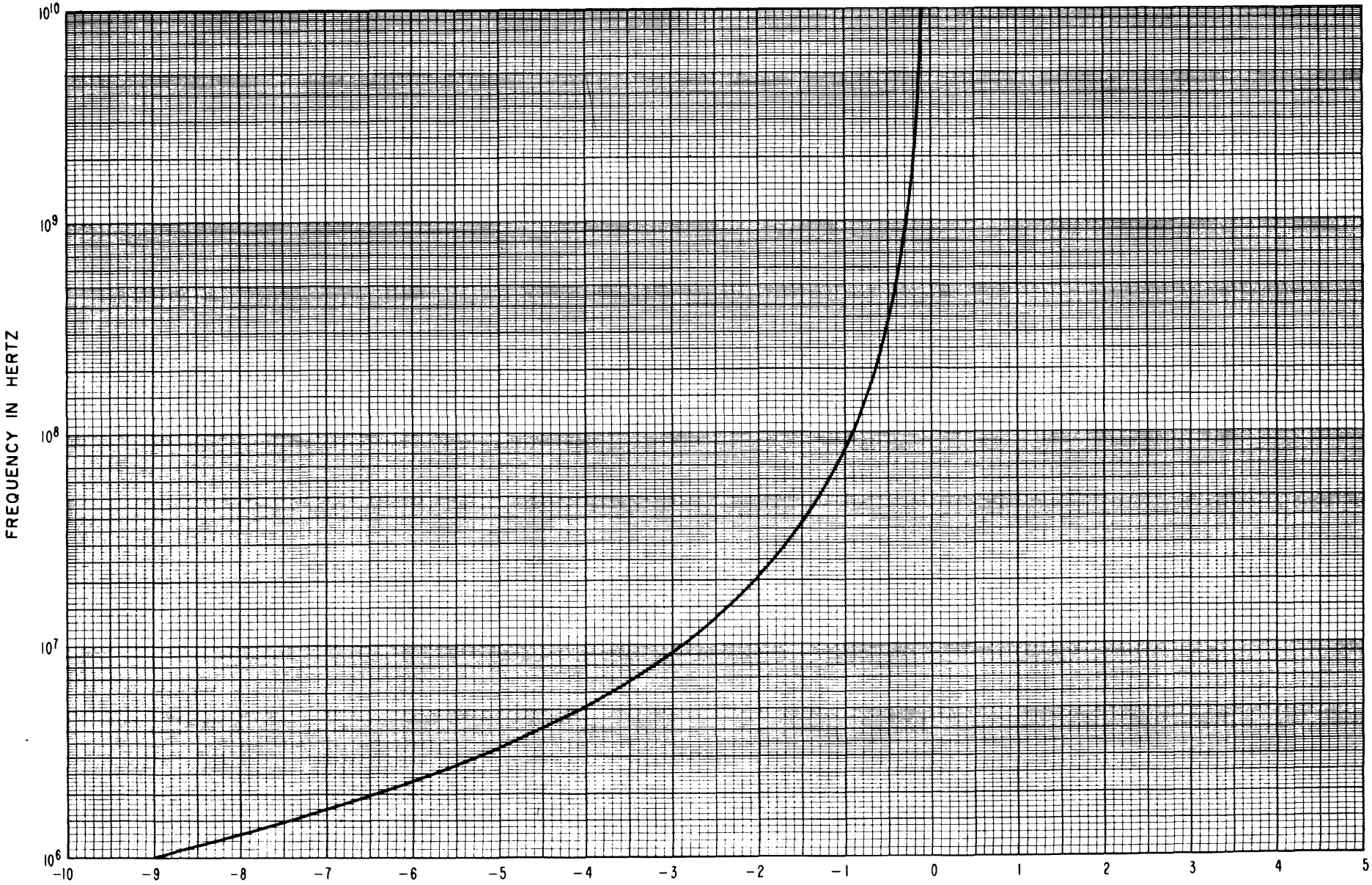

FIGURE 23. *Characteristic impedance phase angle as a function of frequency under standard conditions for line size #2.*

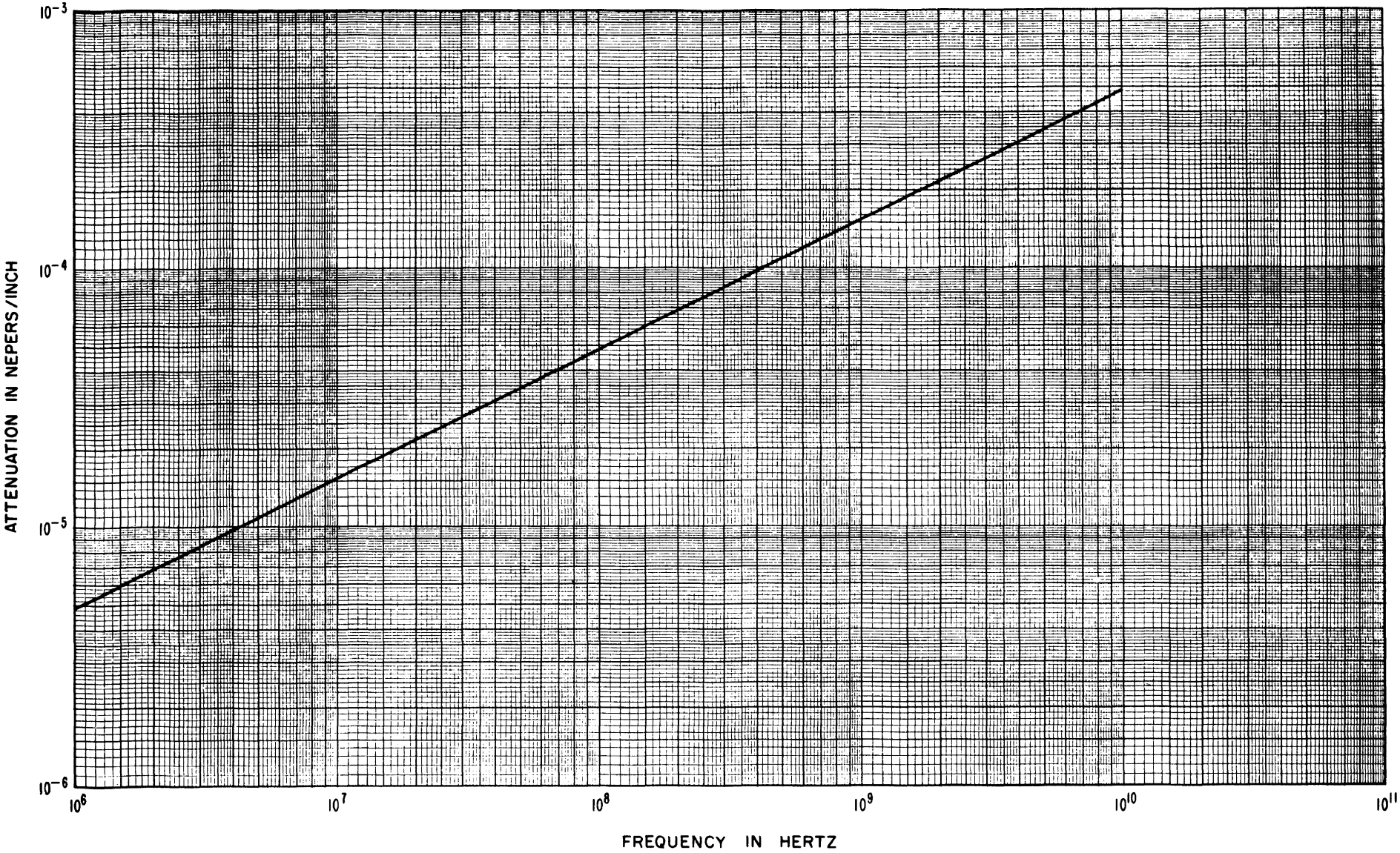

FIGURE 24. *Attenuation per inch as a function of frequency under standard conditions for line size #2.*

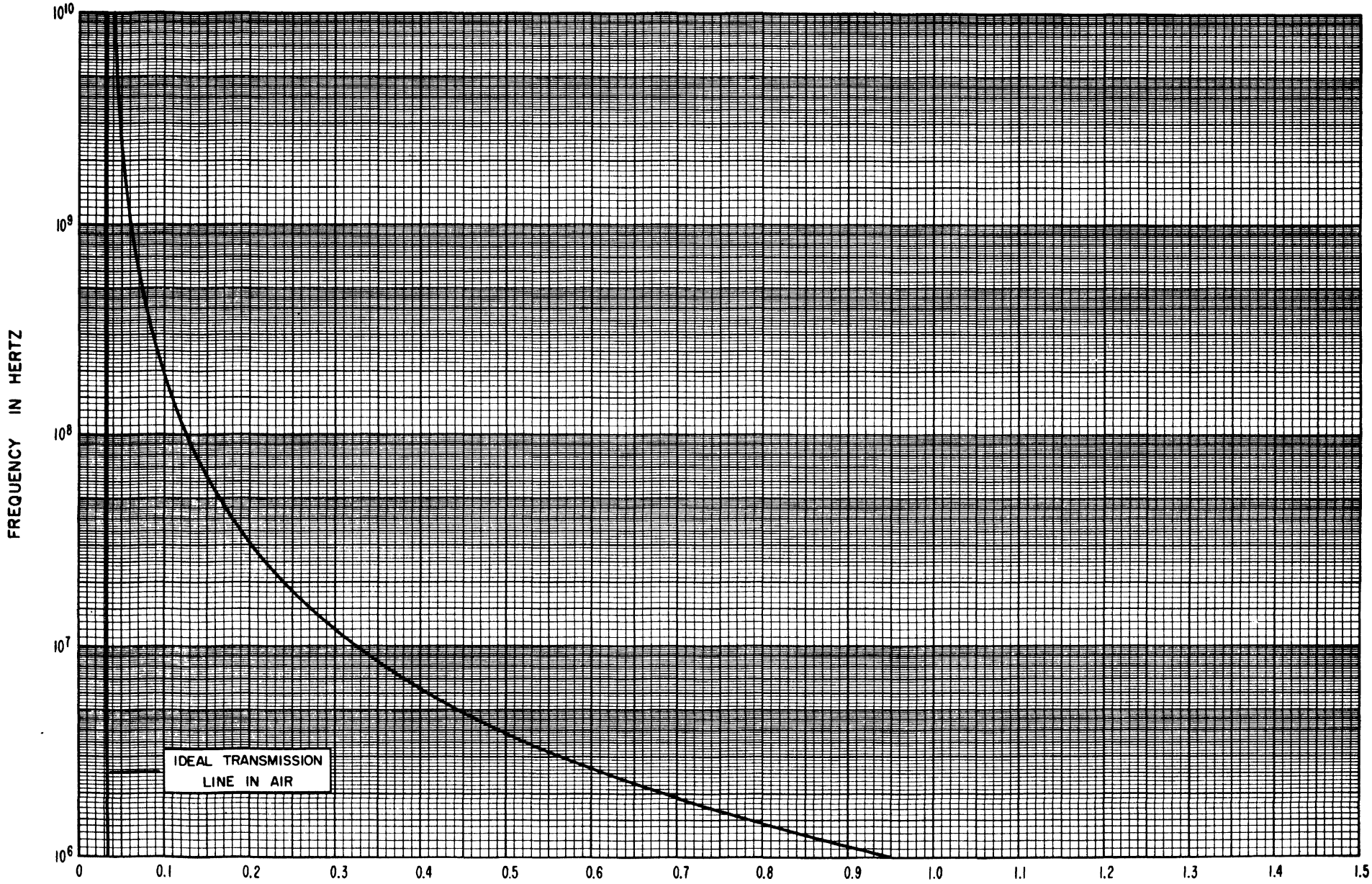

FIGURE 25. *Phase-shift per inch (plotted as a percent deviation from the free space value) as a function of frequency under standard conditions for line size #2.*

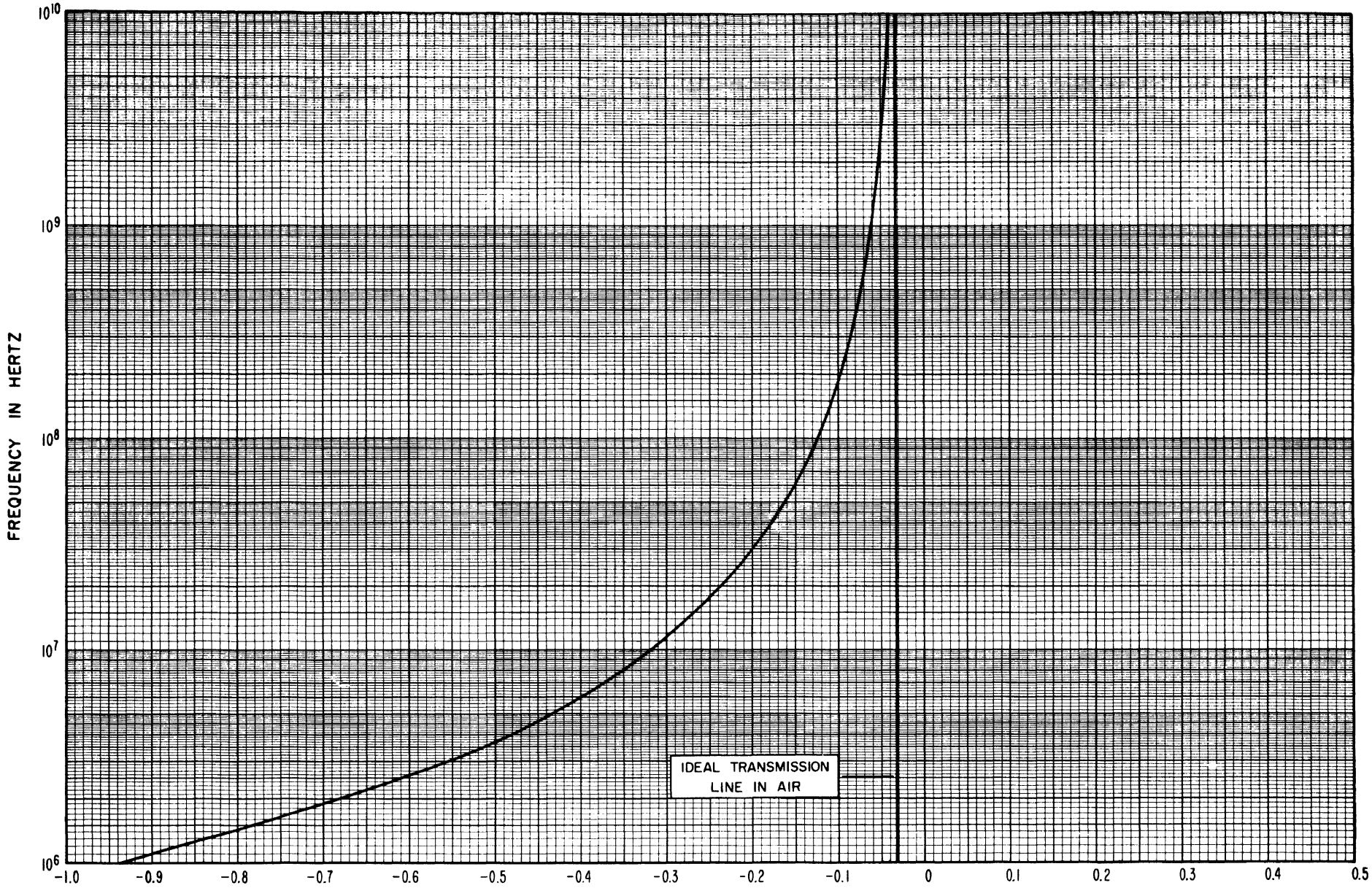

FIGURE 26. *Wavelength (plotted as a percent deviation from the free space value) as a function of frequency under standard conditions for line size #2.*

Line size #2
Variations with resistivity, ρ

Constants used in calculations are the same as those used under standard conditions except that $\rho_i(=\rho_0)$ varies from 0.1×10^{-7} to 0.1×10^{-6} ohm-meters.

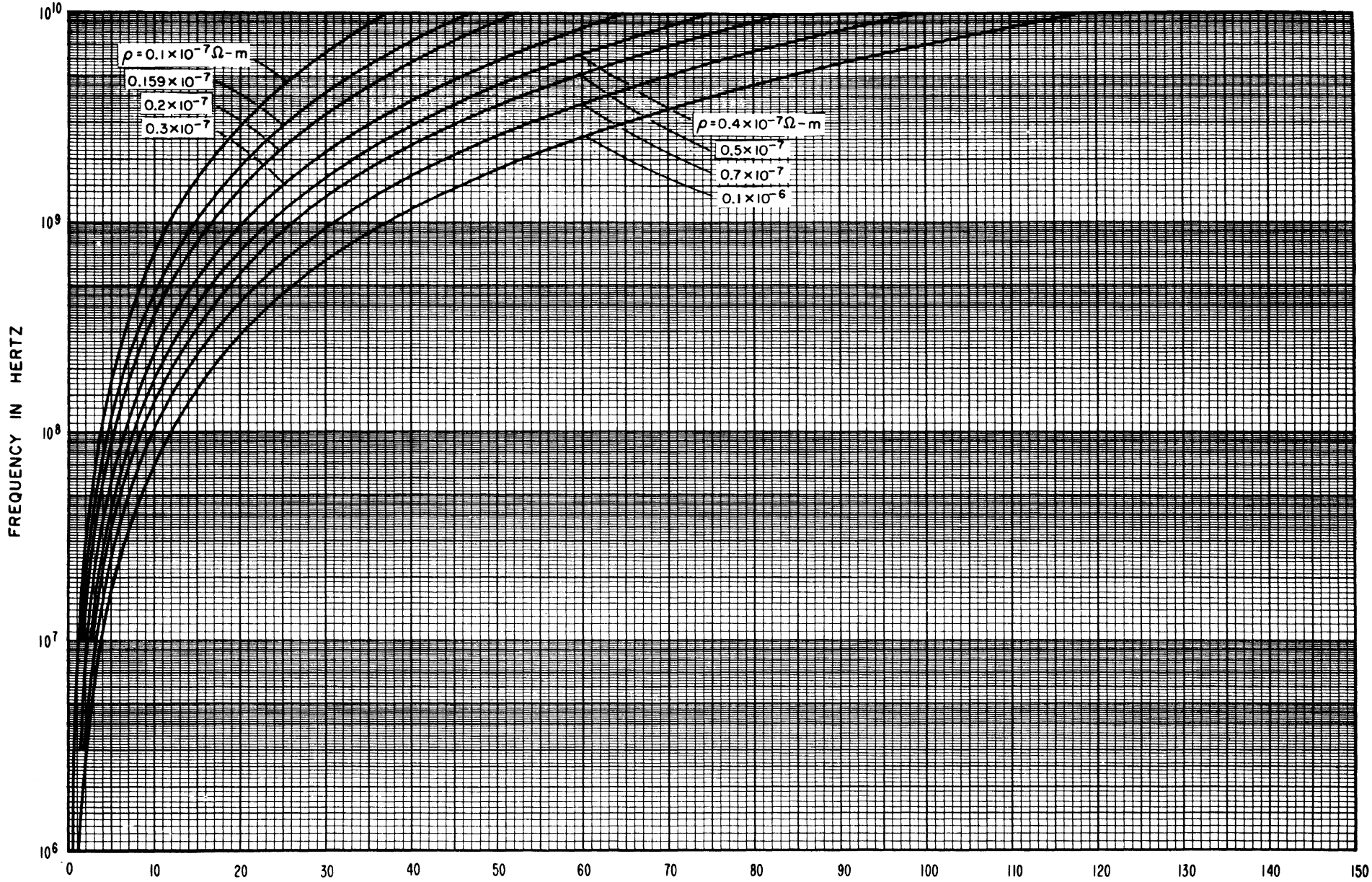

FIGURE 27. *Resistance per inch as a function of frequency for various values of ρ for line size #2.*

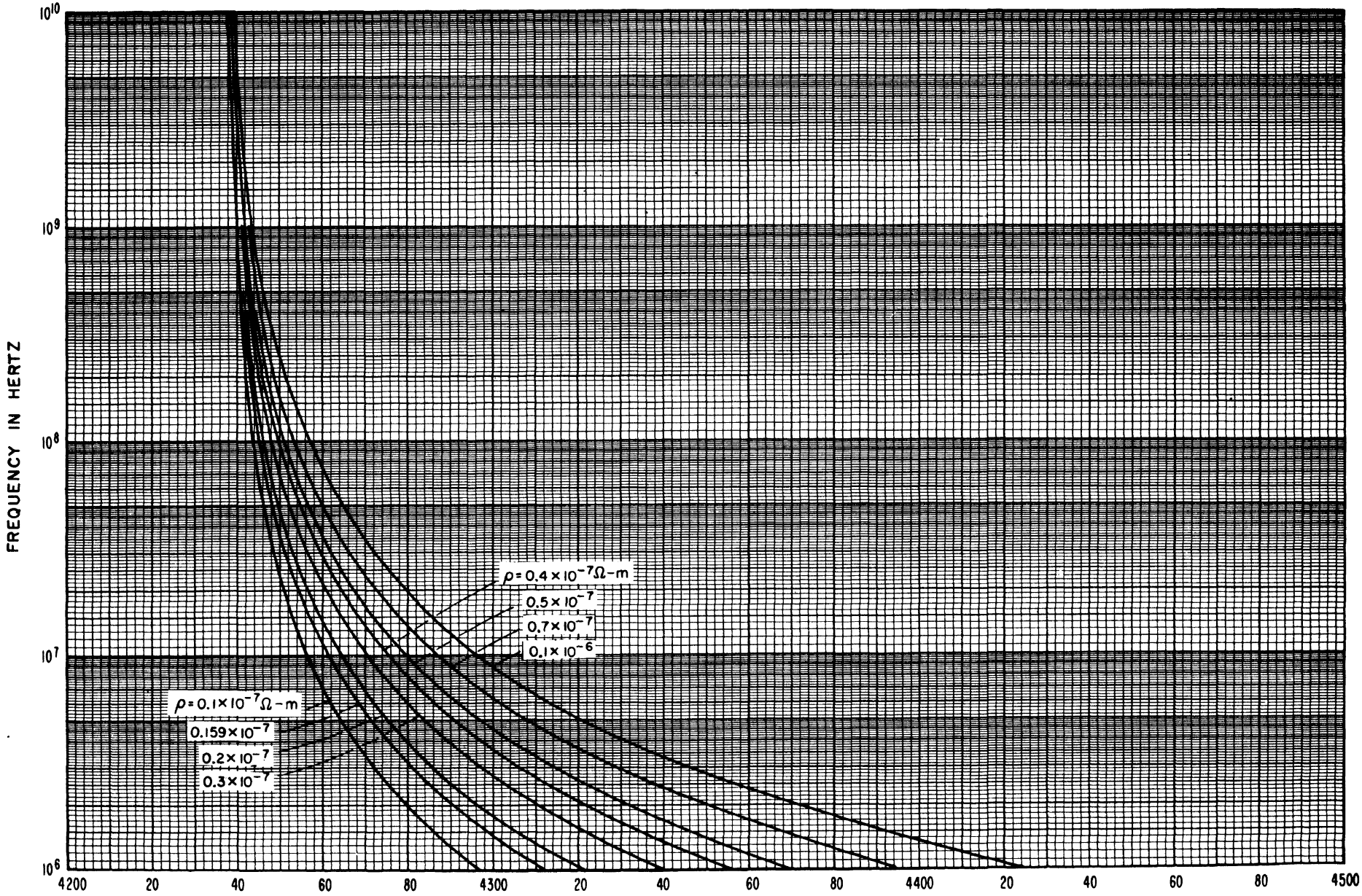

FIGURE 28. *Inductance per inch as a function of frequency for various values of ρ for line size #2.*

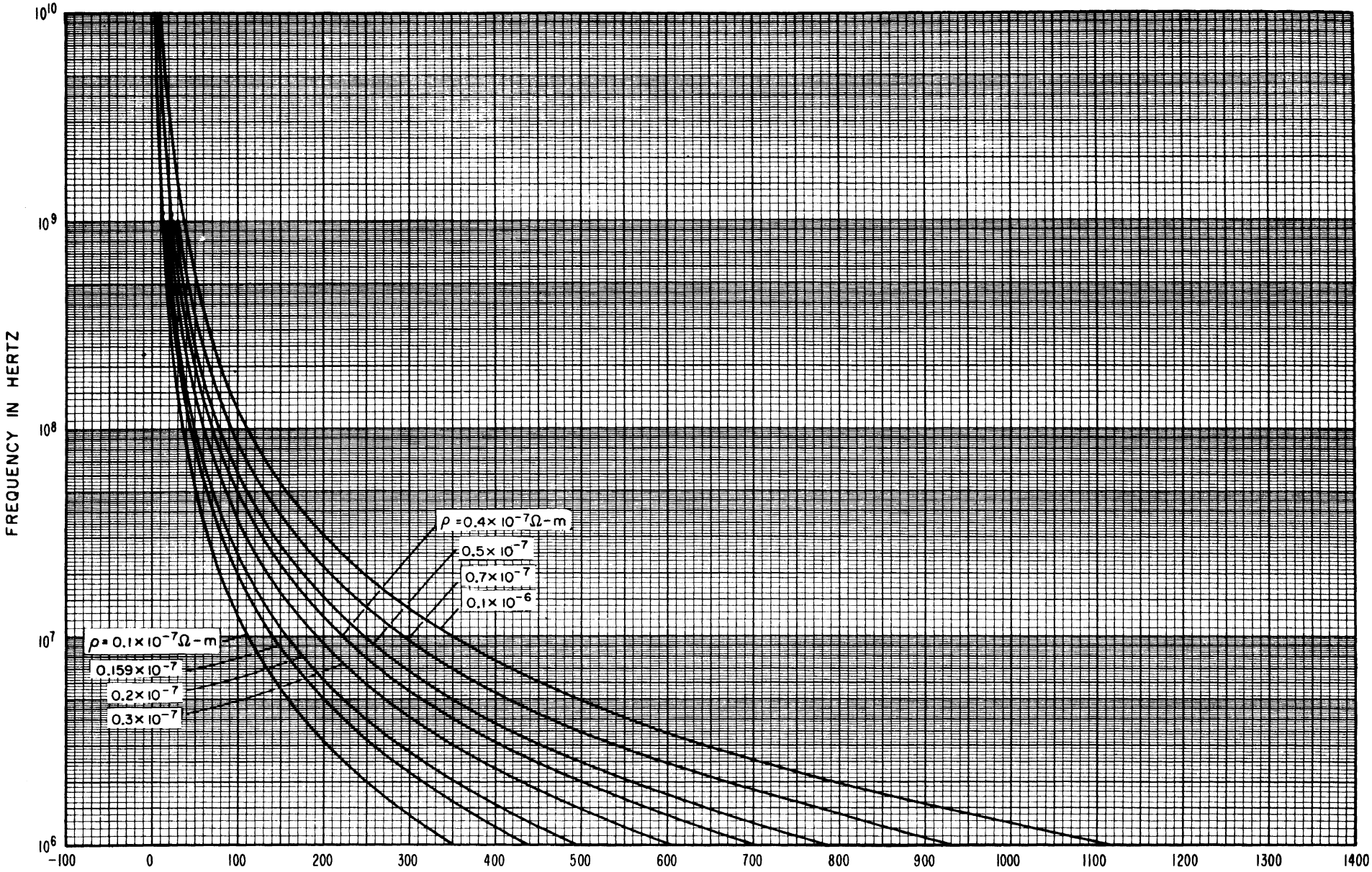

FIGURE 29. *Characteristic impedance magnitude (plotted as a deviation from 50.0 Ω) as a function of frequency for various values of ρ for line size #2.*

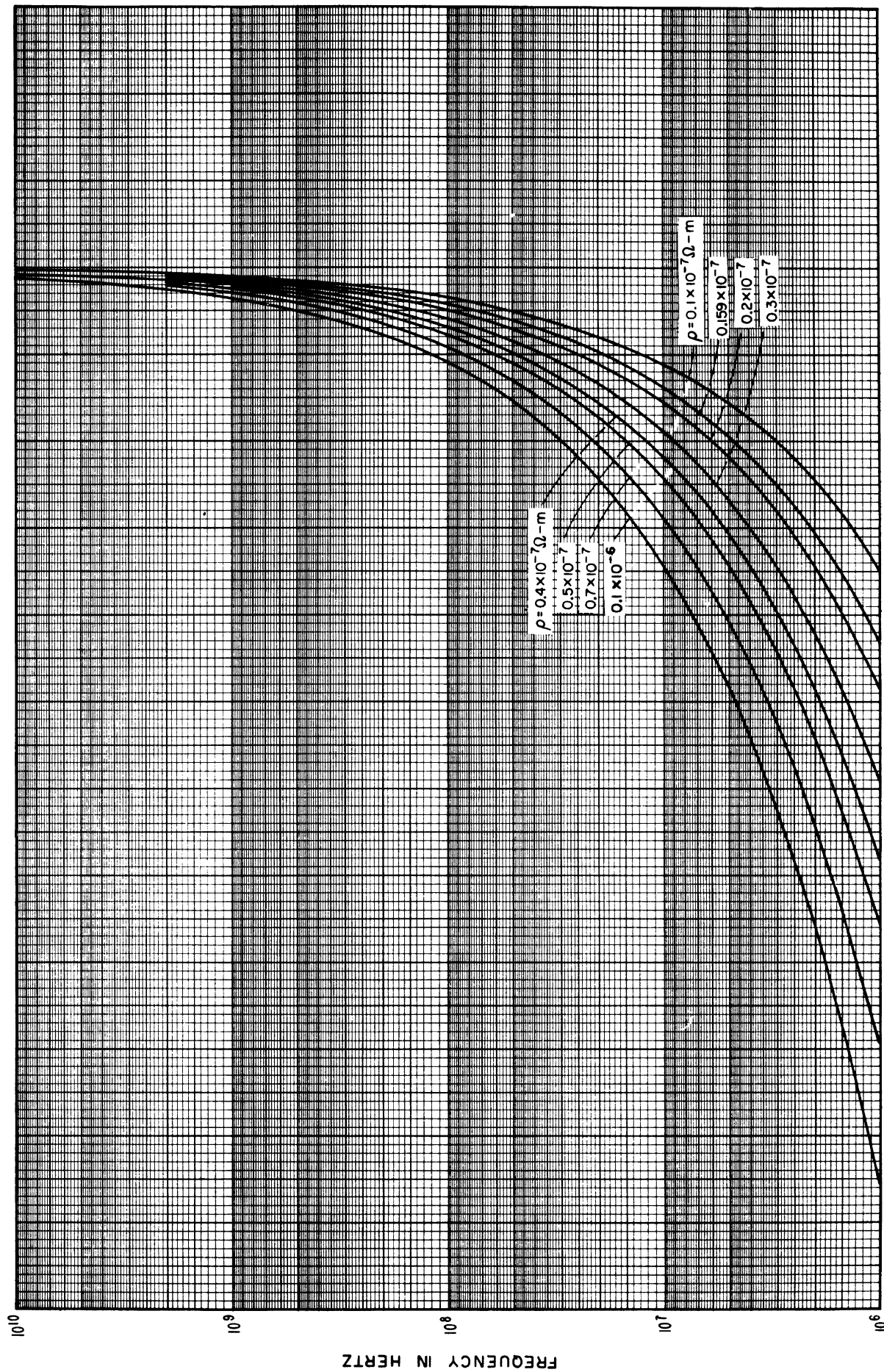

FIGURE 30. *Characteristic impedance phase angle as a function of frequency for various values of ρ for line size #2.*

218-445 O-66—4

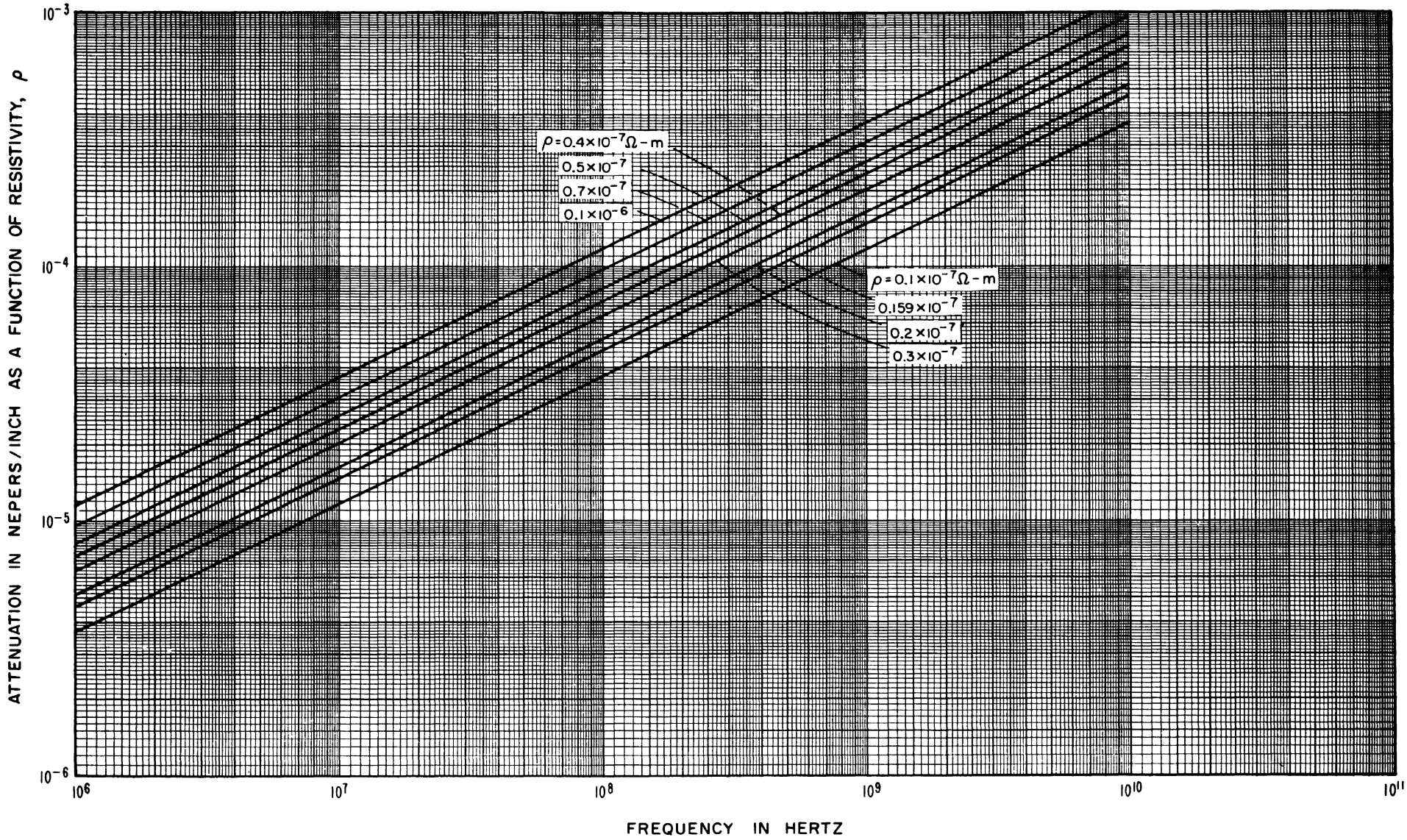

FIGURE 31. *Attenuation per inch as a function of frequency for various values of ρ for line size #2.*

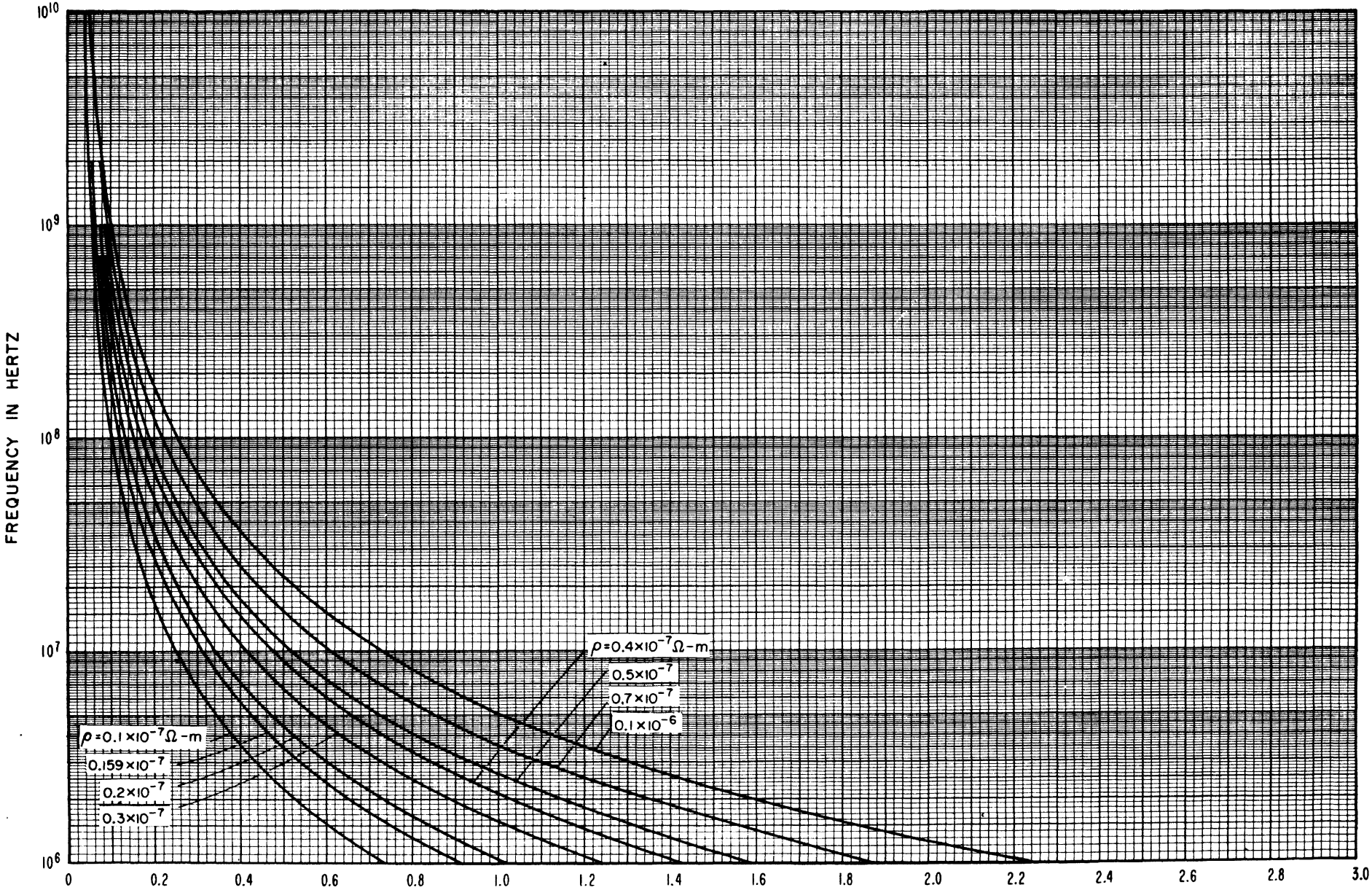

FIGURE 32. *Phase-shift per inch (plotted as a percent deviation from the free space value) as a function of frequency for various values of ρ for line size #2.*

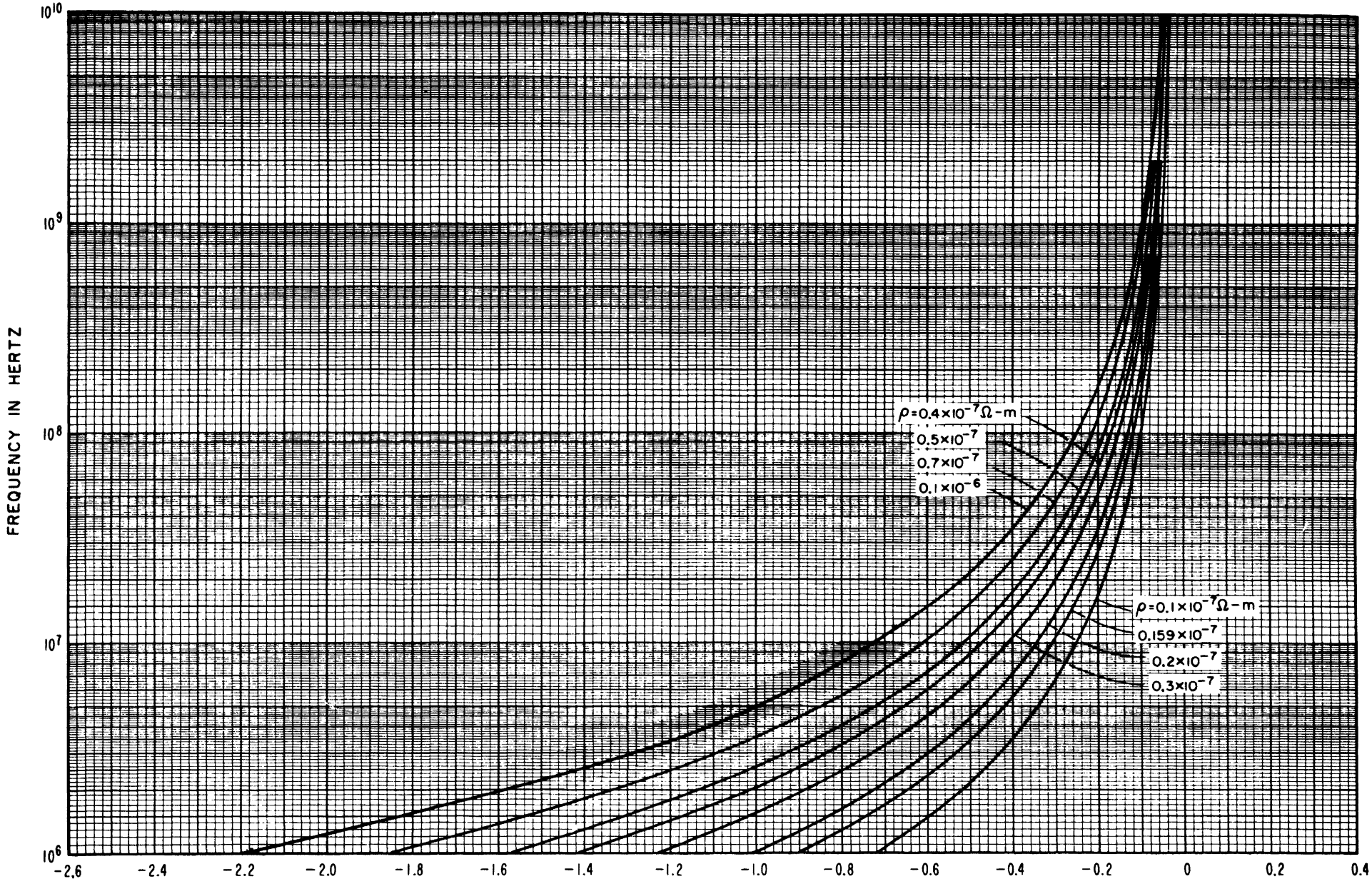

FIGURE 33. *Wavelength (plotted as a percent deviation from the free space value) as a function of frequency for various values of ρ for line size #2.*

Line size #2
Variations with relative dielectric constant, $\frac{\epsilon}{\epsilon_0}$

Constants used in calculations are the same as those used under standard conditions except that $\frac{\epsilon}{\epsilon_0}$ varies from 1.000400 to 1.000800.

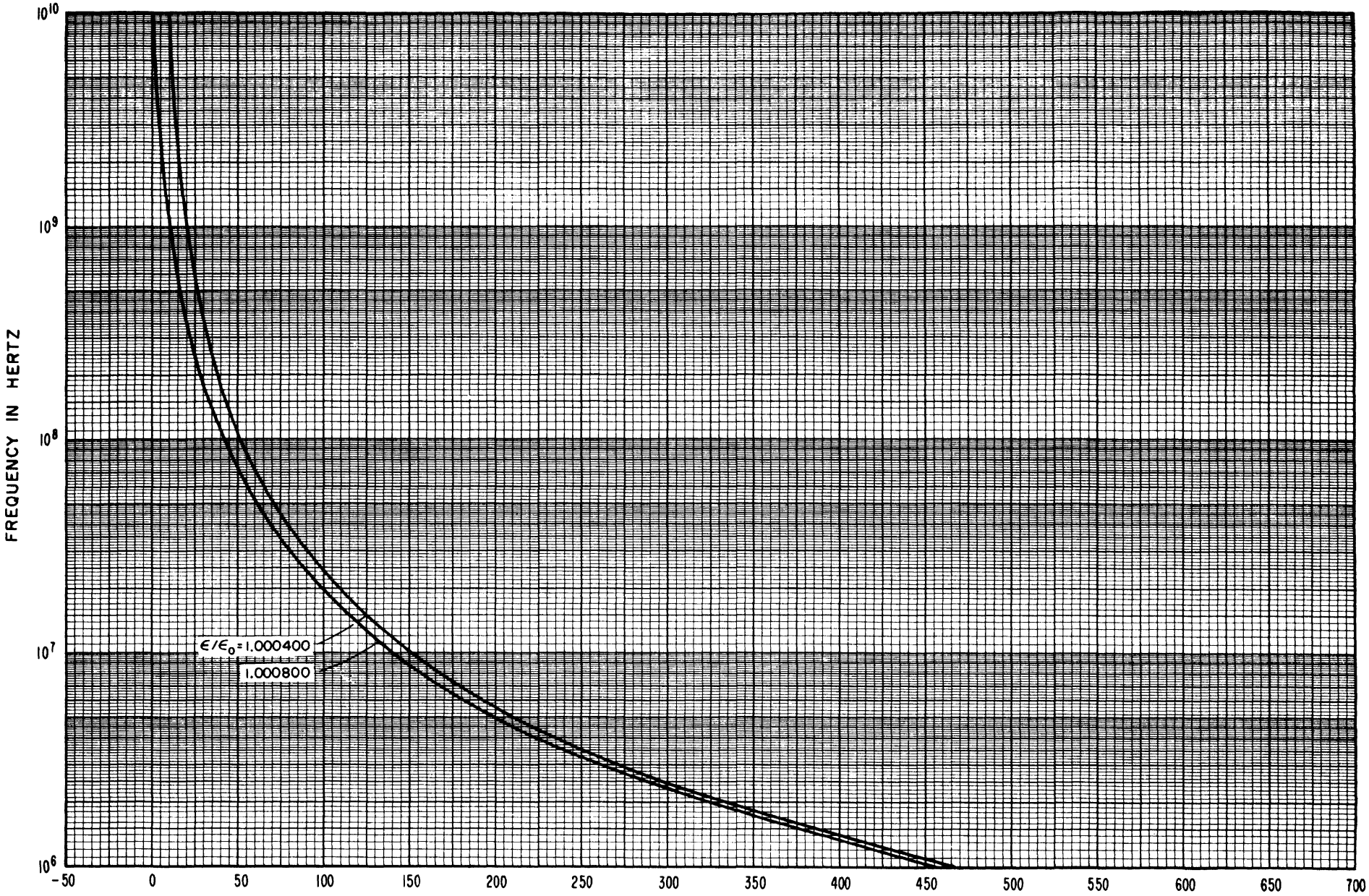

FIGURE 34. *Characteristic impedance magnitude (plotted as a deviation from 50.0 Ω) as a function of frequency for various values of* $\frac{\epsilon}{\epsilon_0}$ *for line size #2.*

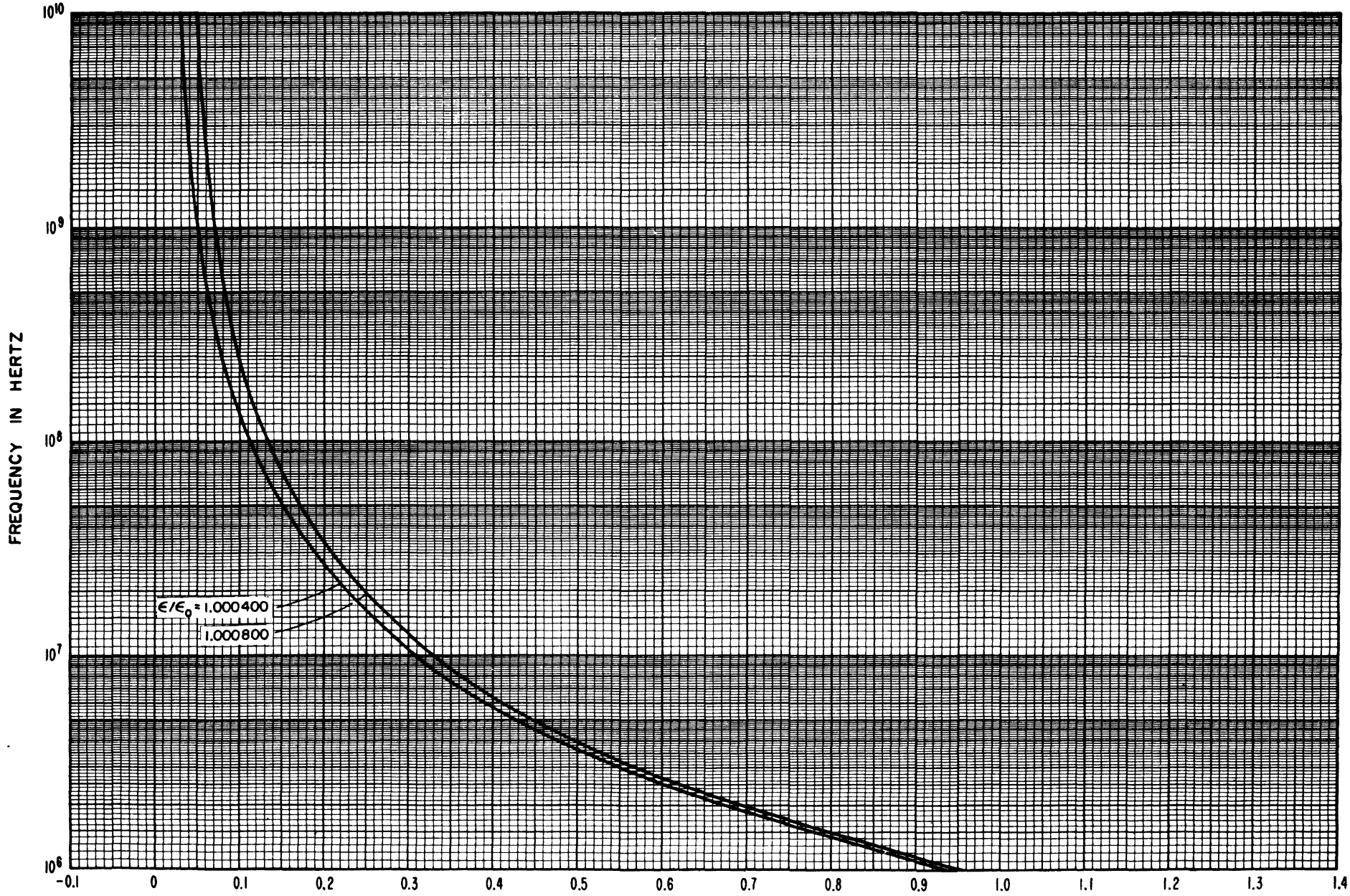

FIGURE 35. *Phase-shift per inch (plotted as a percent deviation from the free space value) as a function of frequency for various values of* $\frac{\epsilon}{\epsilon_0}$ *for line size #2.*

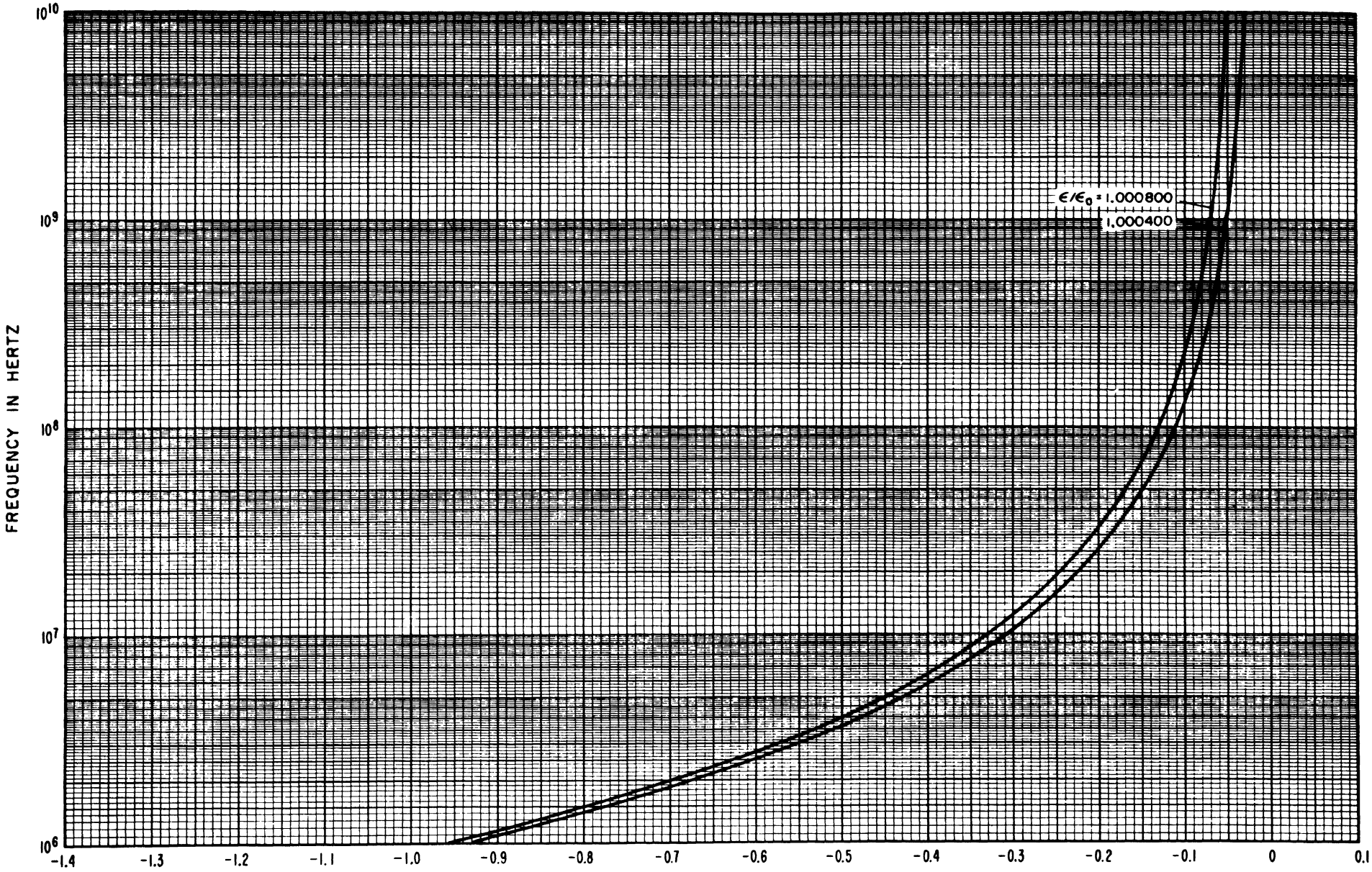

FIGURE 36. *Wavelength (plotted as a percent deviation from the free space value) as a function of frequency for various values of* $\frac{\epsilon}{\epsilon_0}$ *for line size #2.*

Line size #2
Variations with diameters a and b

Constants used in calculations are the same as those used under standard conditions except that a varies ± 0.0001 inch from standard conditions, and b varies ± 0.0002 inch from standard conditions.

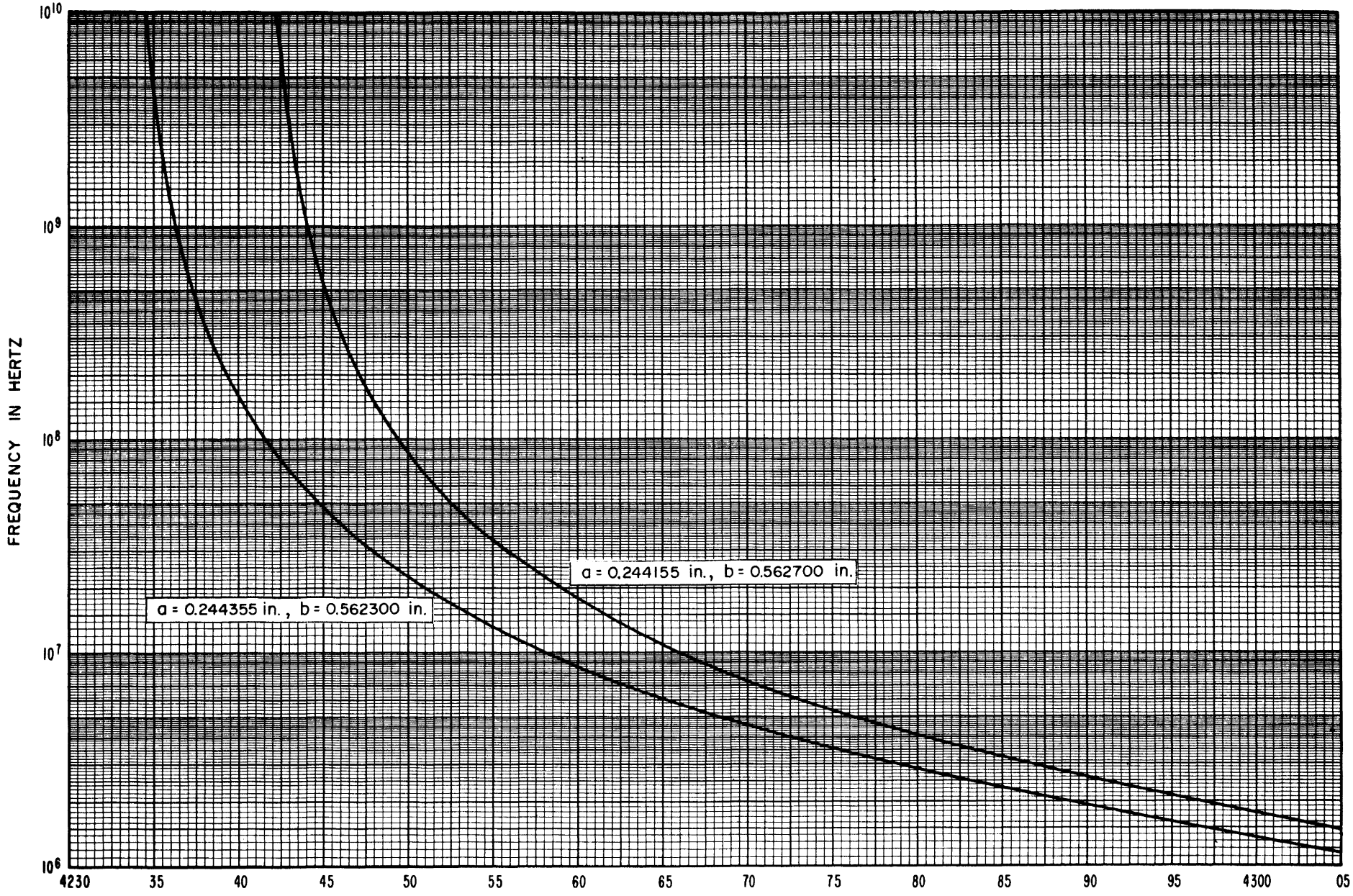

FIGURE 37. *Inductance per inch as a function of frequency for various values of diameters* a *and* b *for line size #2.*

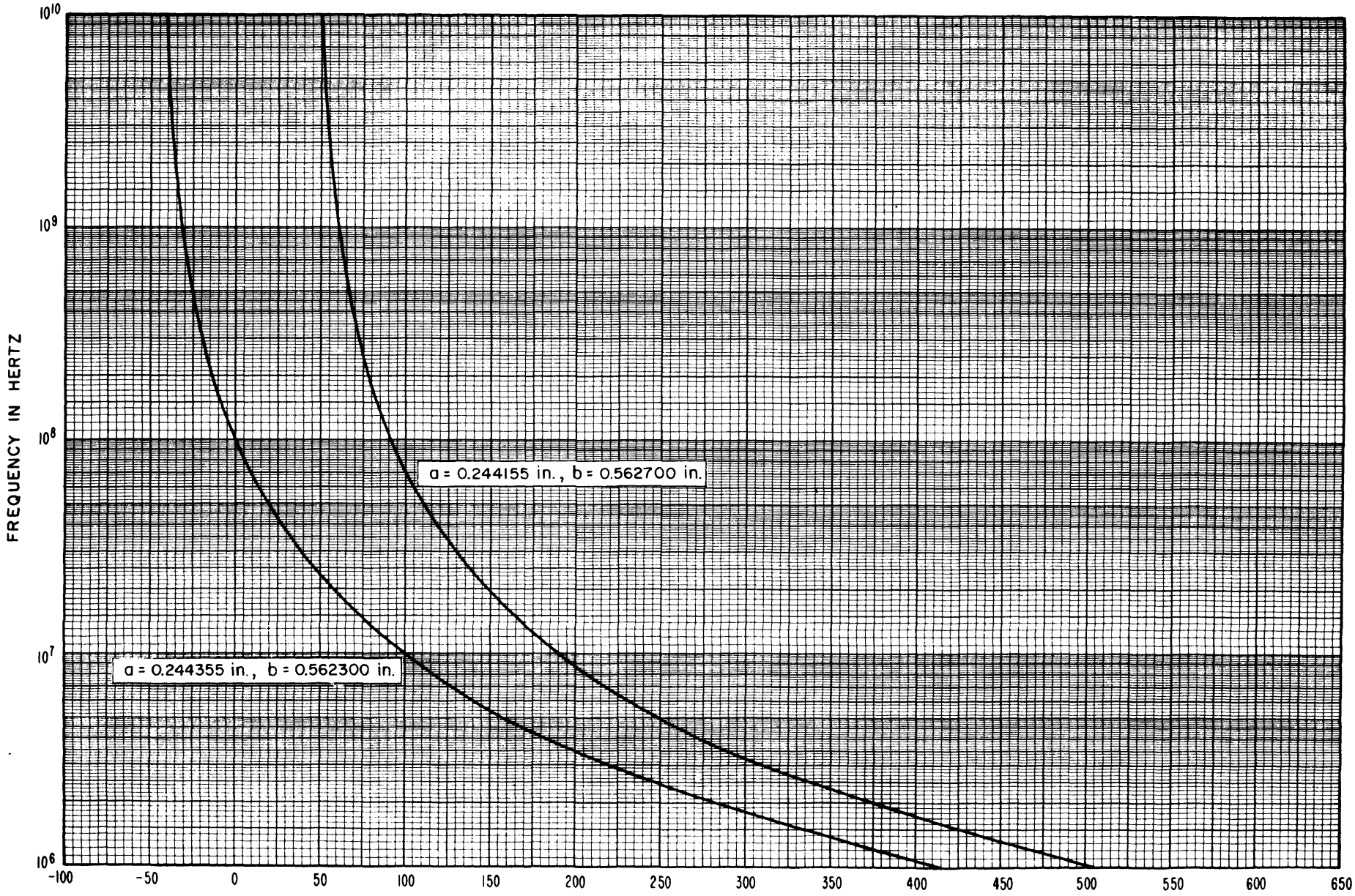

FIGURE 38. *Characteristic impedance magnitude (plotted as a deviation from 50.0 Ω) as a function of frequency for various values of diameters* a *and* b *for line size #2.*

Line size #3

Standard conditions

Constants used in calculations:

$a = 0.325673$ inch

$b = 0.750000$ inch

$\rho_i = \rho_o = 0.17241 \times 10^{-7}$ ohm-meters

$\mu_{o,i} = \mu_o = \mu_d = 4\pi \times 10^{-7}$ henry/meter

$\frac{\epsilon}{\epsilon_o} = 1.000649$

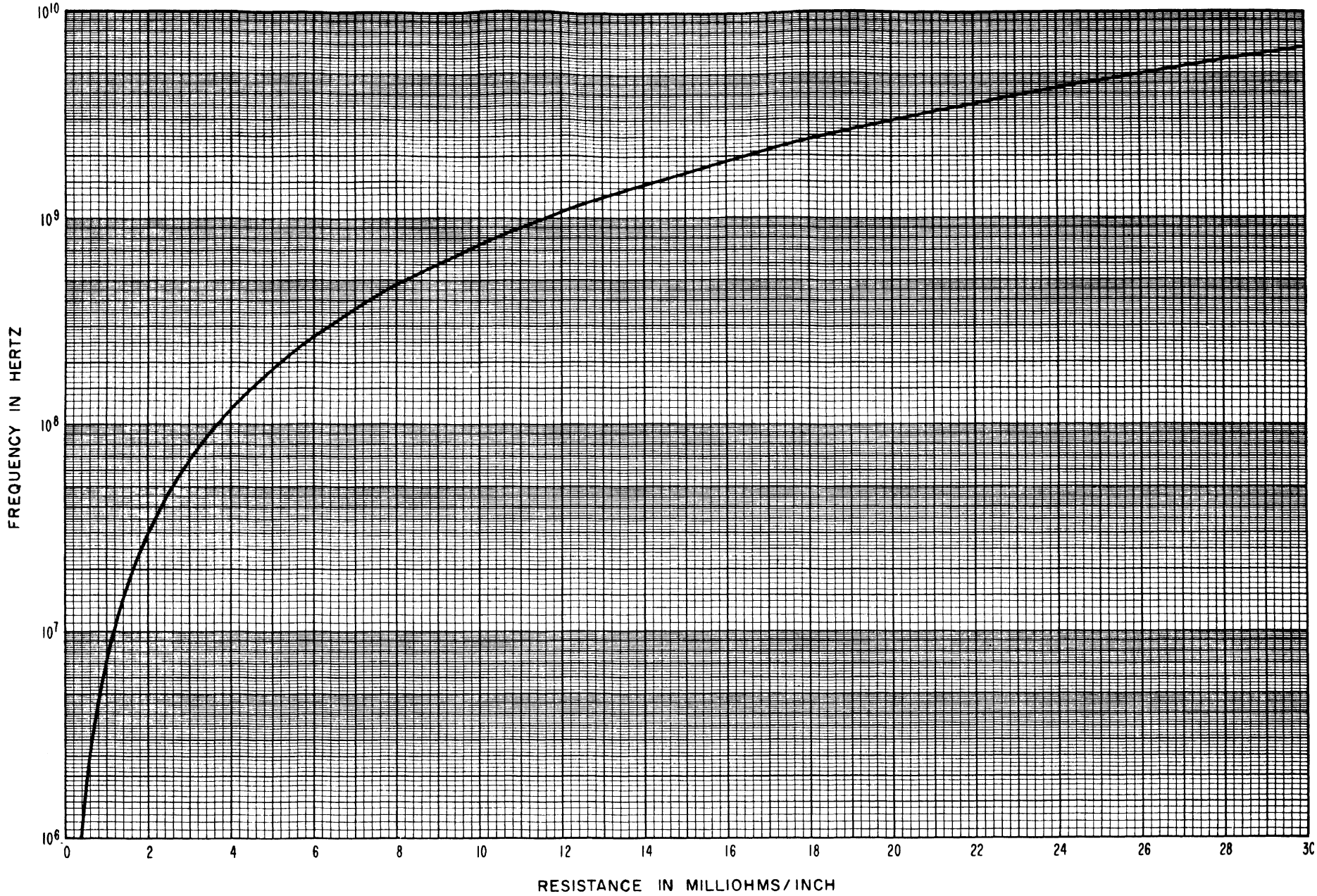

FIGURE 39. *Resistance per inch as a function of frequency under standard conditions for line size #3.*

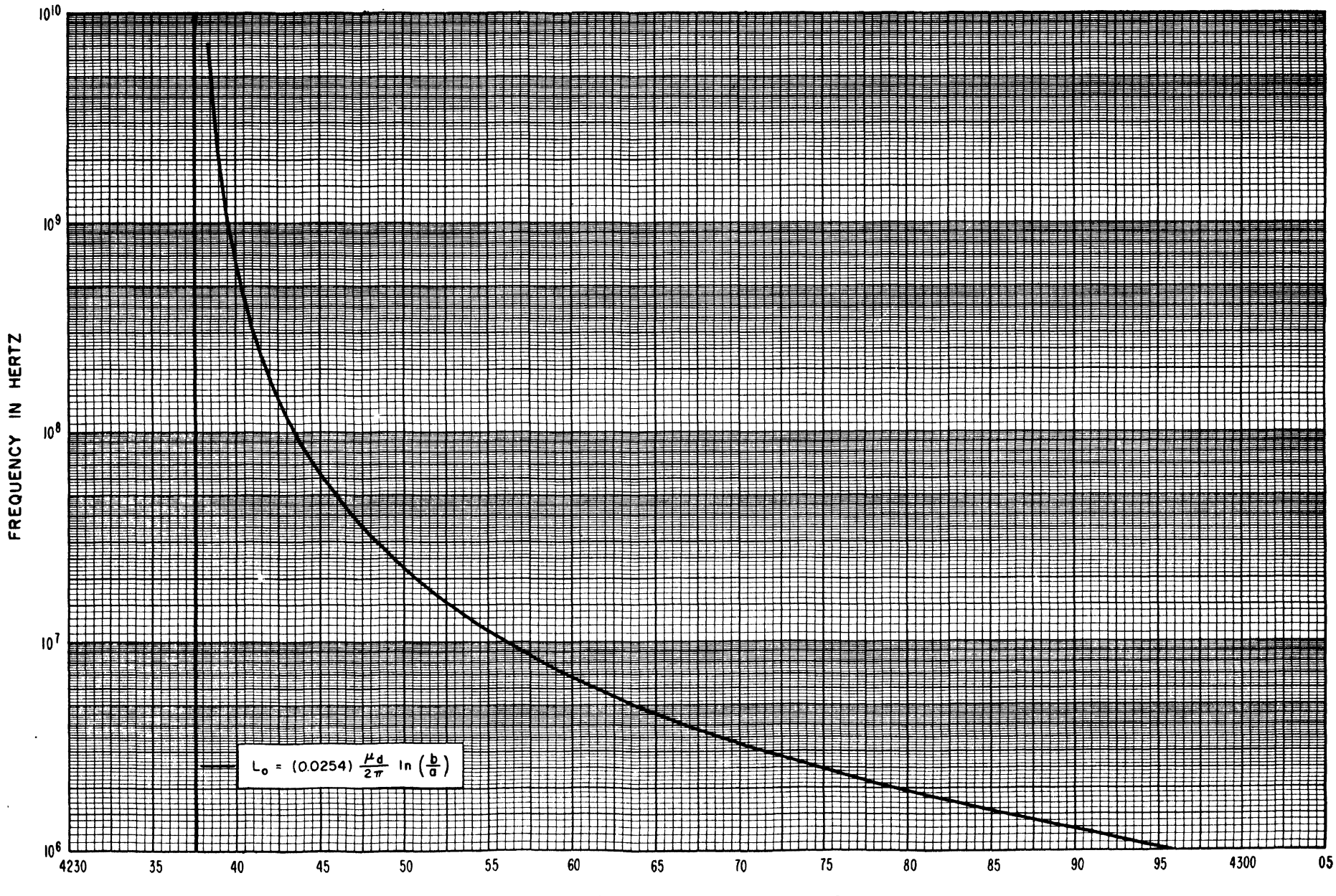

FIGURE 40. *Inductance per inch as a function of frequency under standard conditions for line size #3.*

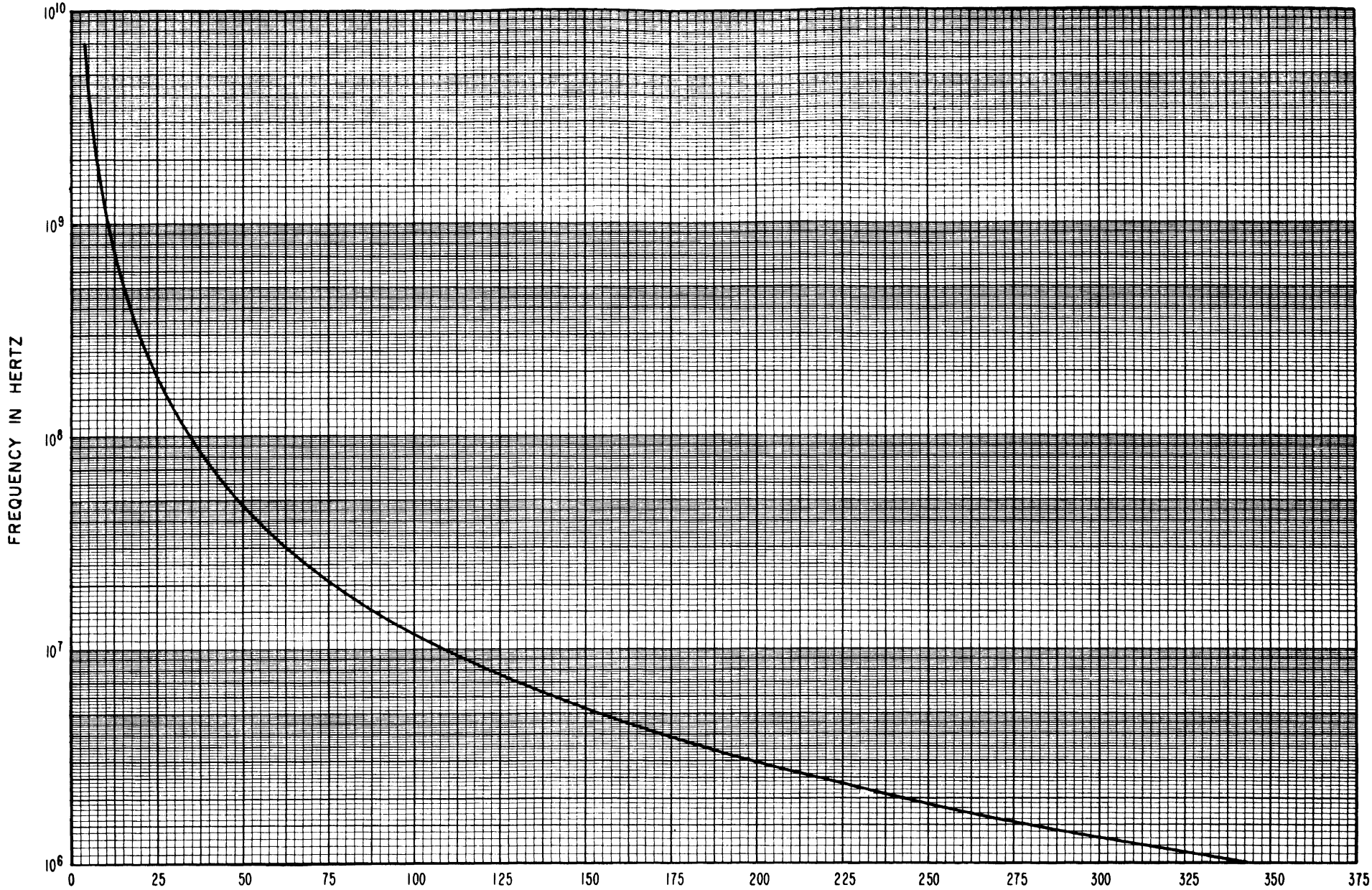

FIGURE 41. *Characteristic impedance magnitude (plotted as a deviation from 50.0 Ω) as a function of frequency under standard conditions for line size #3.*

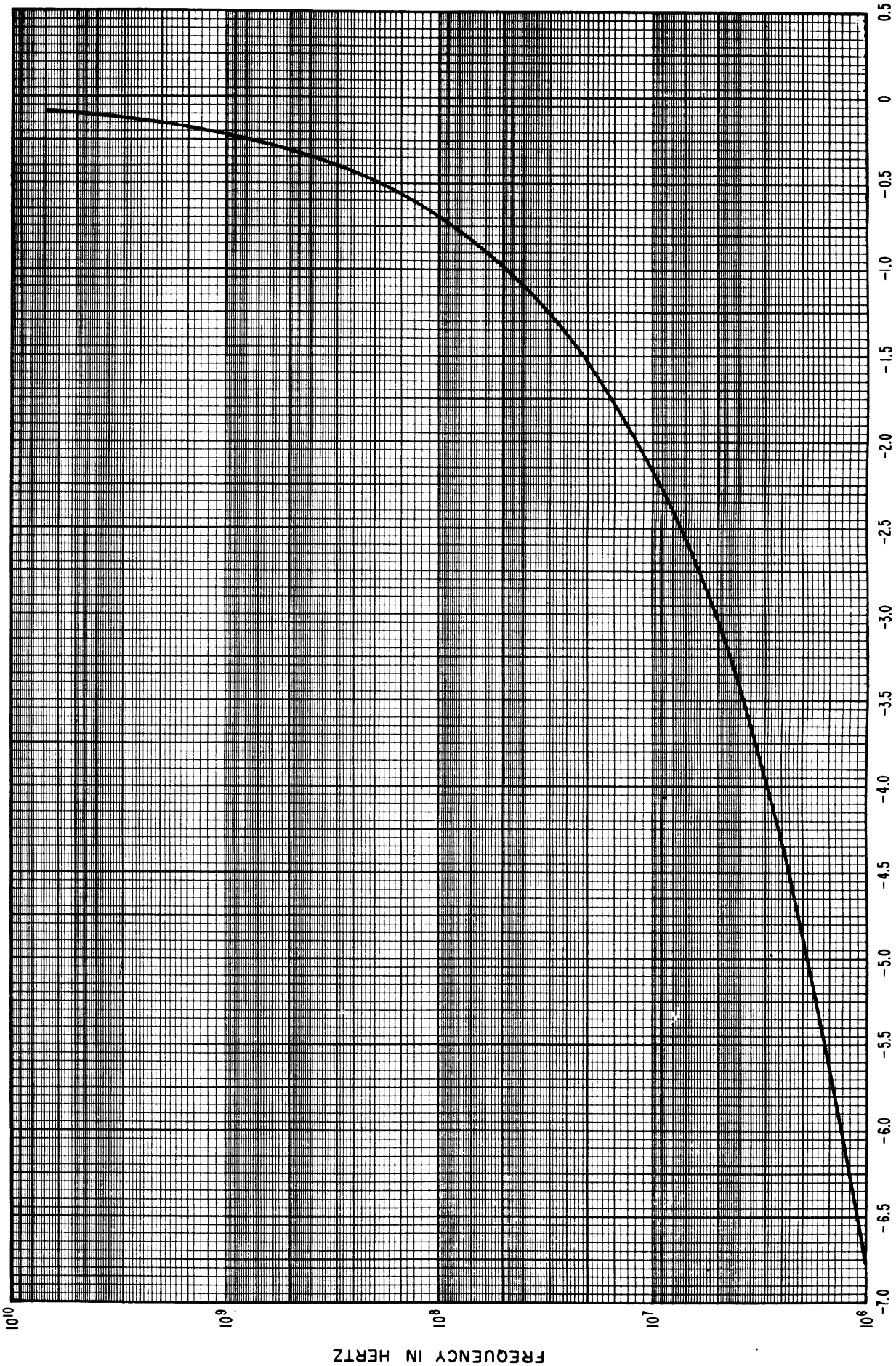

FIGURE 42. *Characteristic impedance phase angle as a function of frequency under standard conditions for line size #3.*

218-445 O-66—5

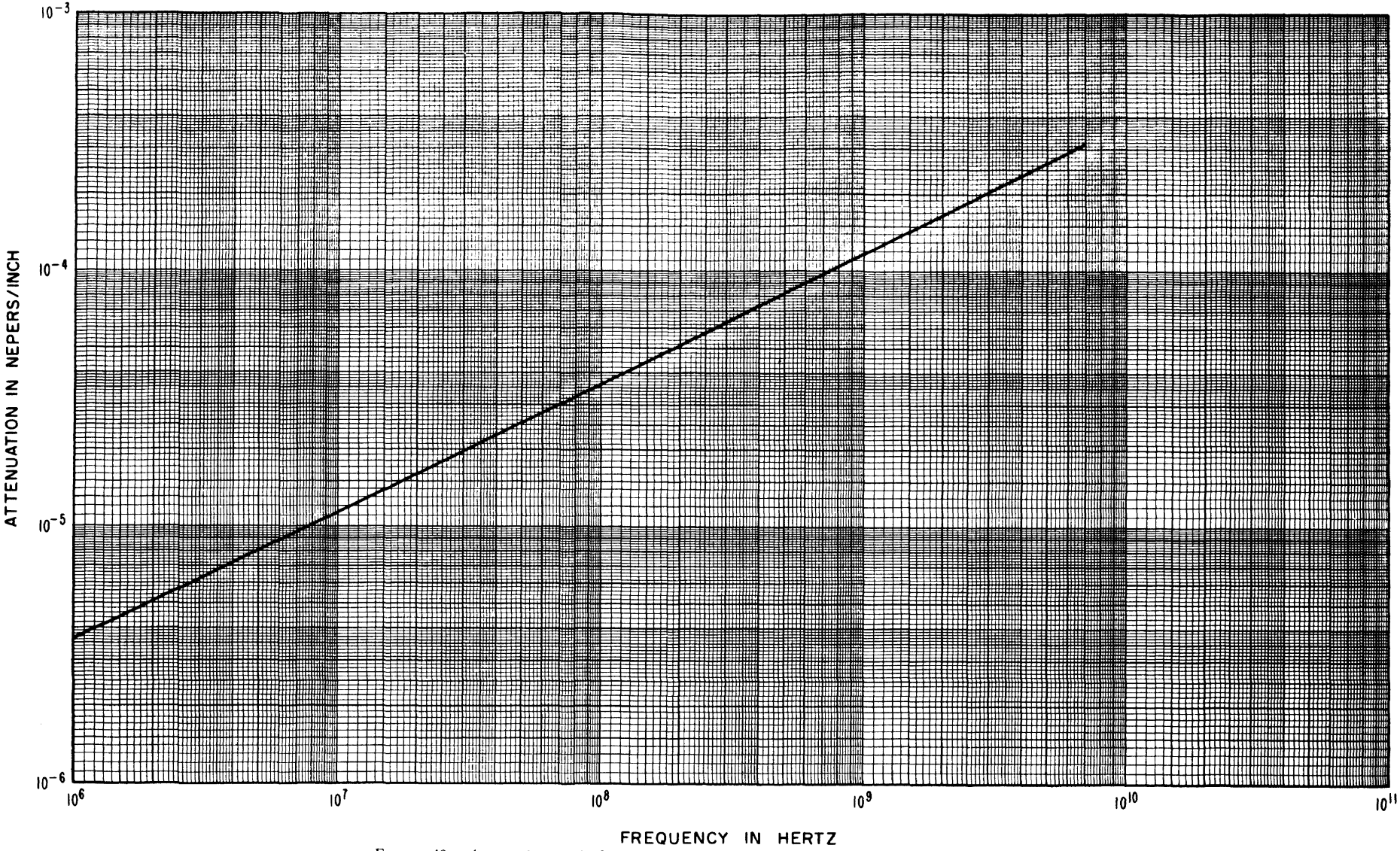

FIGURE 43. *Attenuation per inch as a function of frequency under standard conditions for line size #3.*

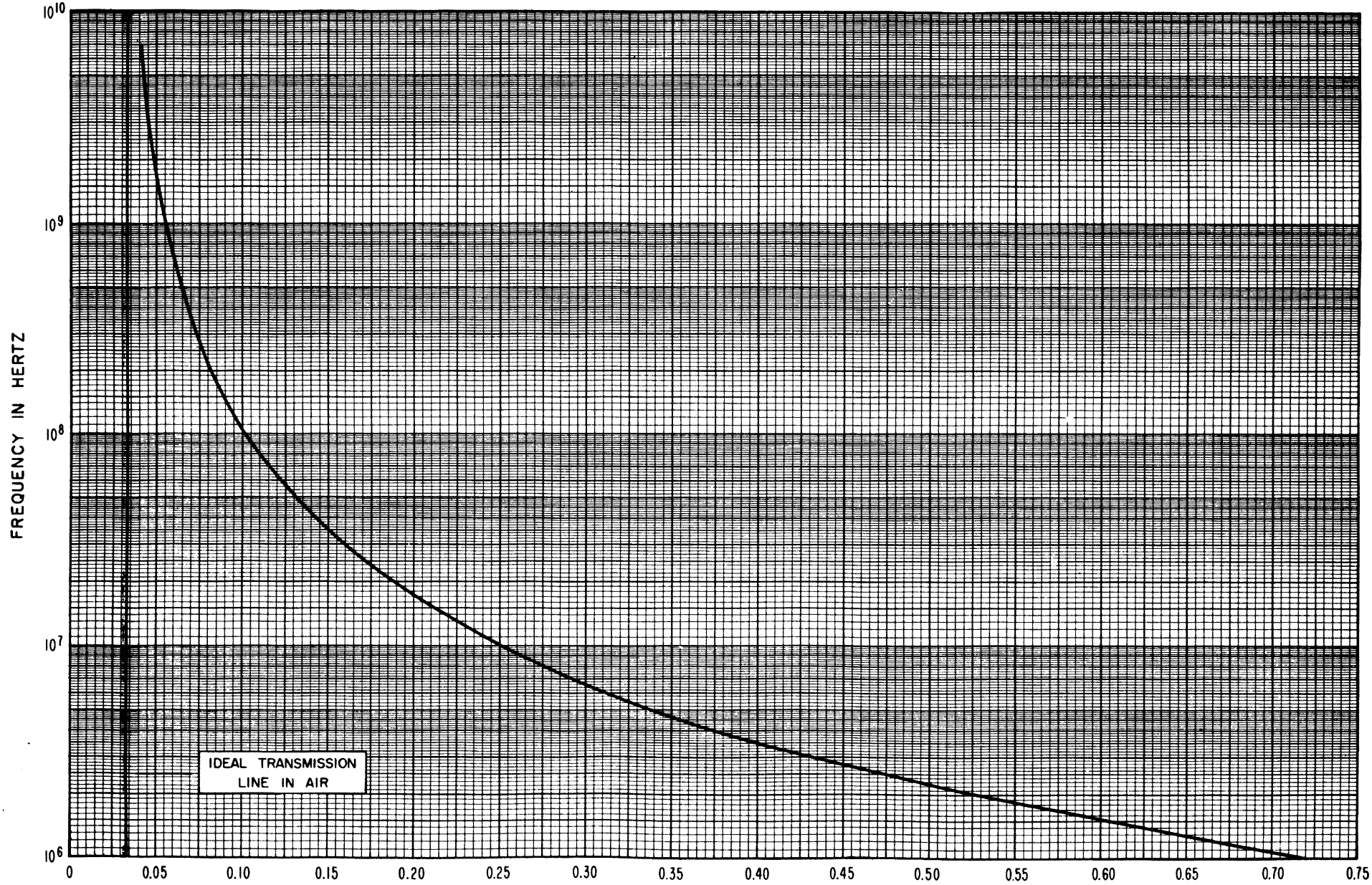

FIGURE 44. *Phase-shift per inch (plotted as a percent deviation from the free space value) as a function of frequency under standard conditions for line size #3.*

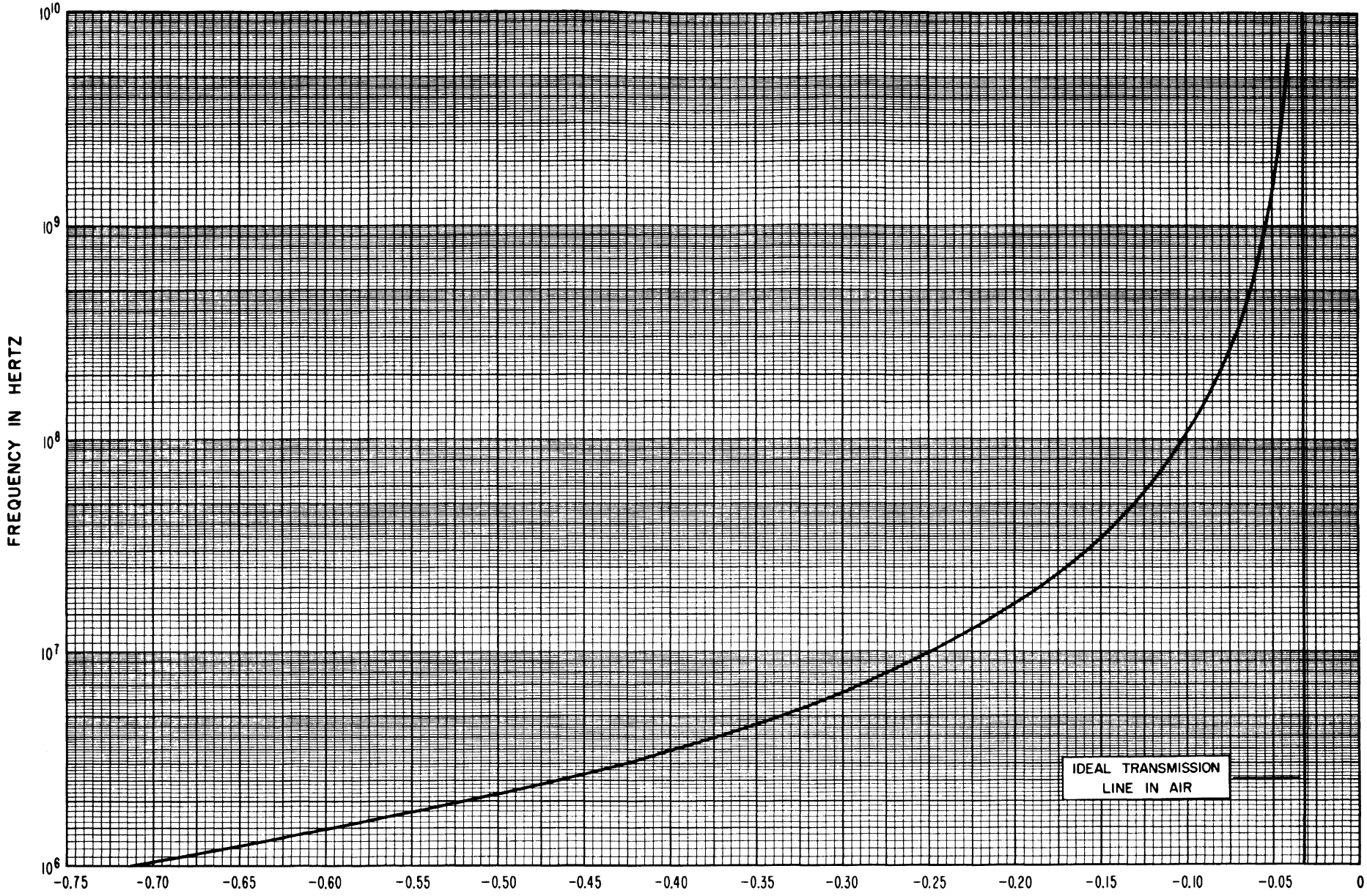

FIGURE 45. *Wavelength (plotted as a percent deviation from the free space value) as a function of frequency under standard conditions for line size #3.*

Line size #3

Variations with resistivity, p

Constants used in calculations are the same as those used under standard conditions except that p (=p) varies from 0.1×10^{-7} to 0.1×10^{-6} ohm-meters.

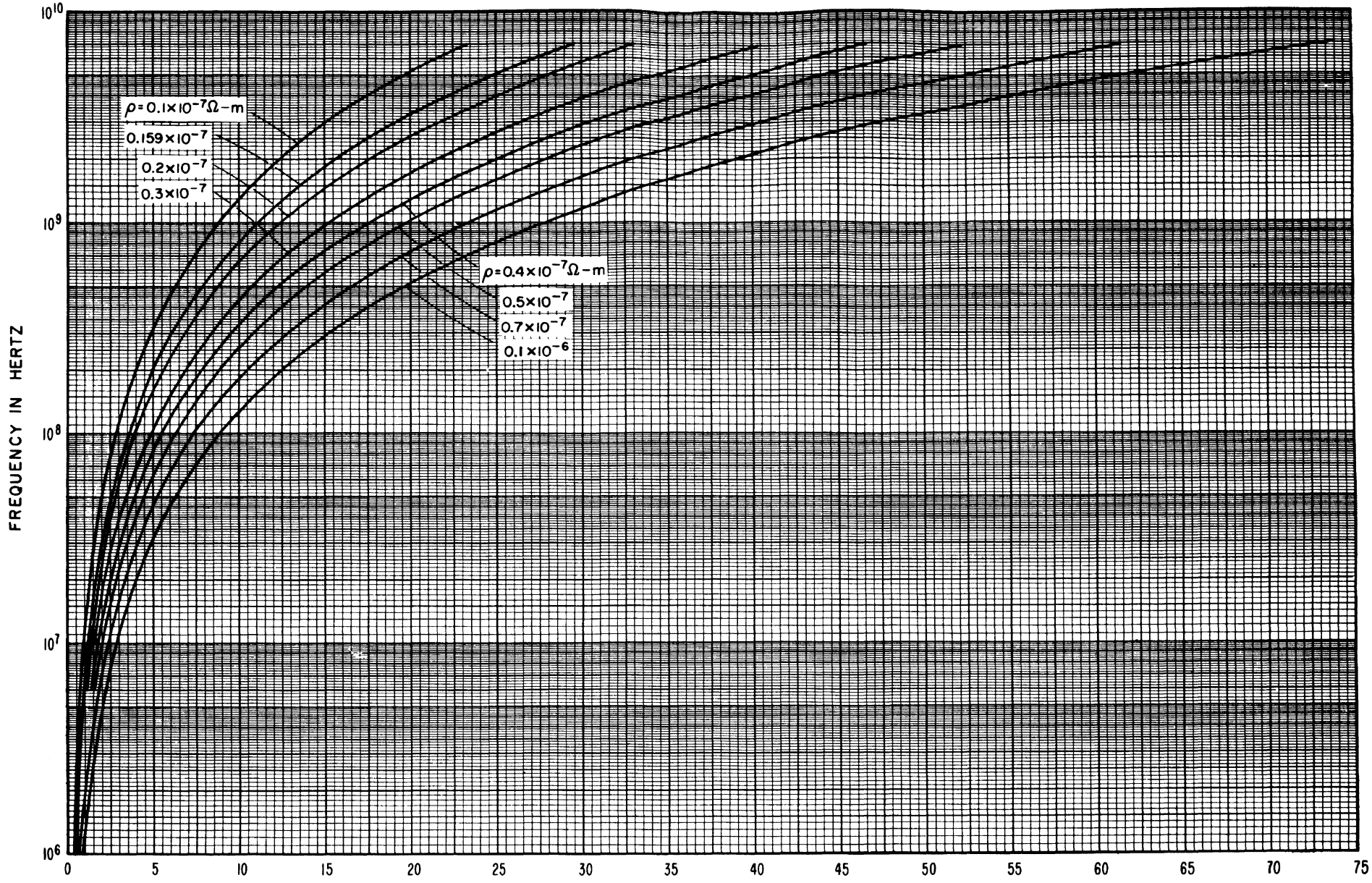

FIGURE 46. *Resistance per inch as a function of frequency for various values of ρ for line size #3.*

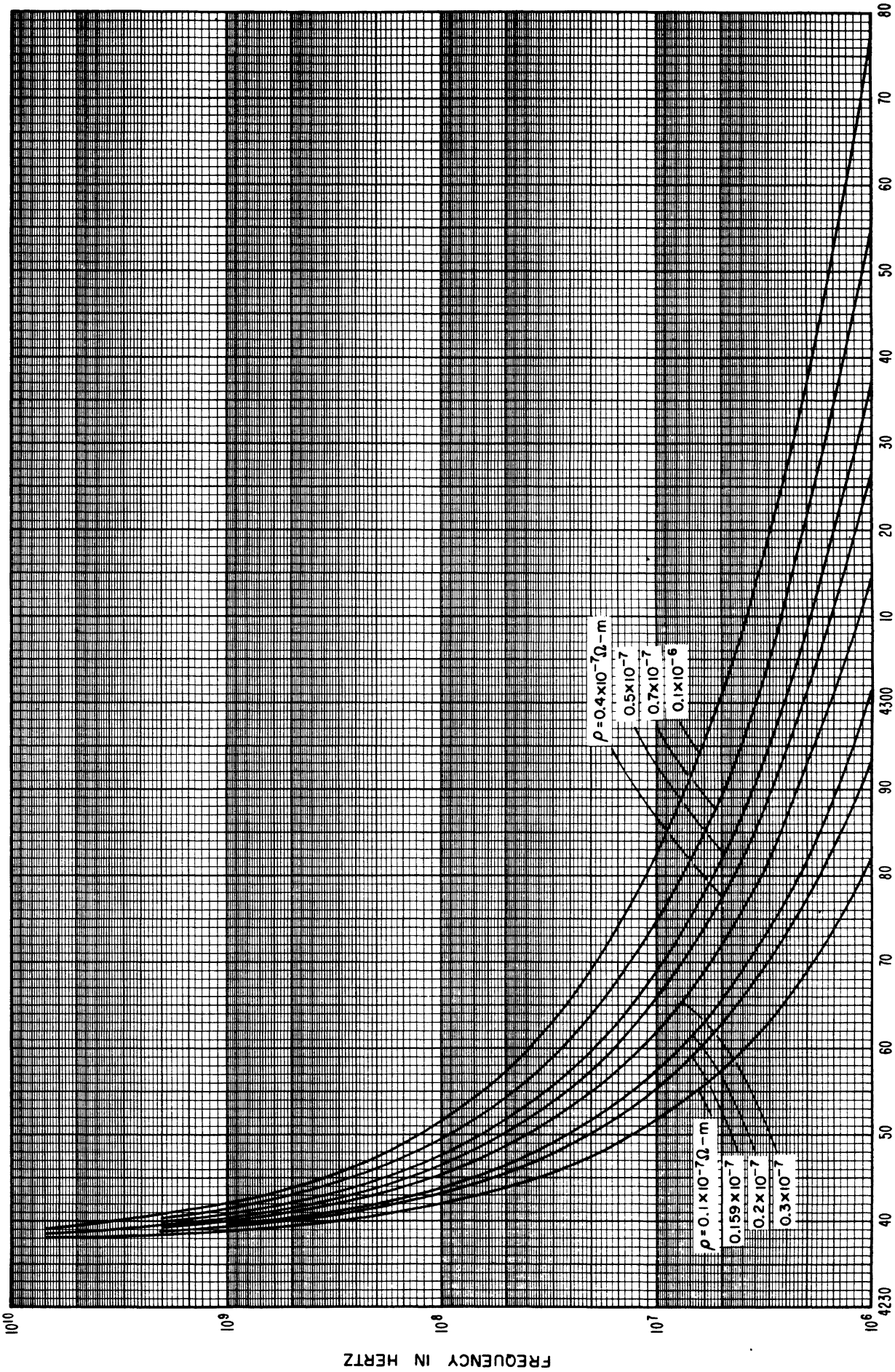

FIGURE 47. *Inductance per inch as a function of frequency for various values of ρ for line size #3.*

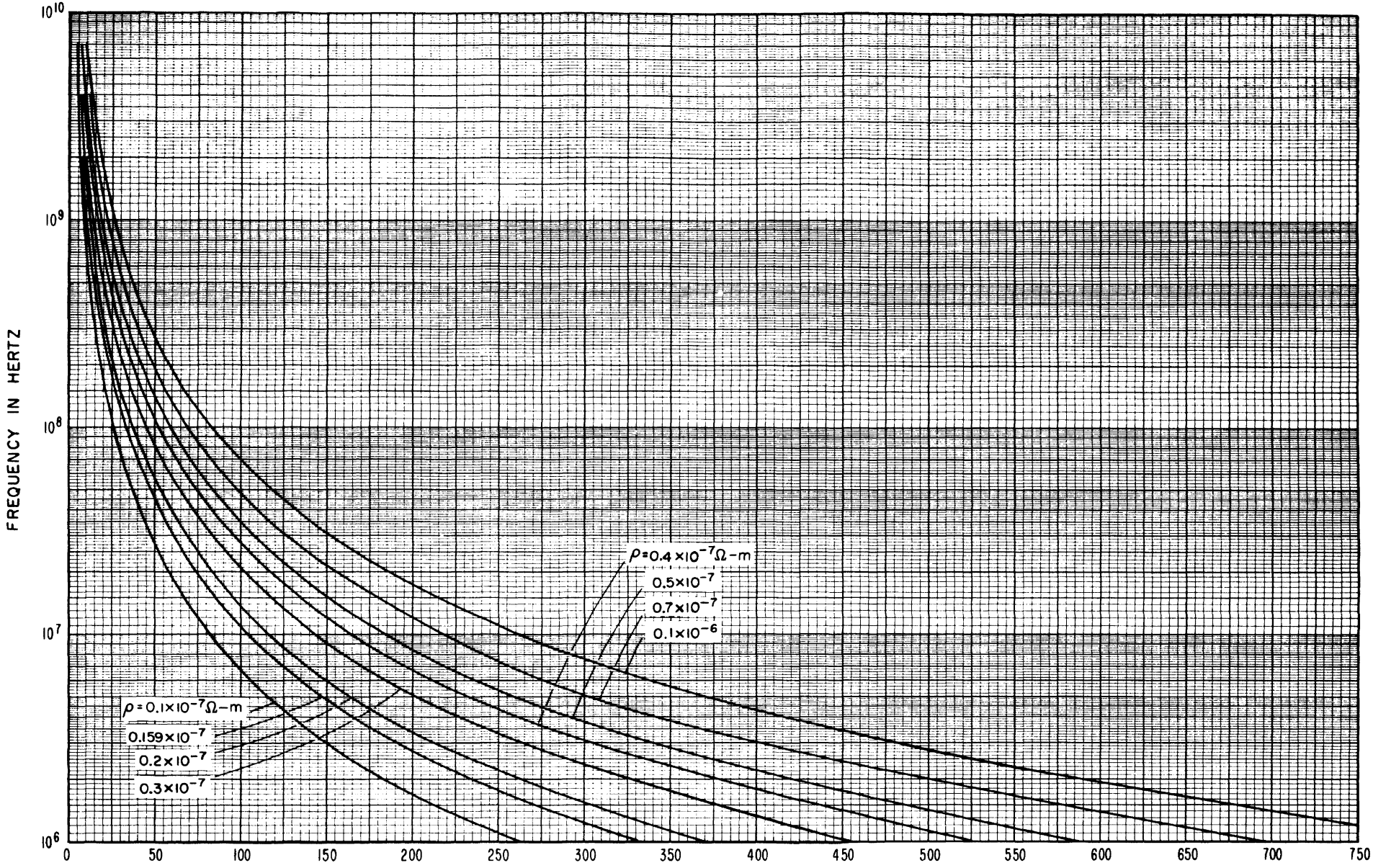

FIGURE 48. *Characteristic impedance magnitude (plotted as a deviation from 50.0 Ω) as a function of frequency for various values of ρ for line size #3.*

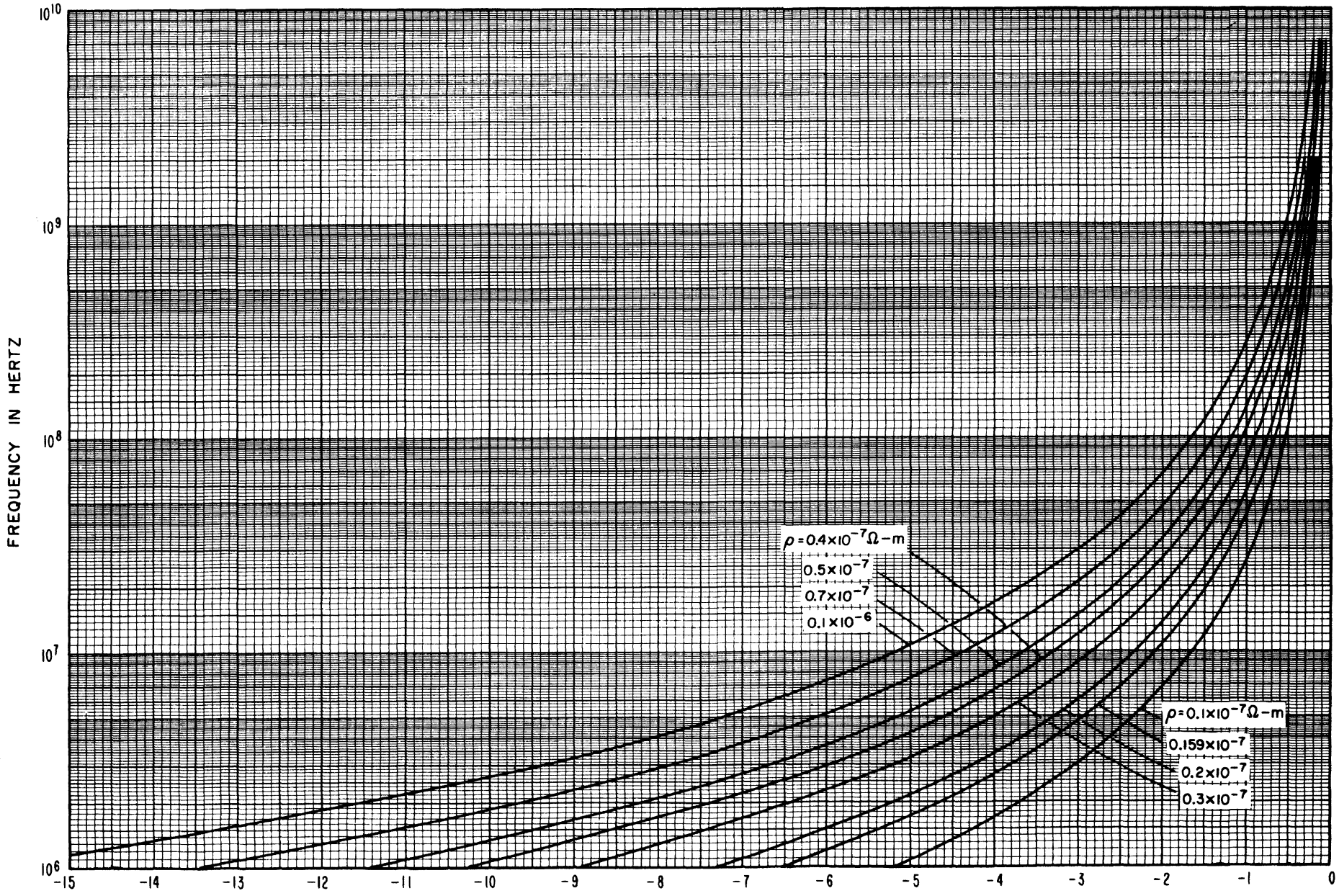

FIGURE 49. *Characteristic impedance phase angle as a function of frequency for various values of ρ for line size #3.*

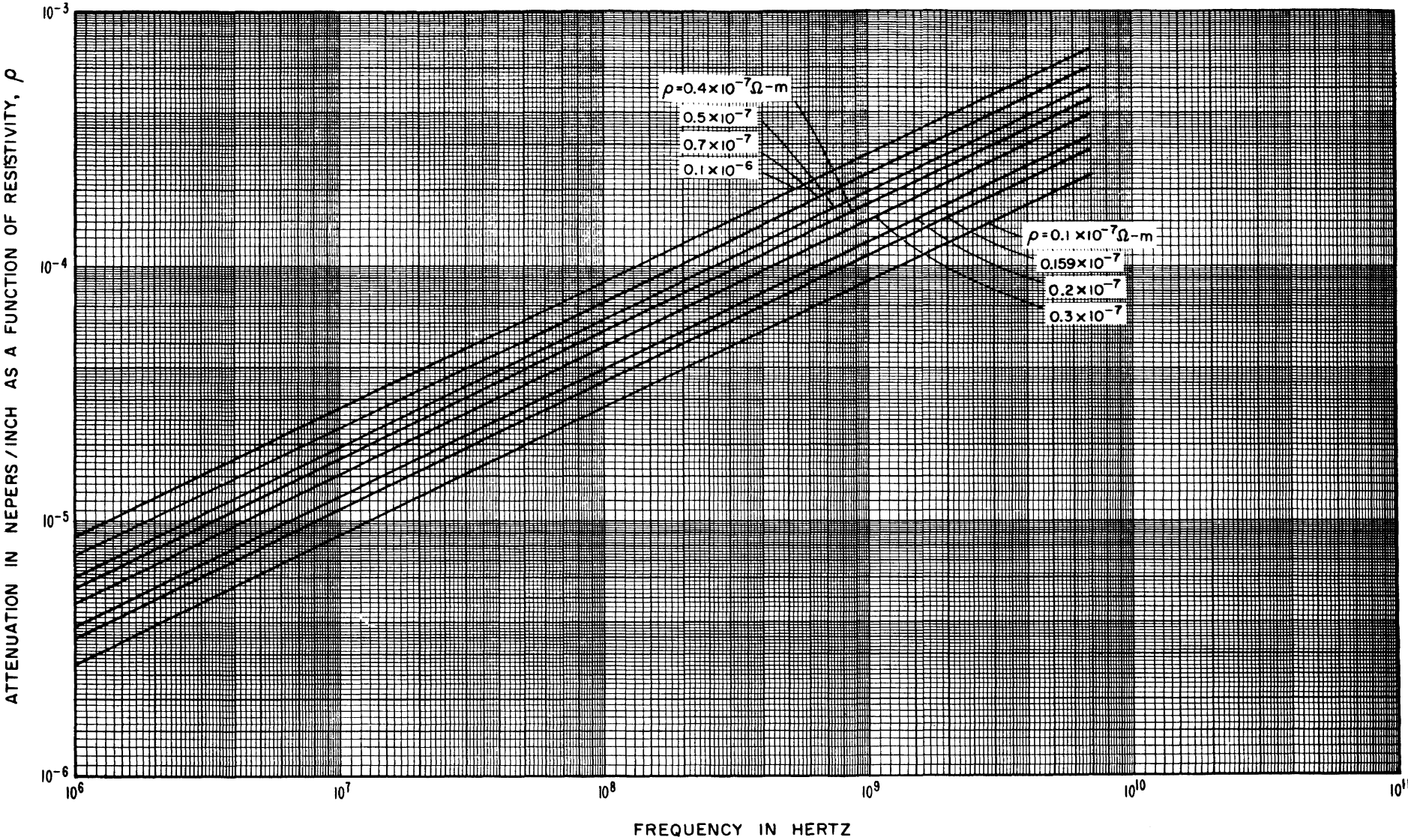

FIGURE 50. *Attenuation per inch as a function of frequency for various values of ρ for line size #3.*

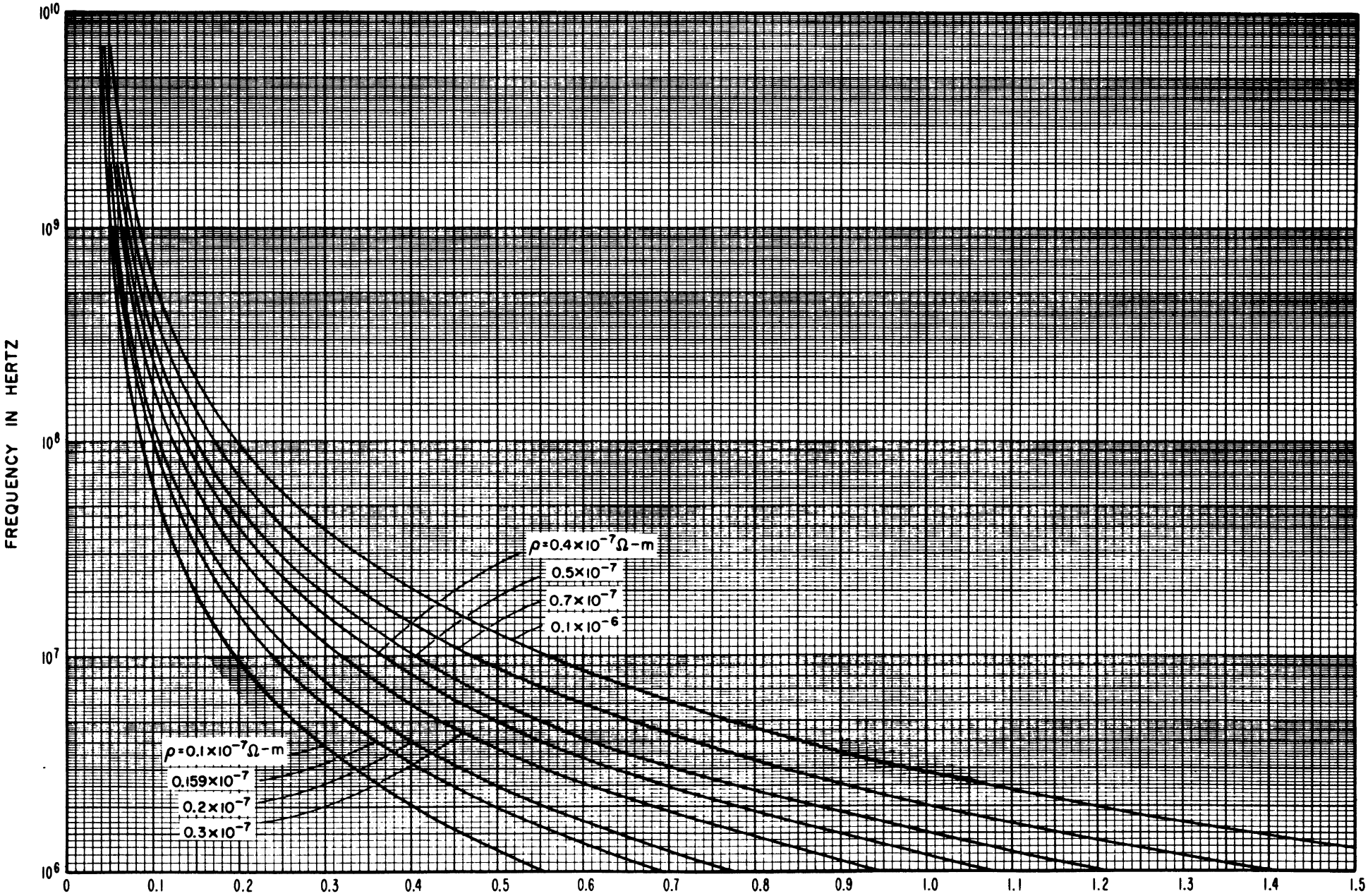

FIGURE 51. *Phase-shift per inch (plotted as a percent deviation from the free space value) as a function of frequency for various values of ρ for line size #3.*

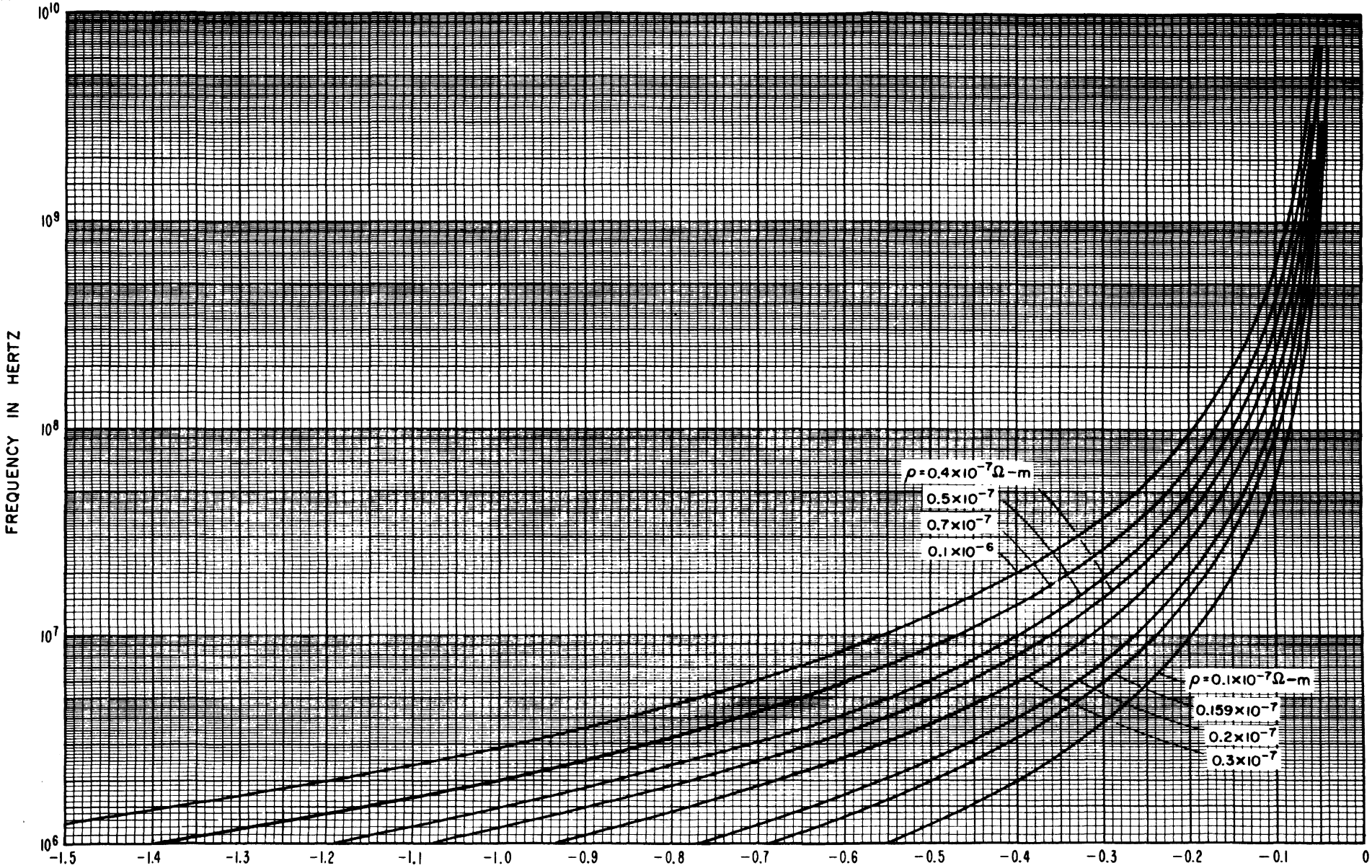

FIGURE 52. *Wavelength (plotted as a percent deviation from the free space value) as a function of frequency for various values of ρ for line size #3.*

Line size #3

Variations with relative dielectric constant, $\frac{\epsilon}{\epsilon_0}$

Constants used in calculations are the same as those used under standard conditions except that $\frac{\epsilon}{\epsilon_0}$ varies from 1.000400 to 1.000800.

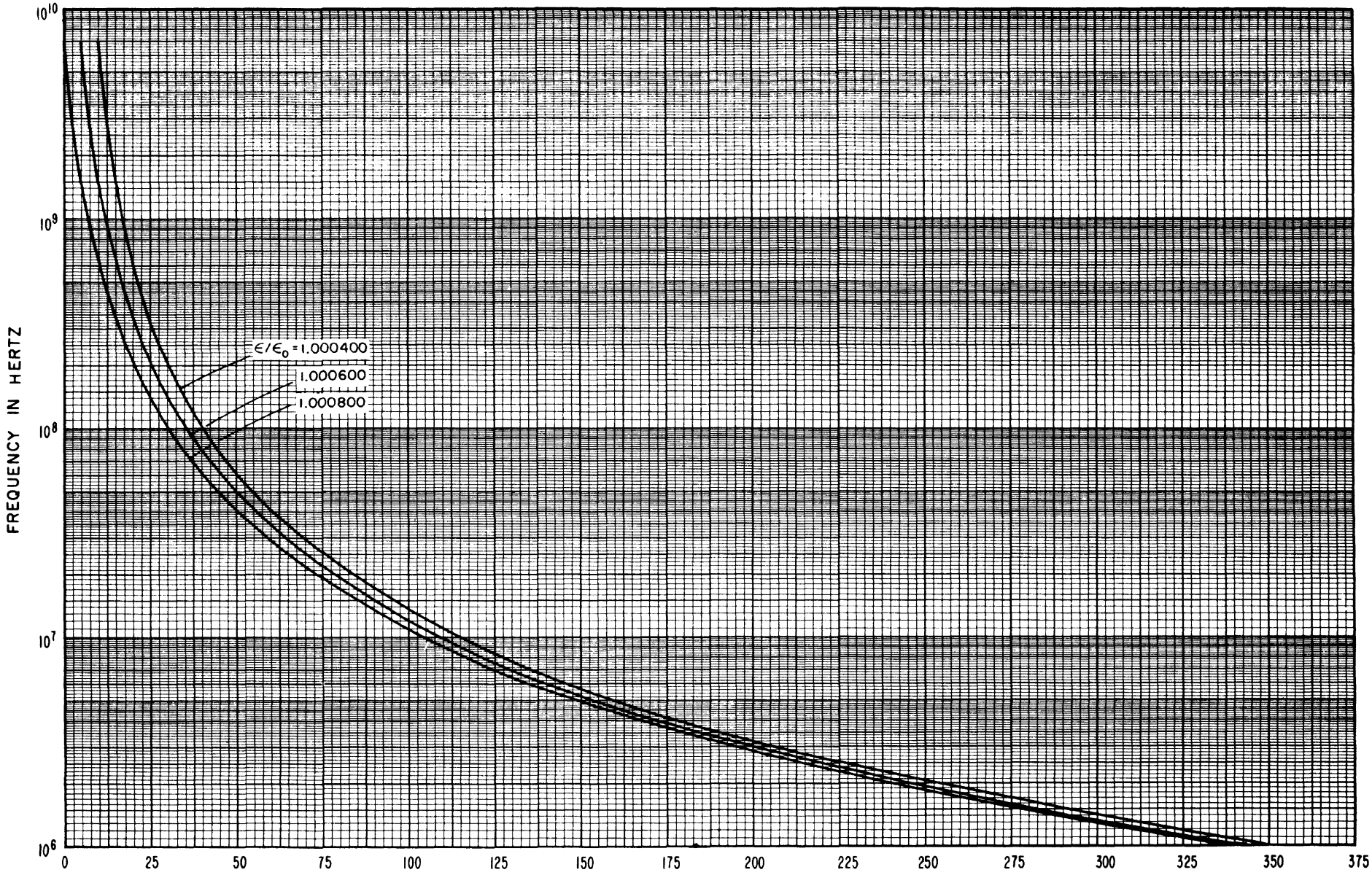

FIGURE 53. *Characteristic impedance magnitude (plotted as a deviation from 50.0 Ω) as a function of frequency for various values of* $\frac{\epsilon}{\epsilon_0}$ *for line size #3.*

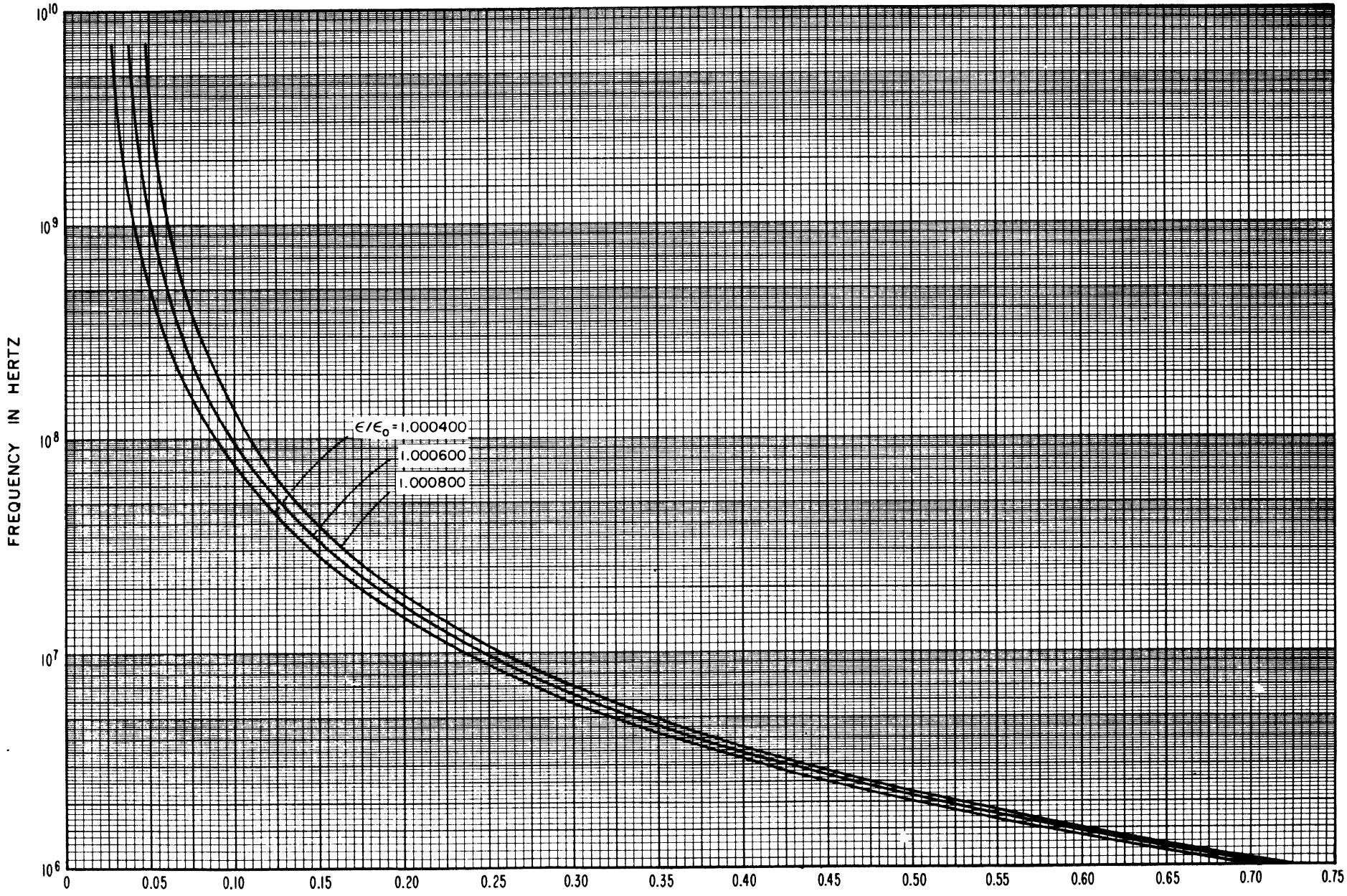

FIGURE 54. *Phase-shift per inch (plotted as a percent deviation from the free space value) as a function of frequency for various values of* $\frac{\epsilon}{\epsilon_0}$ *for line size #3.*

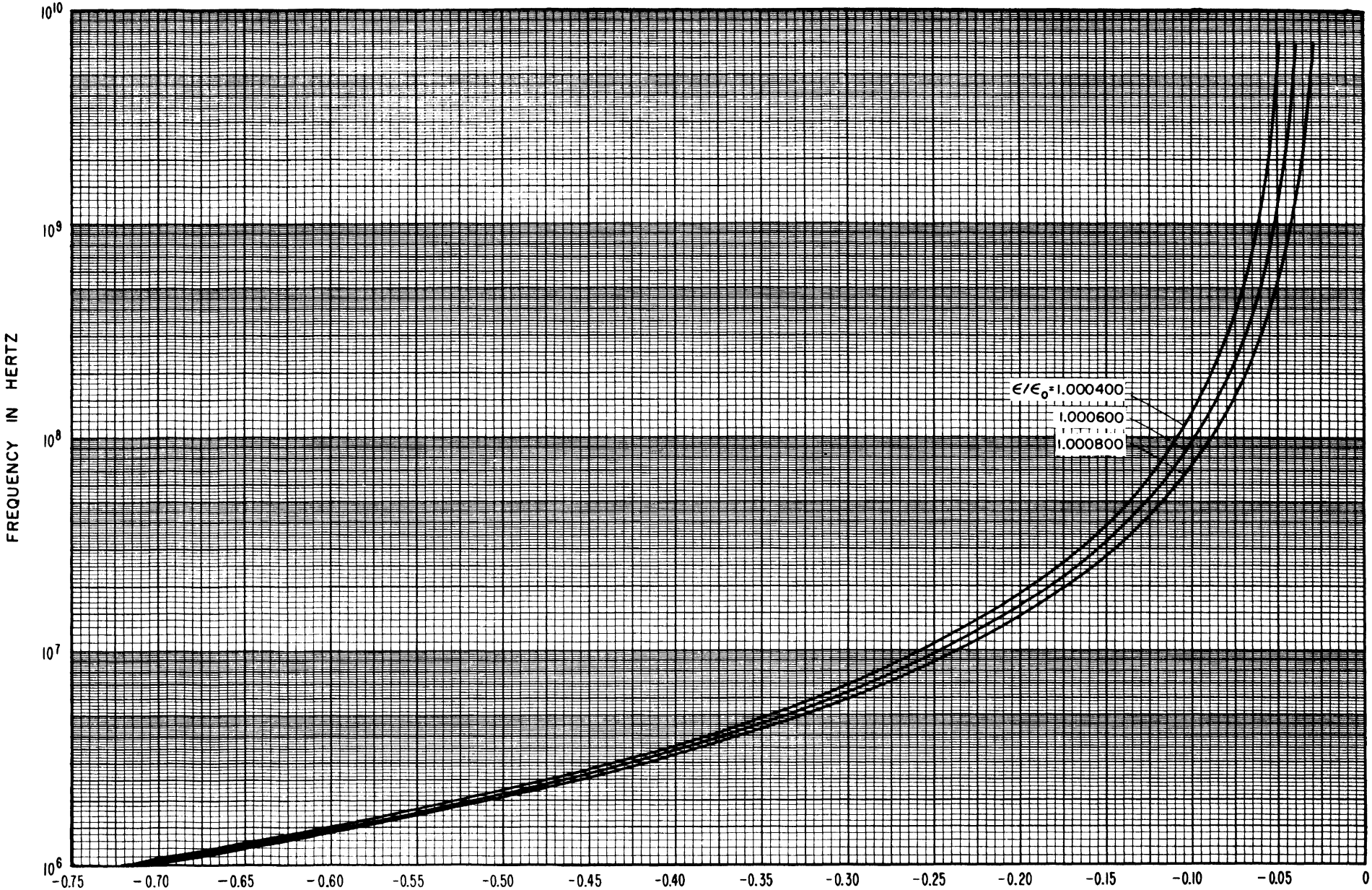

FIGURE 55. *Wavelength (plotted as a percent deviation from the free space value) as a function of frequency for various values of* $\frac{\epsilon}{\epsilon_0}$ *for line size #3.*

Line size #3
Variations with diameters a and b

Constants used in calculations are the same as those used under standard conditions except that a varies ± 0.0001 inch from standard conditions, and b varies ± 0.0002 inch from standard conditions.

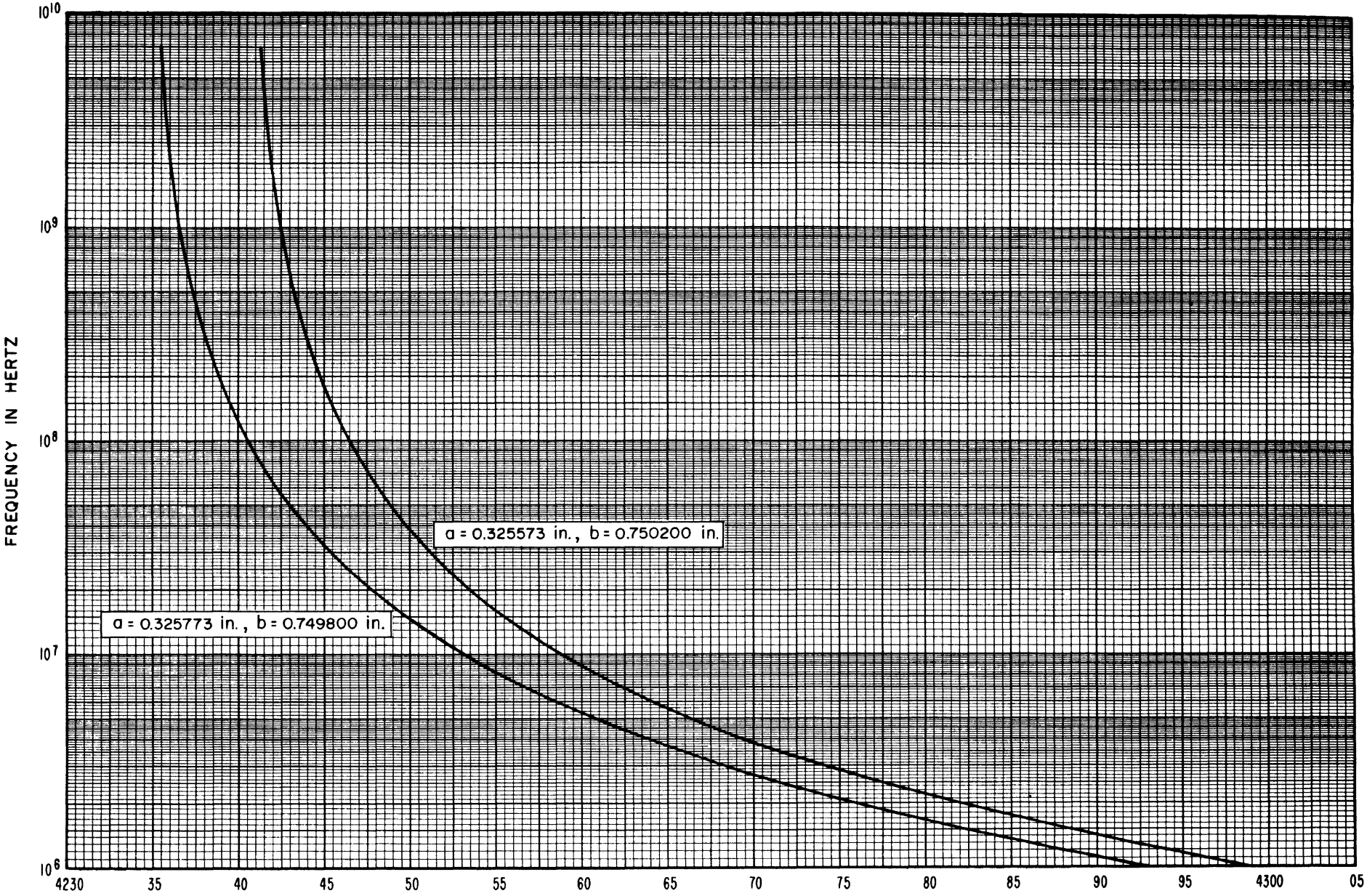

FIGURE 56. *Inductance per inch as a function of frequency for various values of diameters* a *and* b *for line size #3.*

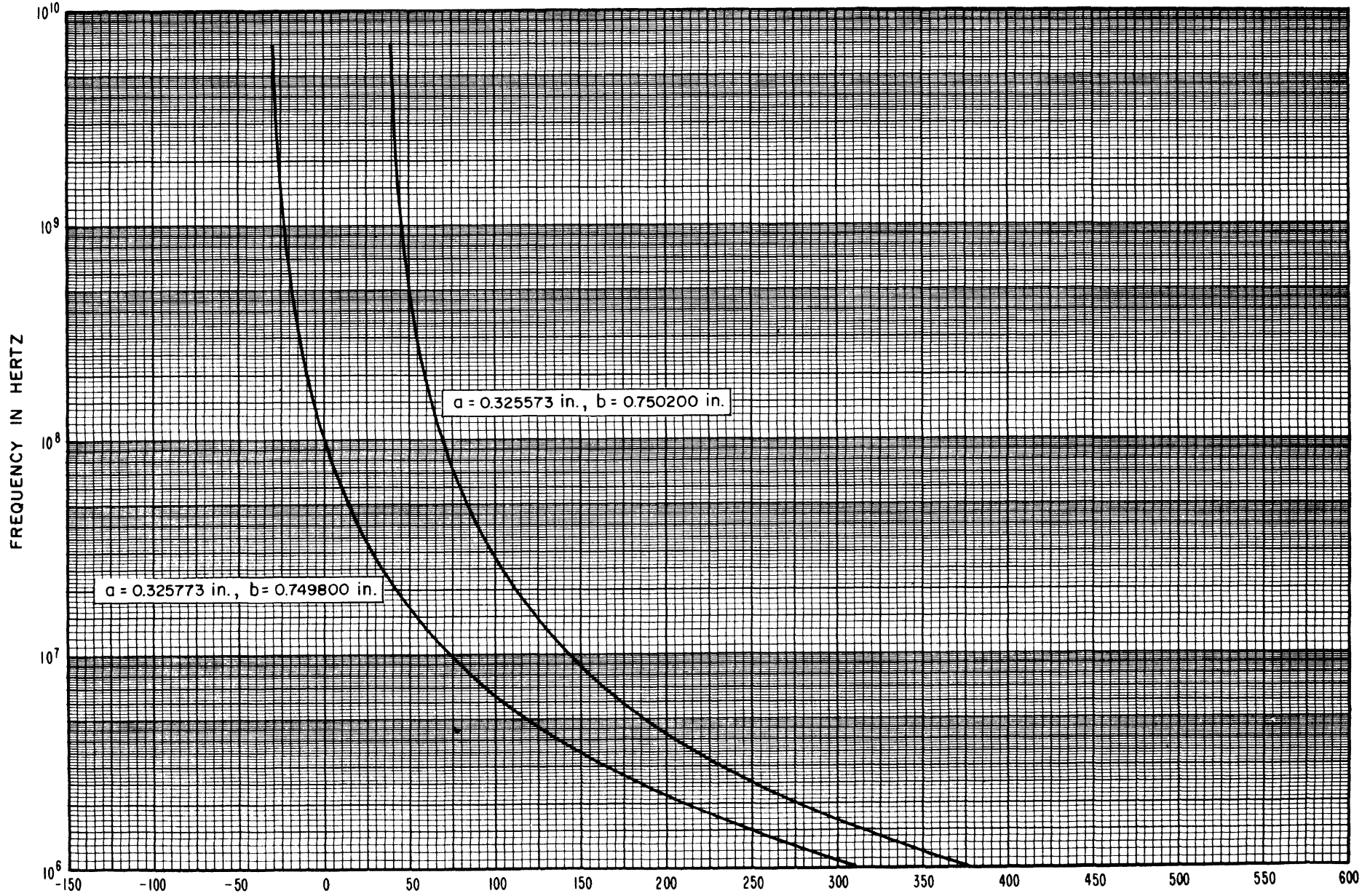

FIGURE 57. *Characteristic impedance magnitude (plotted as a deviation from 50.0 Ω) as a function of frequency for various values of diameters* a *and* b *for line size #3.*

Line size #4
Standard conditions

Constants used in calculations:

$a = 0.359010$ inch

$b = 0.826772$ inch

$\rho_i = \rho_0 = 0.17241 \times 10^{-7}$ ohm-meters

$\mu_{ci} = \mu_{co} = \mu_d = 4\pi \times 10^{-7}$ henry/meter

$\frac{\epsilon}{\epsilon_0} = 1.000649$

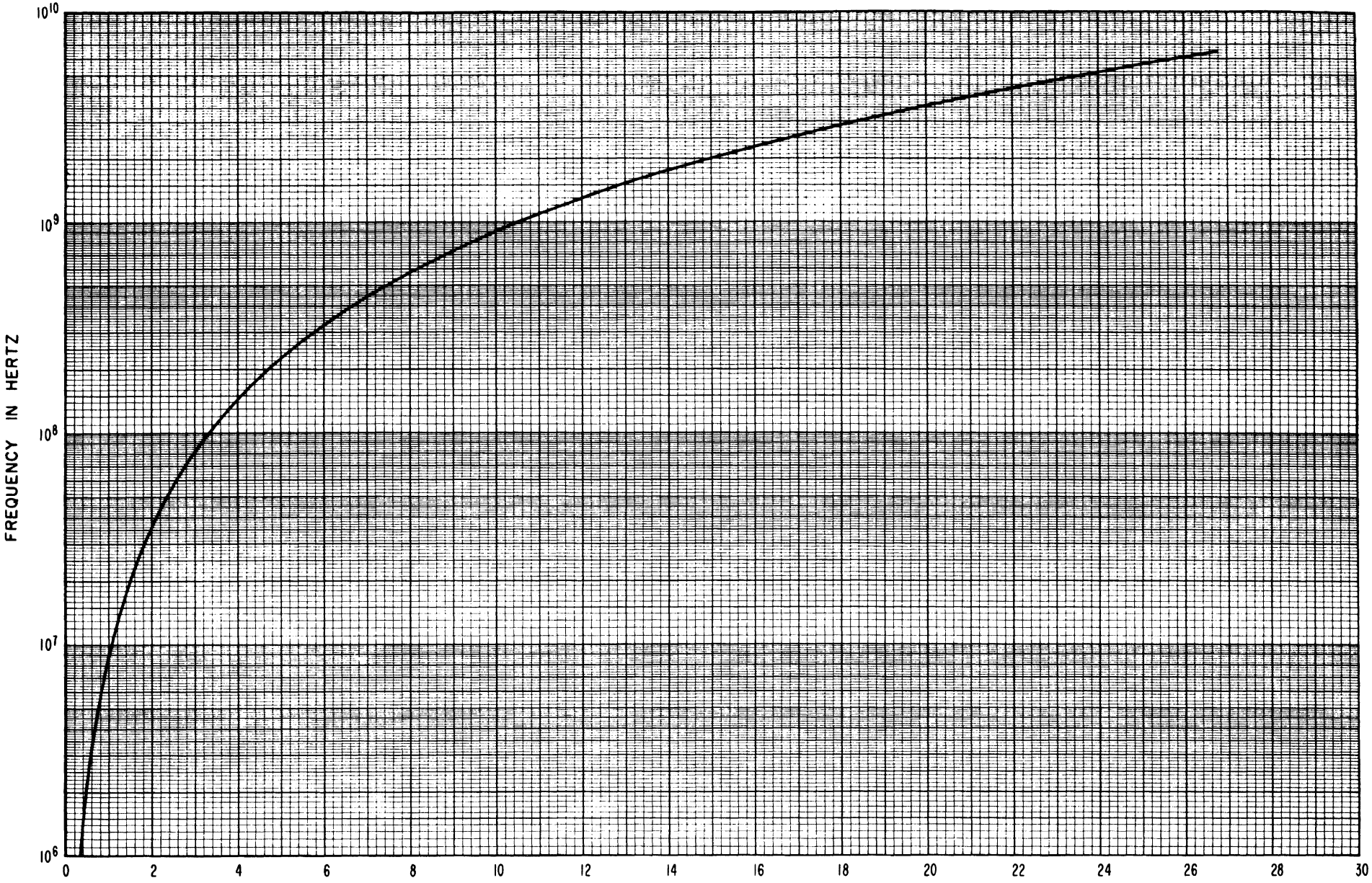

FIGURE 58. *Resistance per inch as a function of frequency under standard conditions for line size #4.*

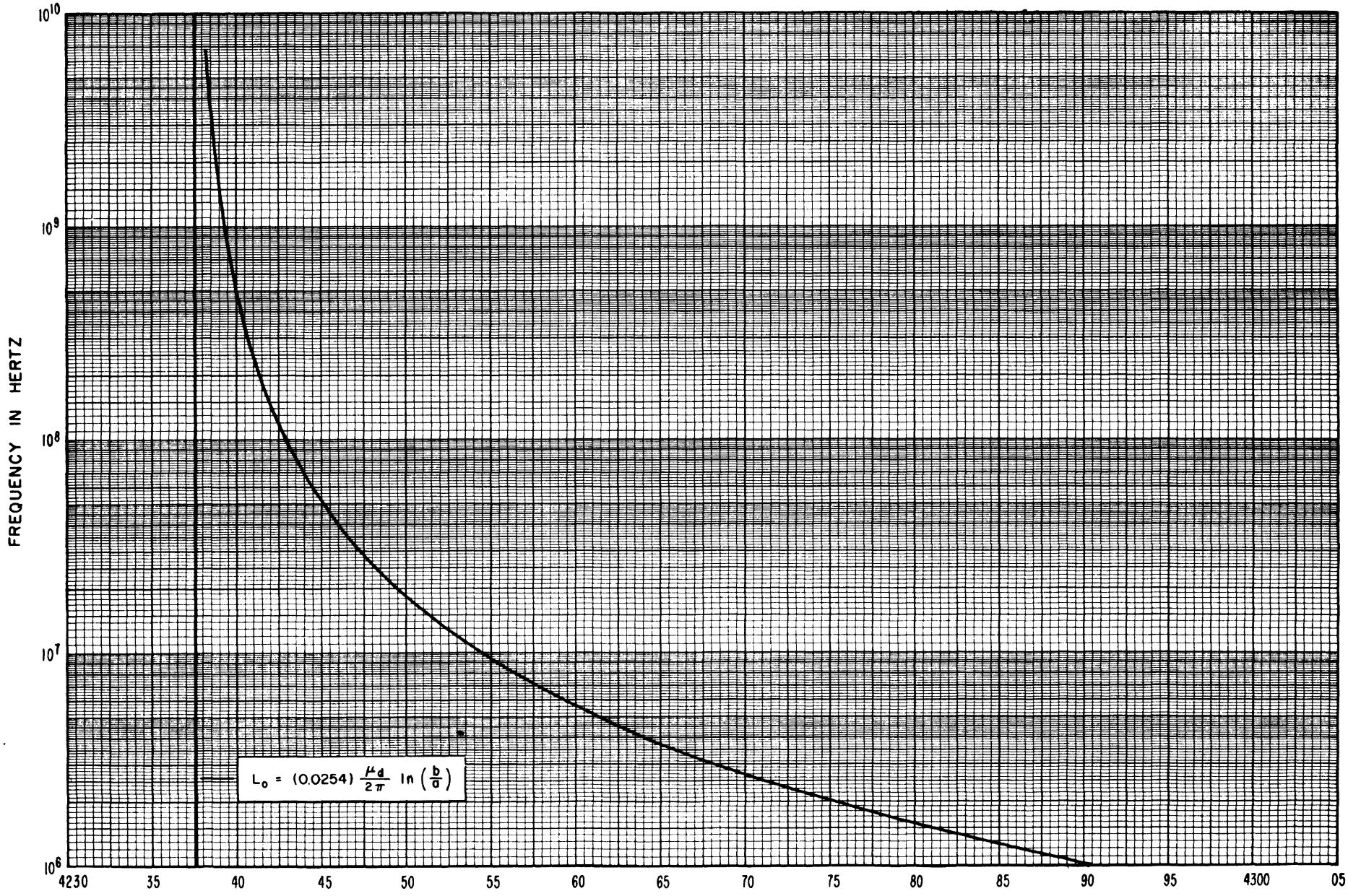

FIGURE 59. *Inductance per inch as a function of frequency under standard conditions for line size #4.*

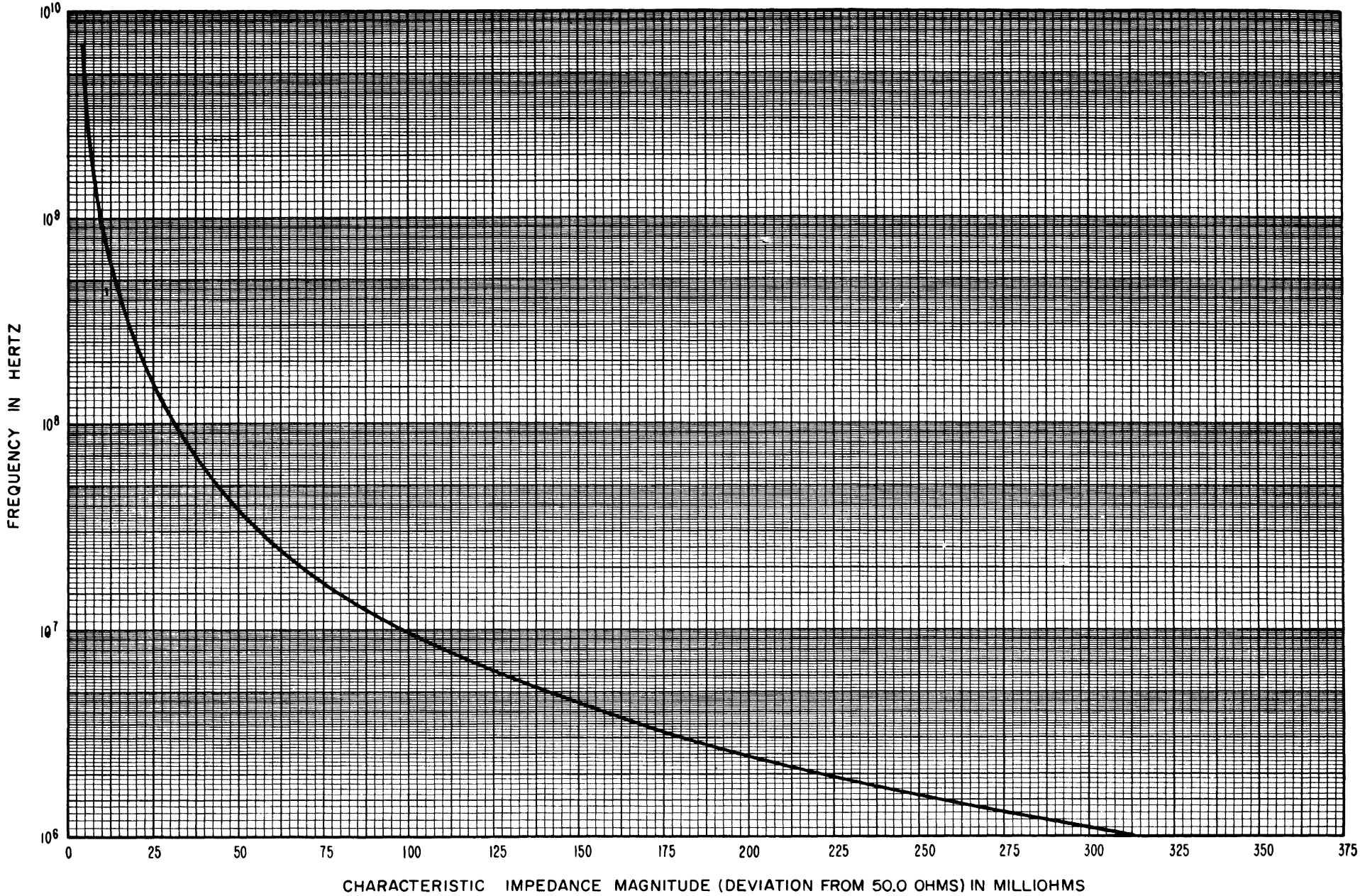

FIGURE 60. *Characteristic impedance magnitude (plotted as a deviation from 50.0 Ω) as a function of frequency under standard conditions for line size #4.*

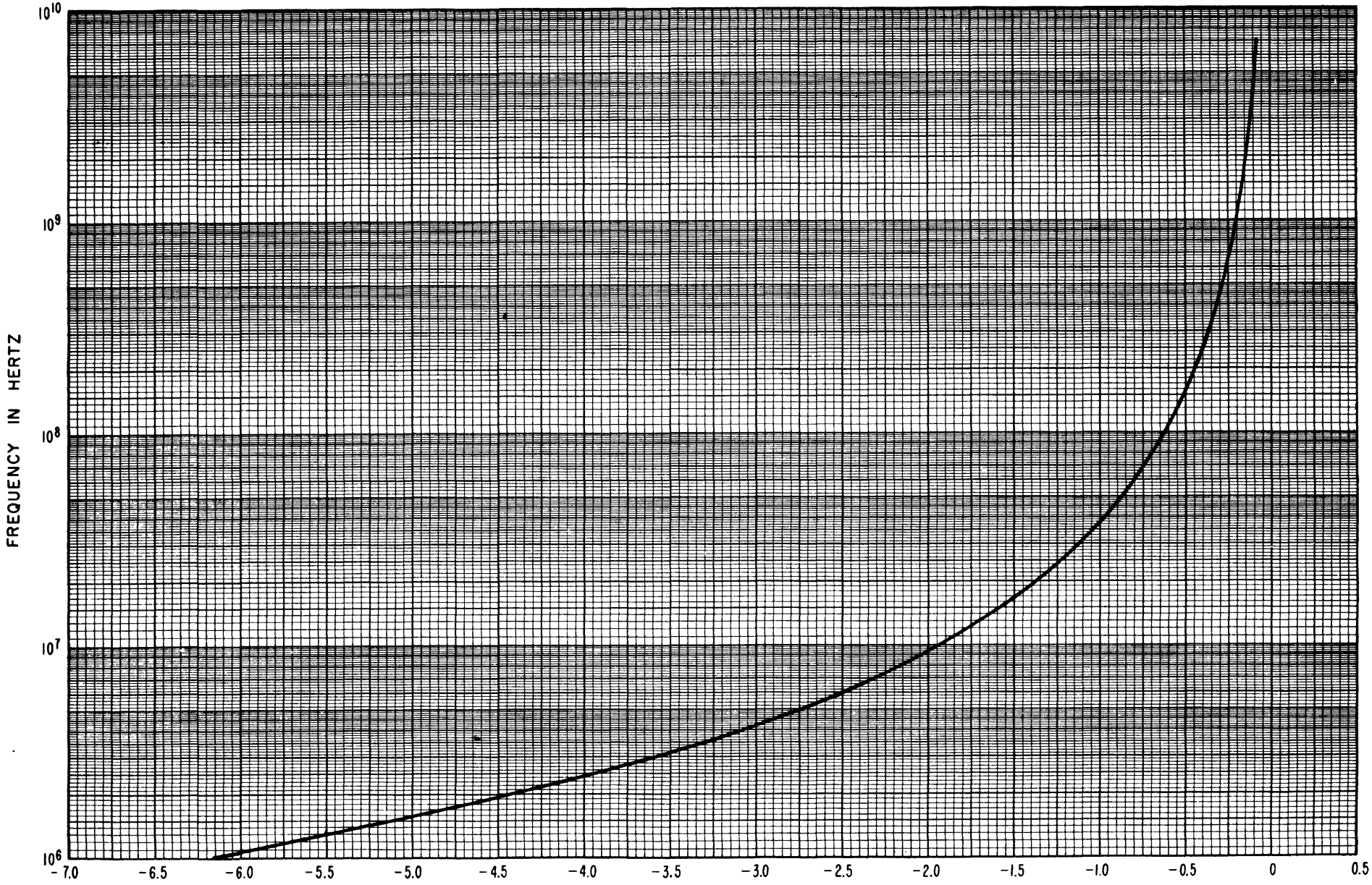

FIGURE 61. *Characteristic impedance phase angle as a function of frequency under standard conditions for line size #4.*

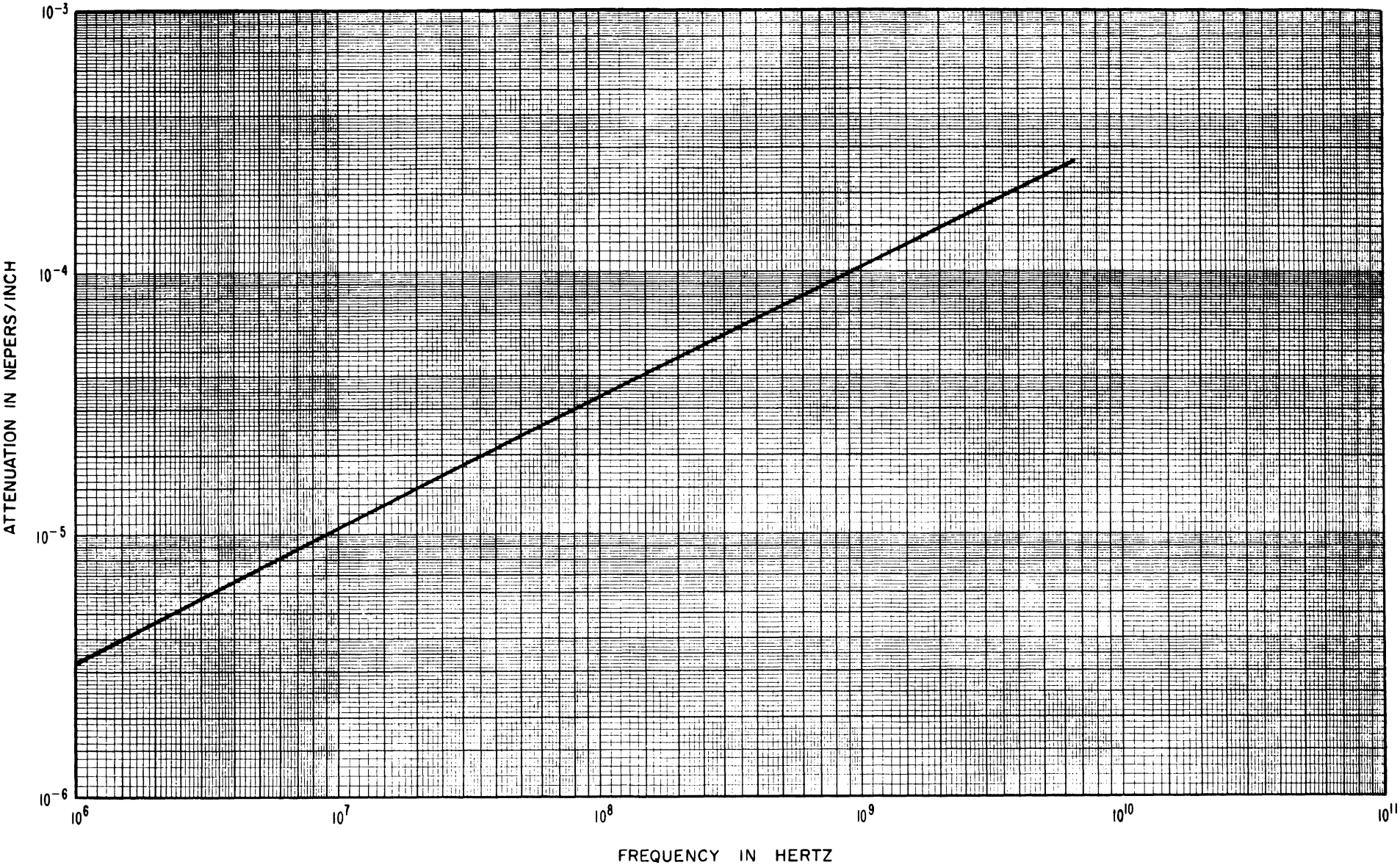

FIGURE 62. *Attenuation per inch as a function of frequency under standard conditions for line size #4.*

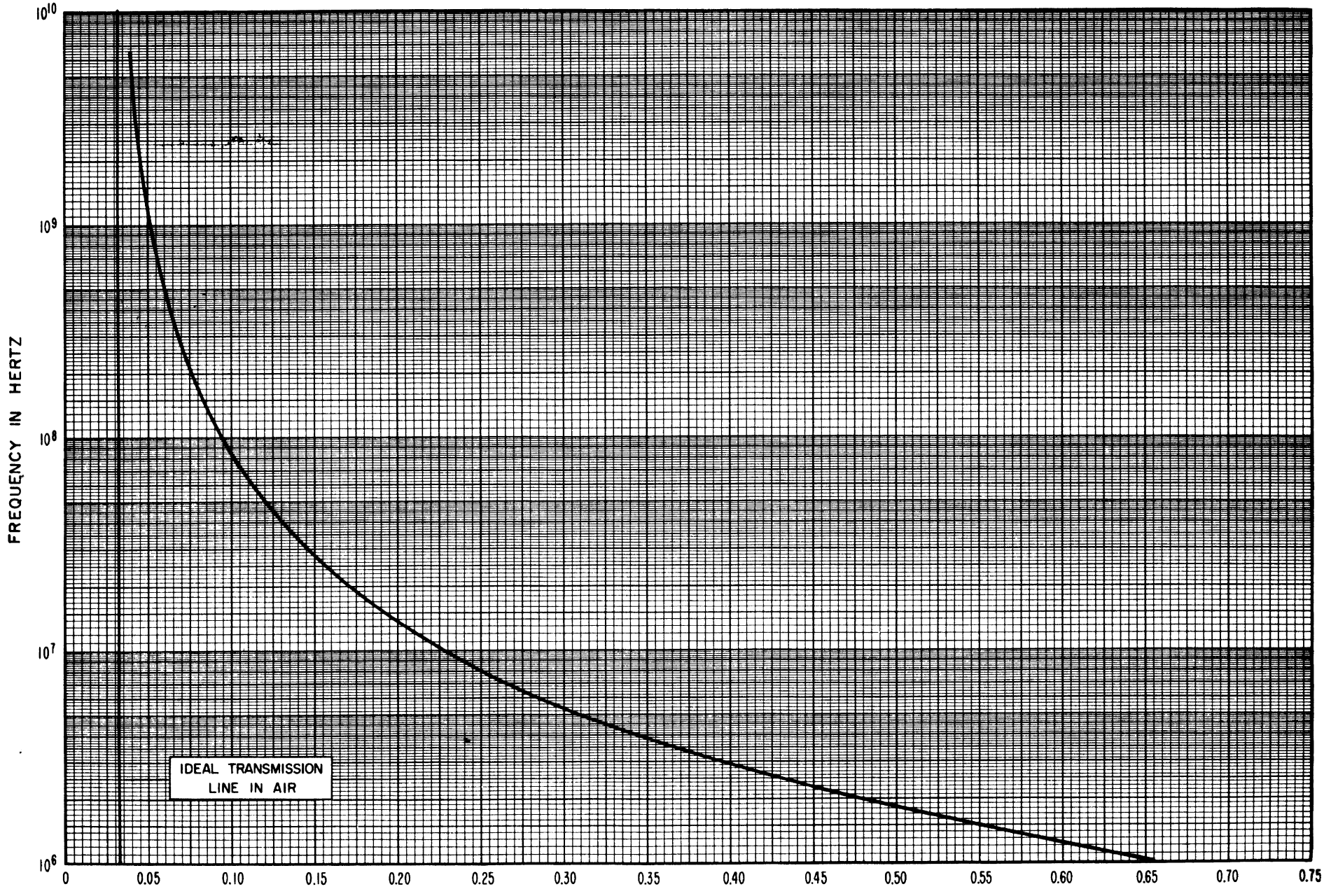

FIGURE 63. *Phase-shift per inch (plotted as a percent deviation from the free space value) as a function of frequency under standard conditions for line size #4.*

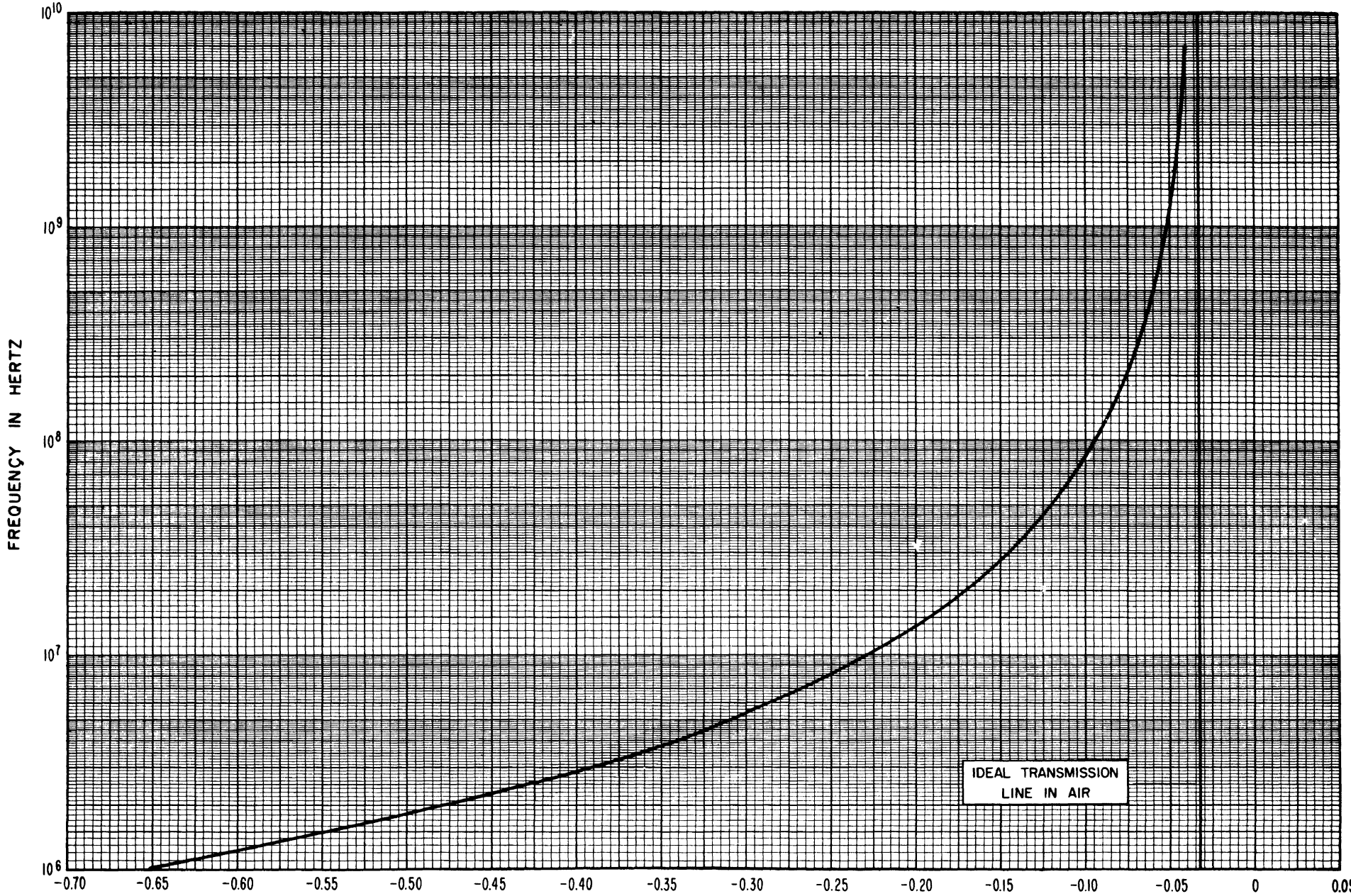

FIGURE 64. *Wavelength (plotted as a percent deviation from the free space value) as a function of frequency under standard conditions for line size #4.*

Line size #4
Variations with resistivity, ρ

Constants used in calculations are the same as those used under standard conditions except that $\rho_i (= \rho_0)$ varies from 0.1×10^{-7} to 0.1×10^{-6} ohm-meters.

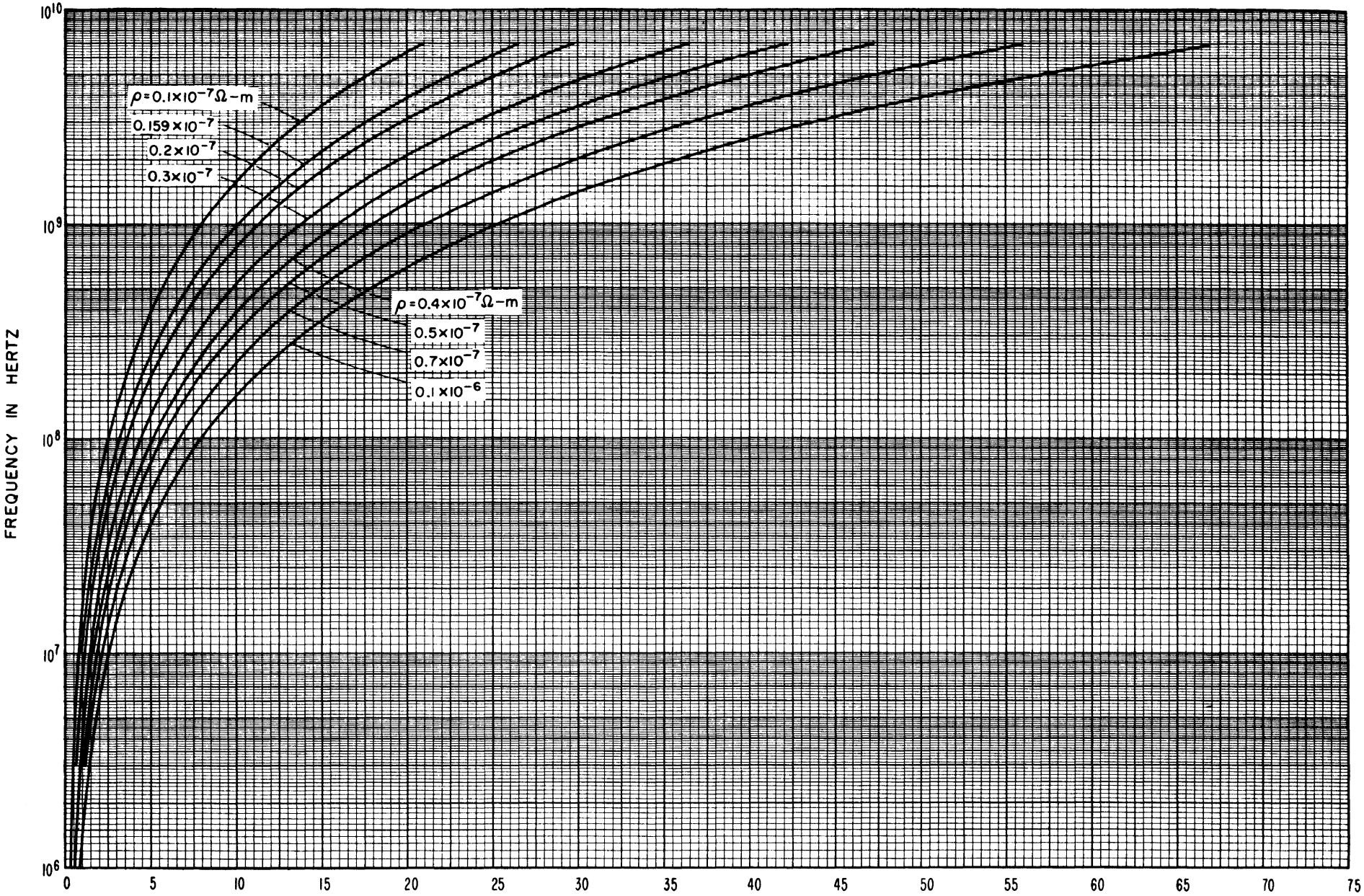

FIGURE 65. *Resistance per inch as a function of frequency for various values of ρ for line size #4.*

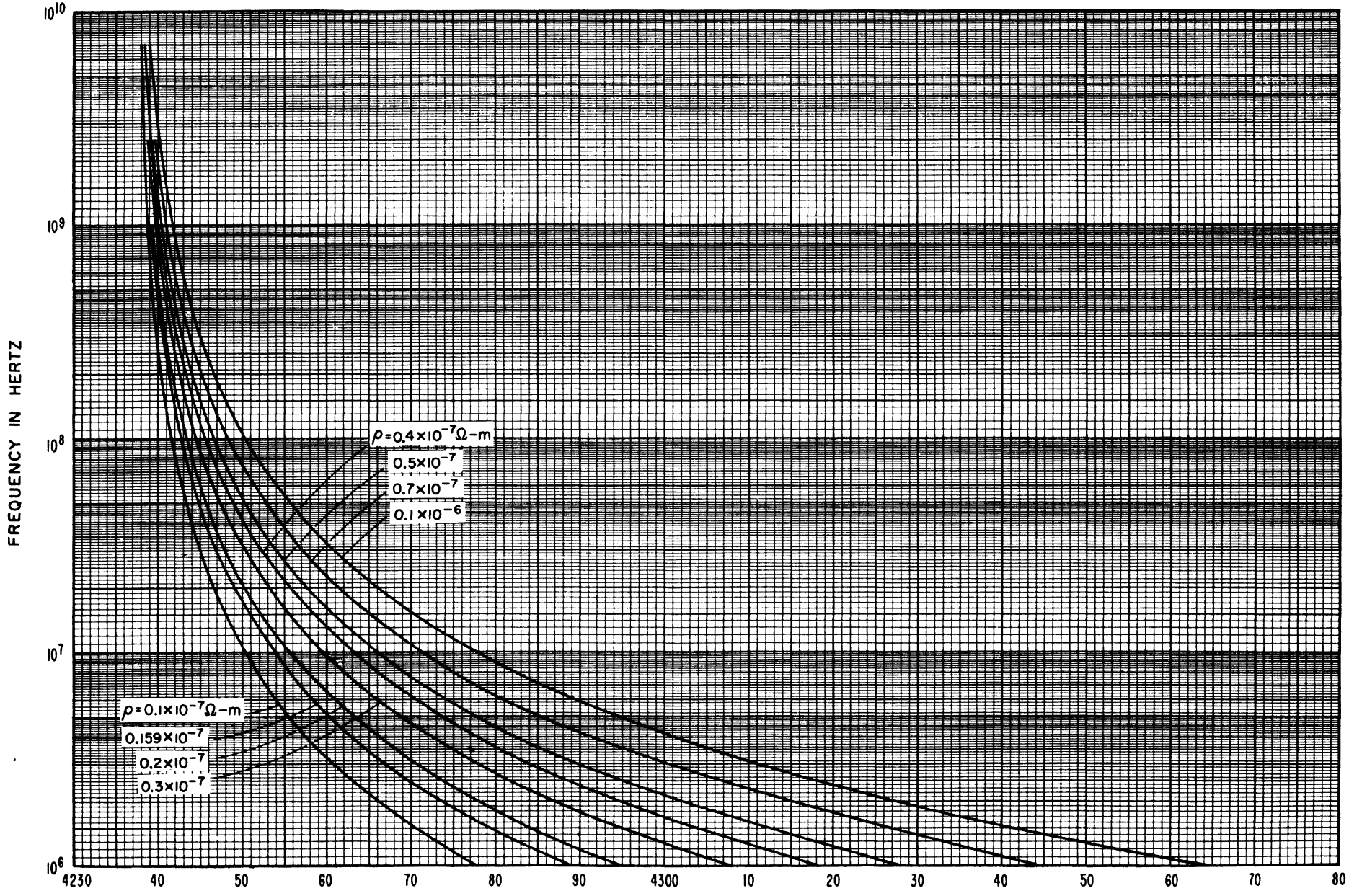

FIGURE 66. *Inductance per inch as a function of frequency for various values of ρ for line size #4.*

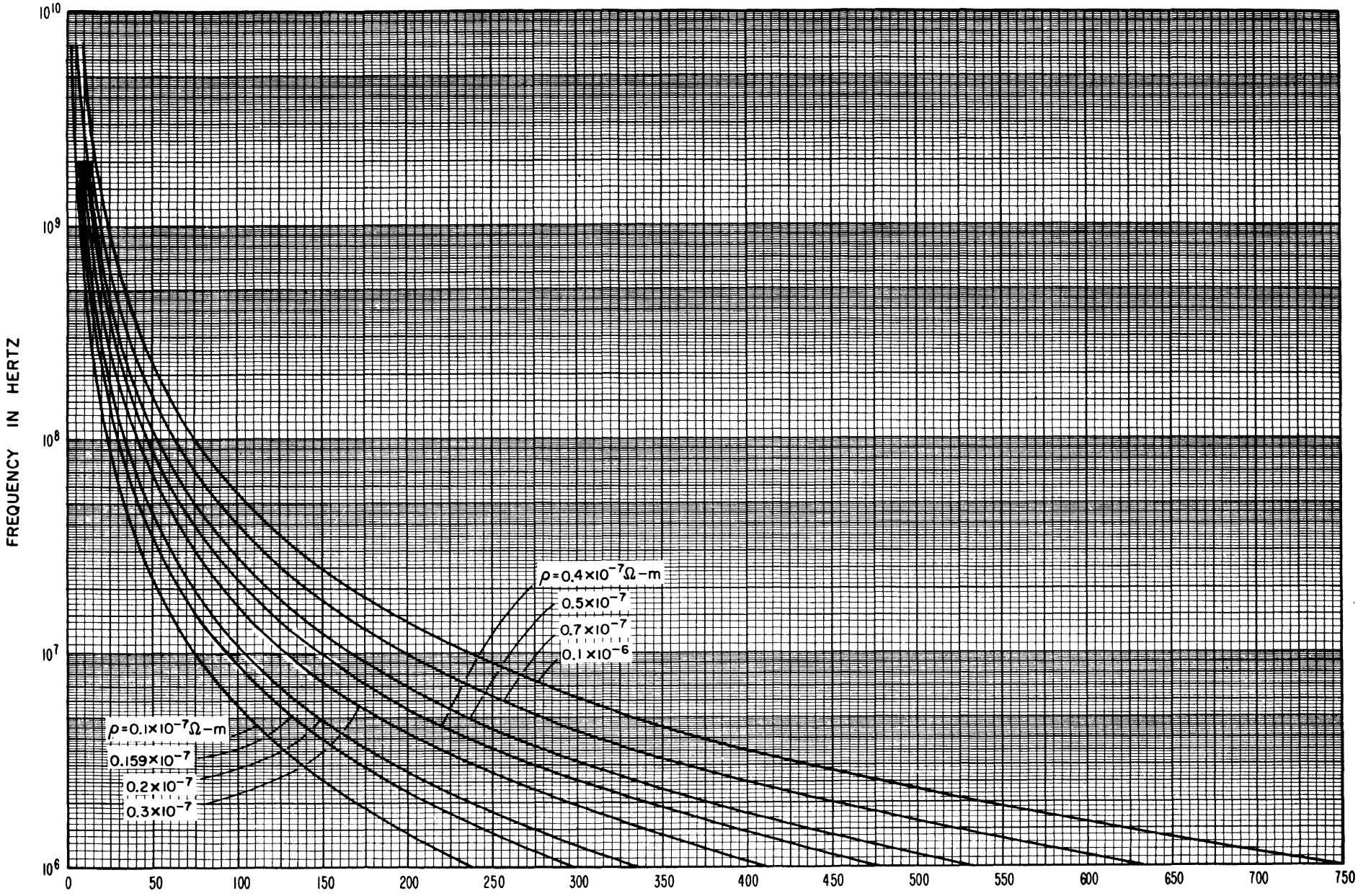

FIGURE 67. *Characteristic impedance magnitude (plotted as a deviation from 50.0 Ω) as a function of frequency for various values of ρ for line size #4.*

218-445 O-66—7

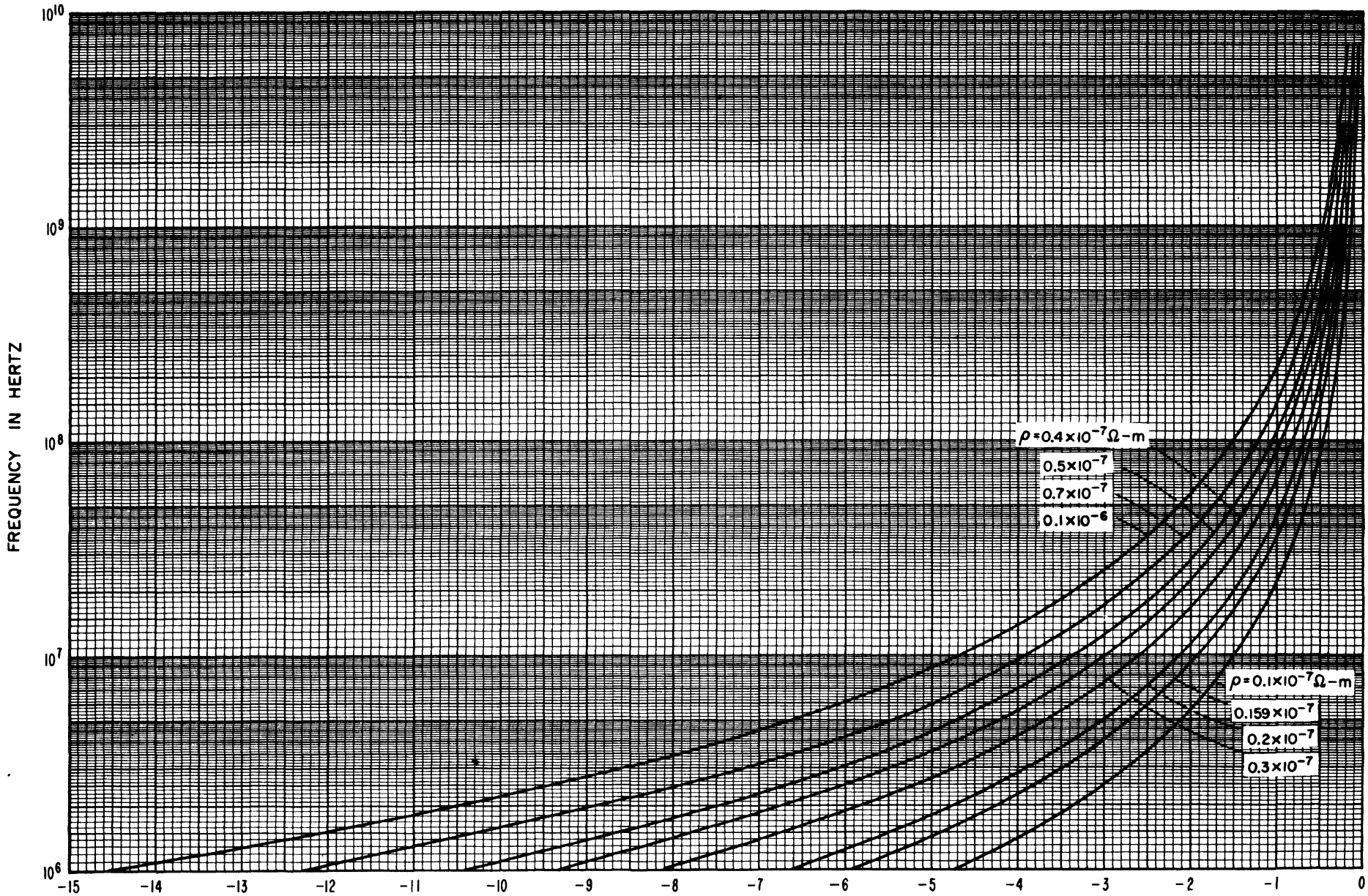

FIGURE 68. *Characteristic impedance phase angle as a function of frequency for various values of ρ for line size #4.*

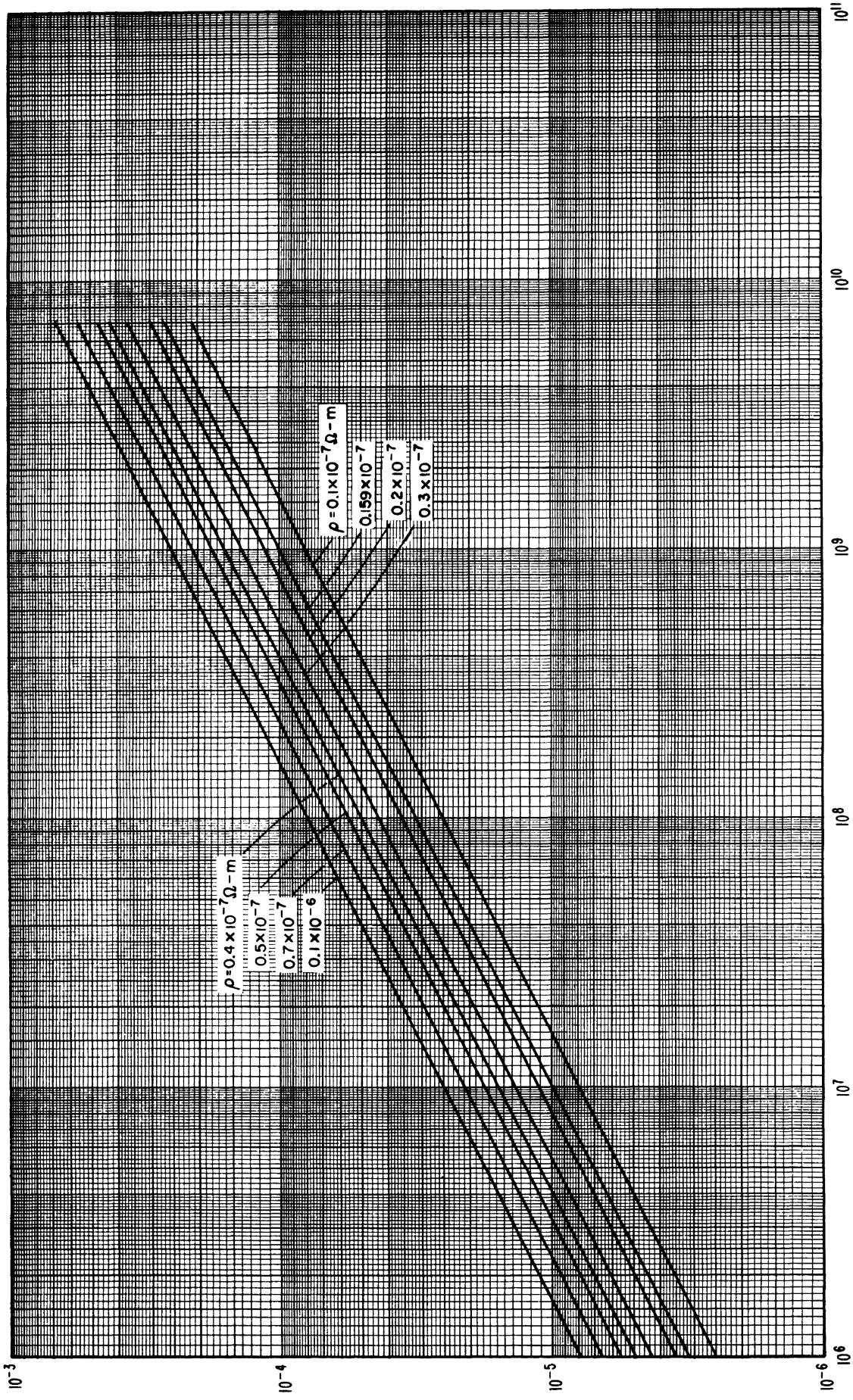

FIGURE 69. *Attenuation per inch as a function of frequency for various values of ρ for line size #4.*

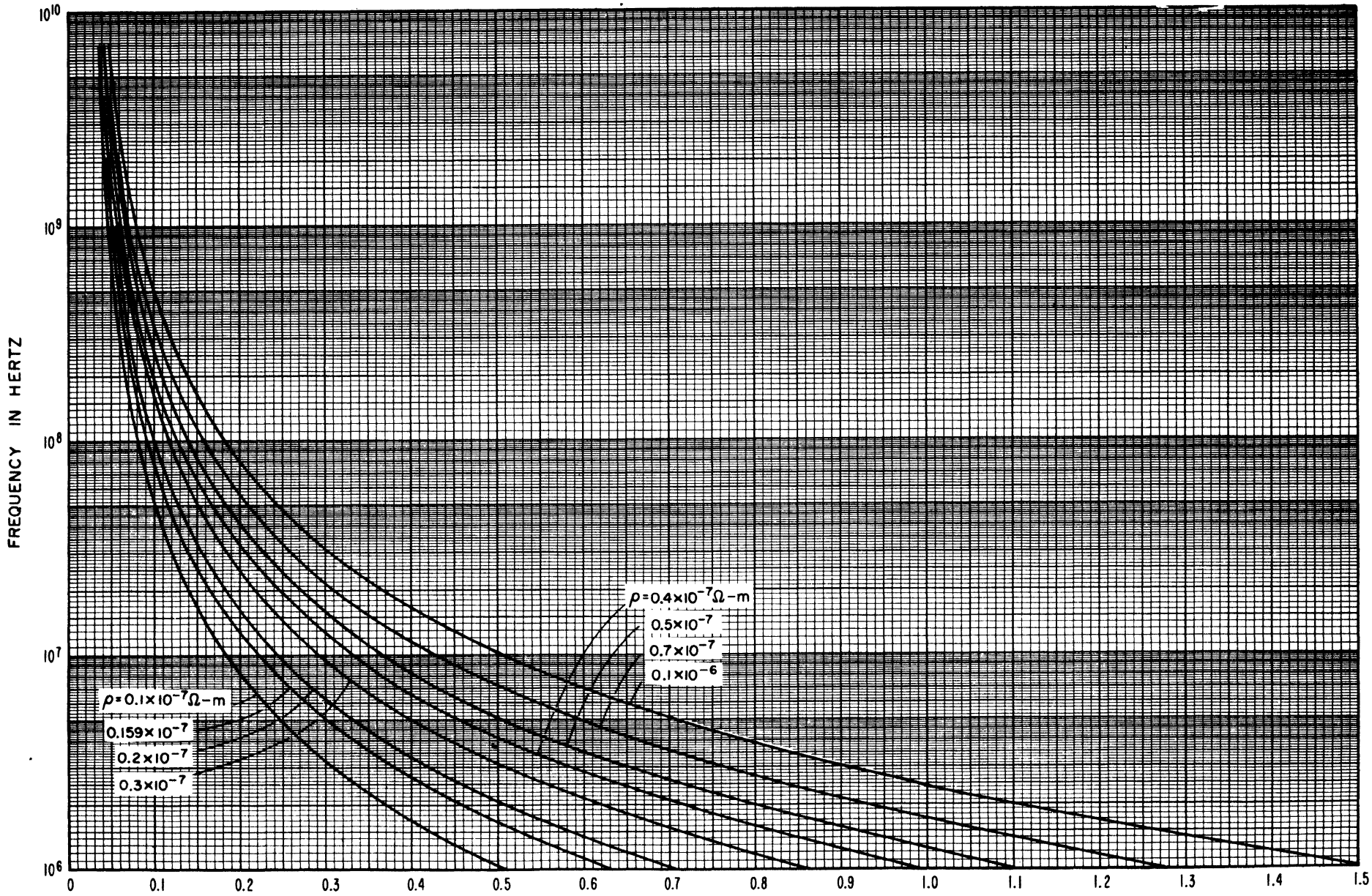

FIGURE 70. *Phase-shift per inch (plotted as a percent deviation from the free space value) as a function of frequency for various values of ρ for line size #4.*

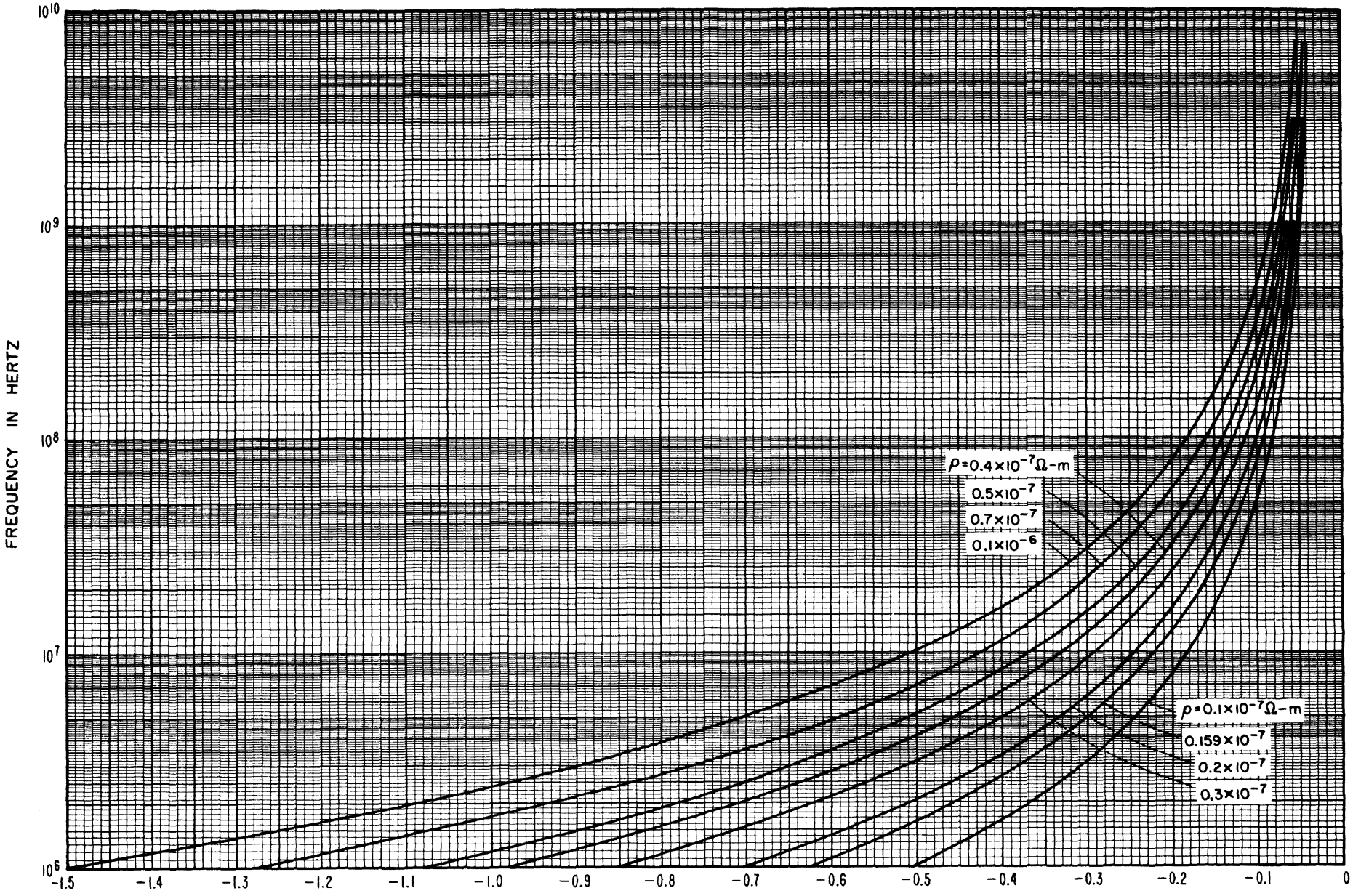

FIGURE 71. *Wavelength (plotted as a percent deviation from the free space value) as a function of frequency for various values of ρ for line size #4.*

Line size #4

Variations with relative dielectric constant, $\frac{\epsilon}{\epsilon_0}$

Constants used in calculations are the same as those used under standard conditions except that $\frac{\epsilon}{\epsilon_0}$ varies from 1.000400 to 1.000800.

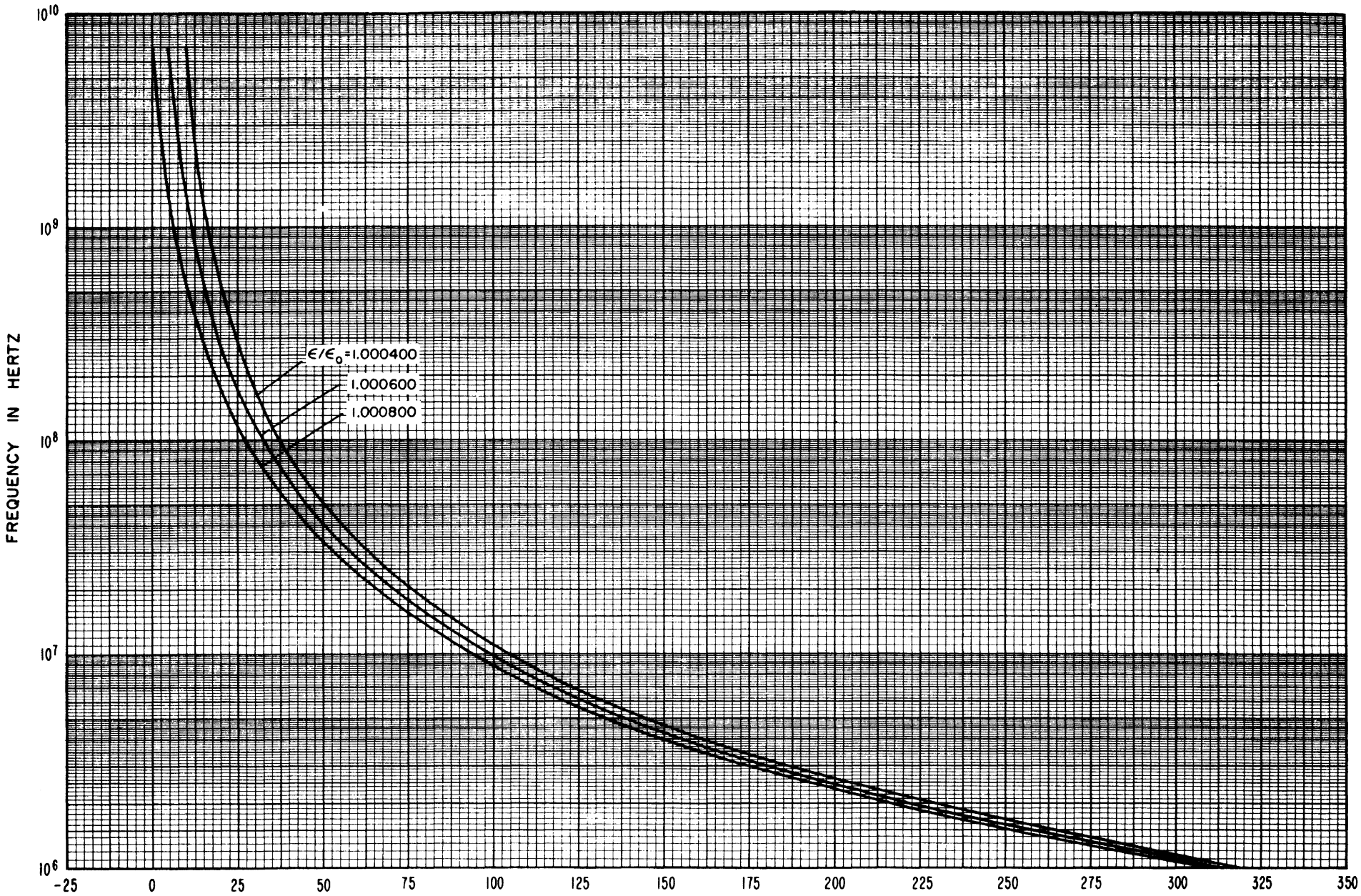

FIGURE 72. *Characteristic impedance magnitude (plotted as a deviation from 50.0 Ω) as a function of frequency for various values of* $\frac{\epsilon}{\epsilon_0}$ *for line size #4.*

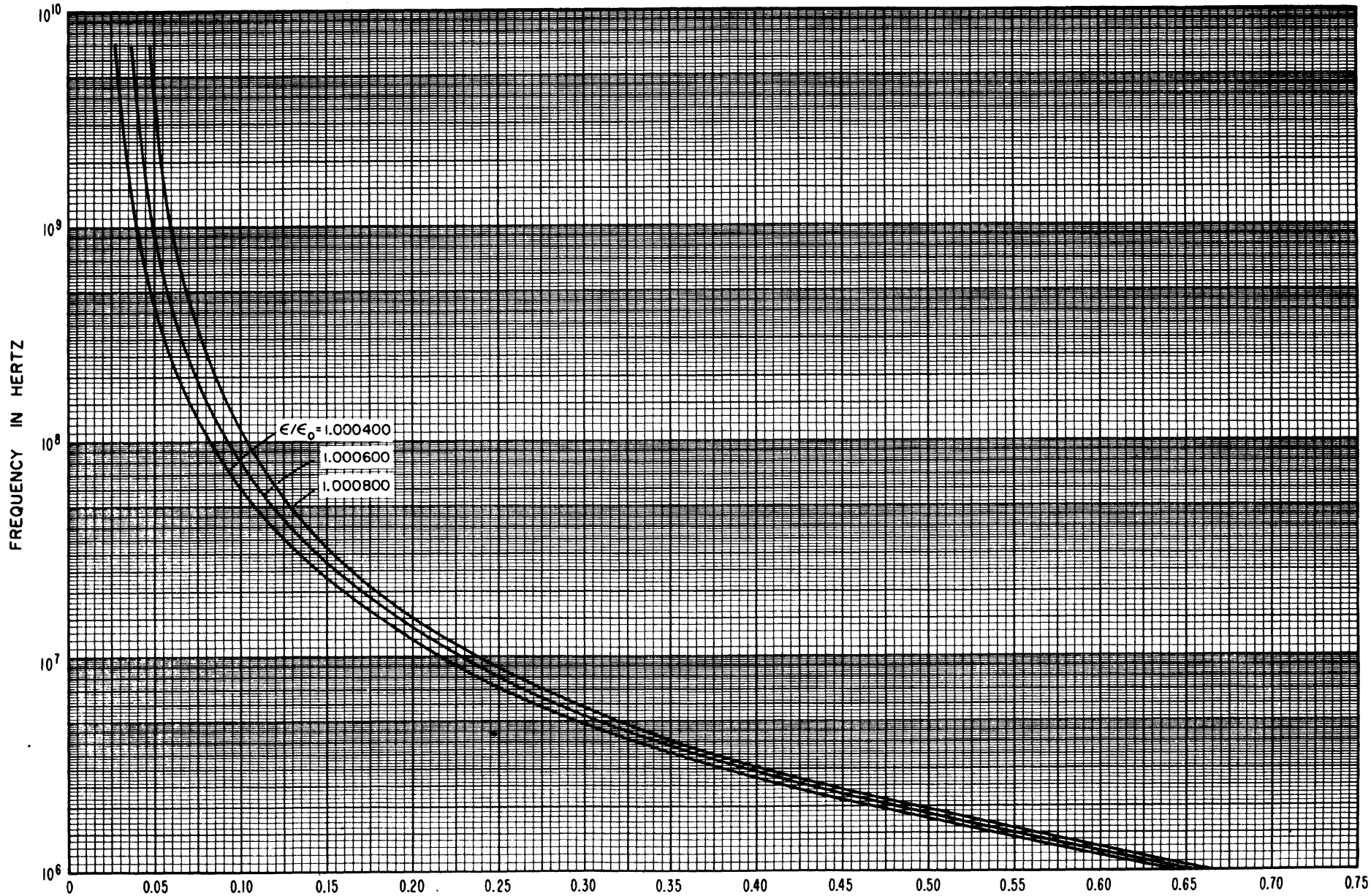

FIGURE 73. *Phase-shift per inch (plotted as a percent deviation from the free space value) as a function of frequency for various values of* $\frac{\epsilon}{\epsilon_0}$ *for line size #4.*

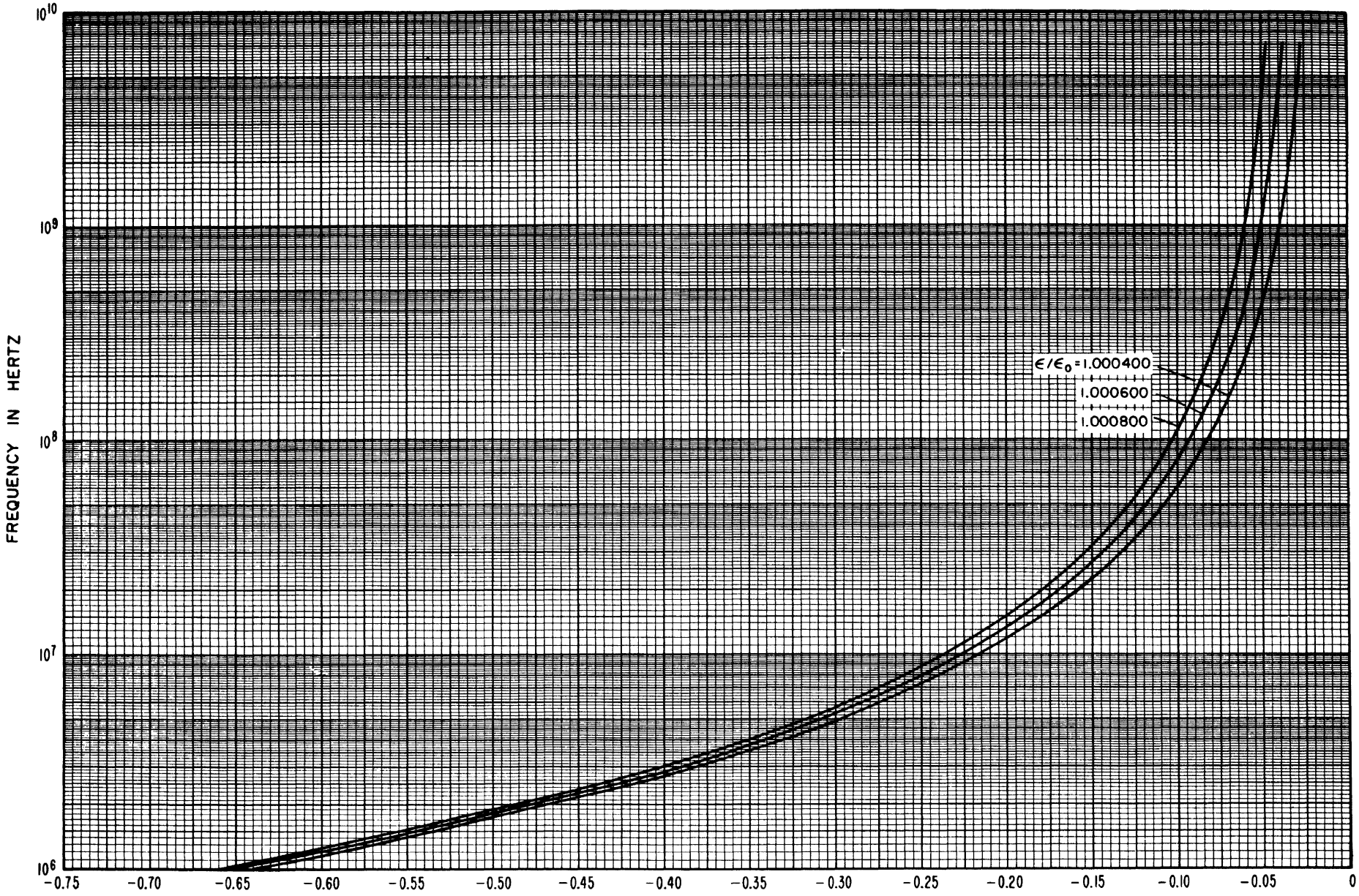

FIGURE 74. *Wavelength (plotted as a percent deviation from the free space value) as a function of frequency for various values of* $\frac{\epsilon}{\epsilon_0}$ *for line size #4.*

Line size #4
Variations with diameters a and b

Constants used in calculations are the same as those used under standard conditions except that a varies ± 0.0001 inch from standard conditions, and b varies ± 0.0002 inch from standard conditions.

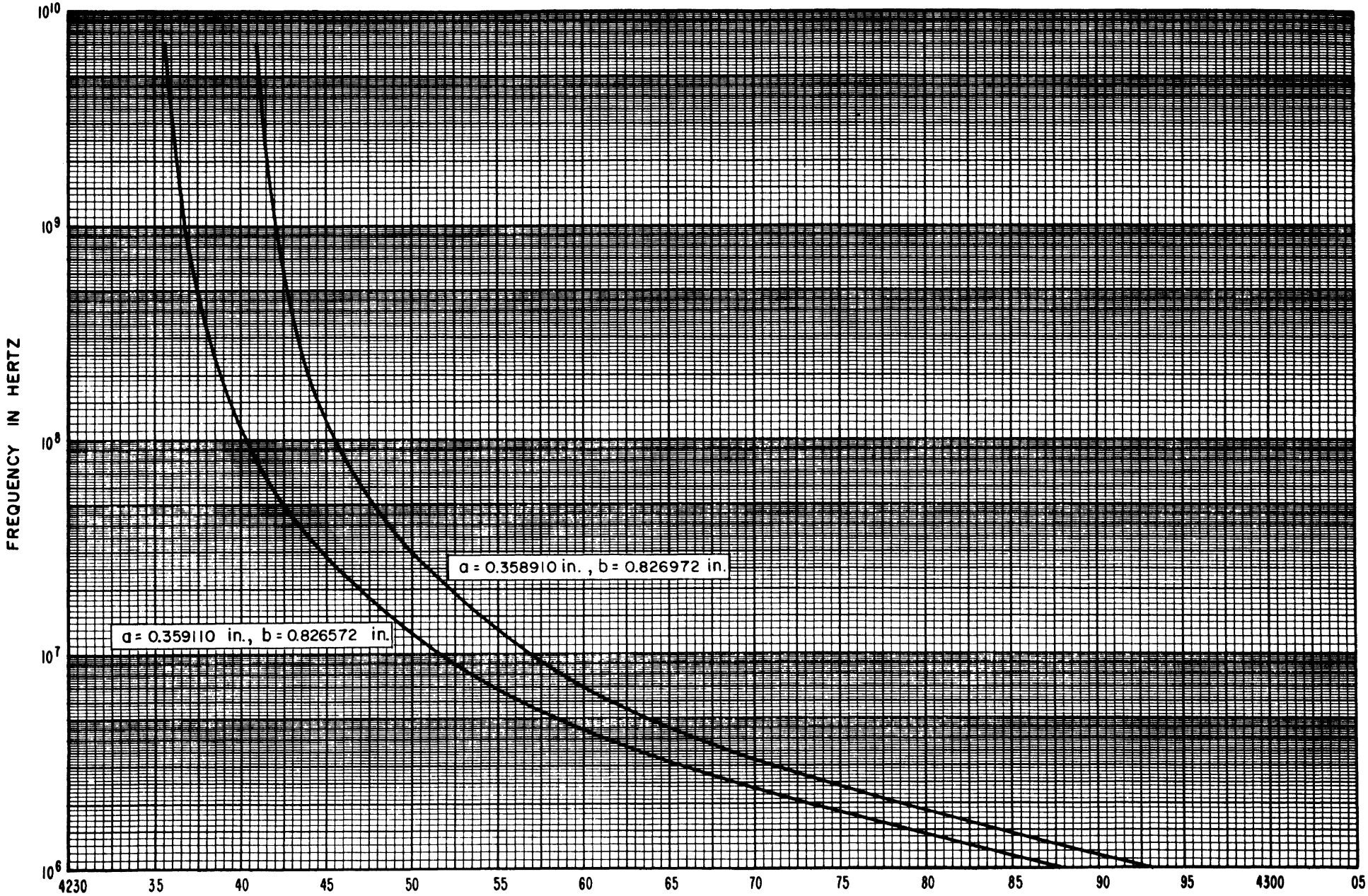

FIGURE 75. *Inductance per inch as a function of frequency for various values of diameters* a *and* b *for line size #4.*

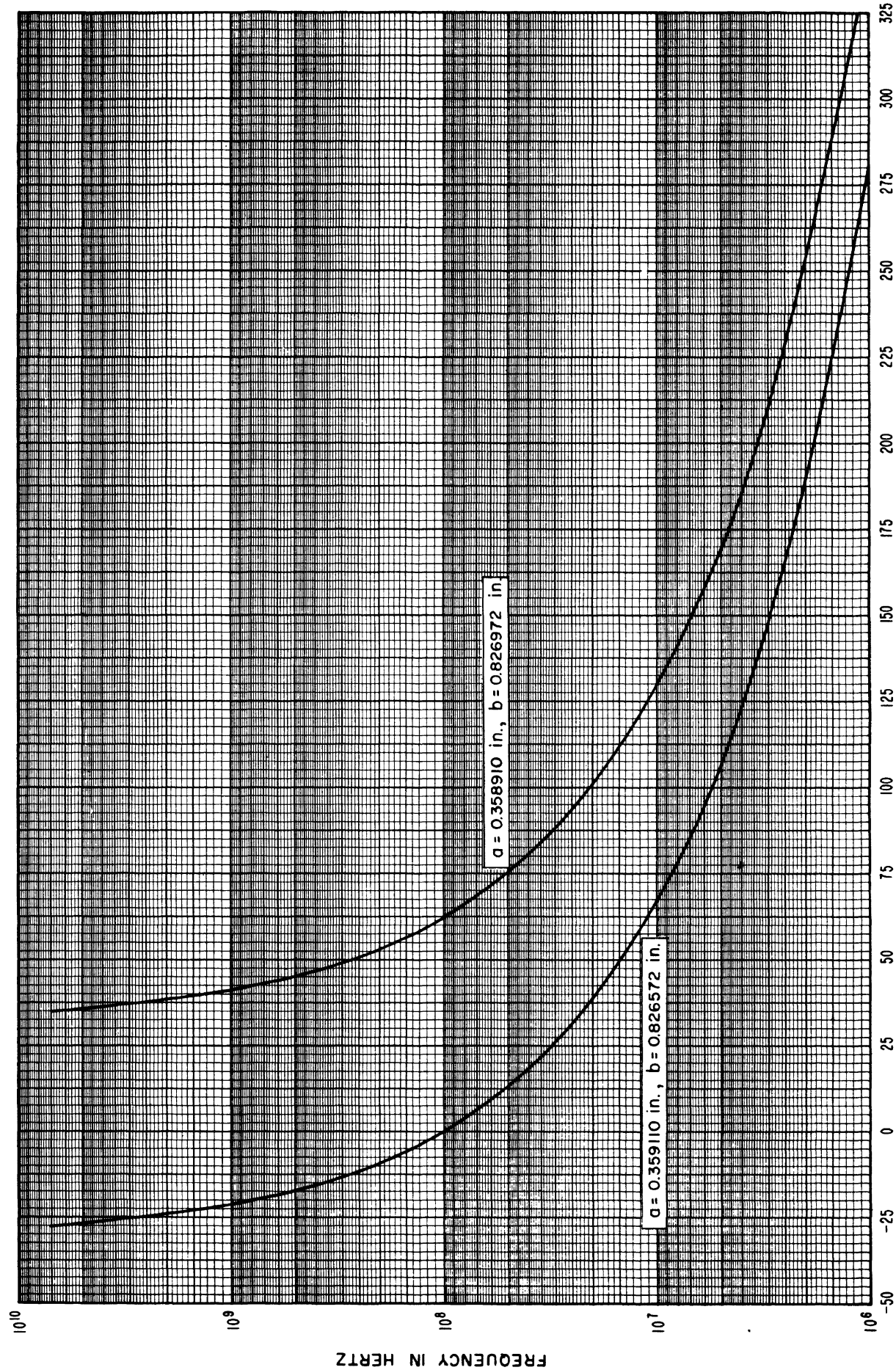

FIGURE 76. *Characteristic impedance magnitude (plotted as a deviation from 50.0 Ω) as a function of frequency for various values of diameters* a *and* b *for line size #4.*

U.S. GOVERNMENT PRINTING OFFICE : 1966 OL—218-445

July 25, 1966

Errata to accompany NBS Monograph 96

Electrical Parameters of Precision, Coaxial, Air-Dielectric Transmission Lines

Robert E. Nelson and Marlene R. Coryell

Page

iii Page number for "3. Computational methods...":

now reads : page 3

should read: page 2

3 Equation for $bei_\nu z$:

now reads : $bei_\nu z \sim \frac{e^{z/\sqrt{2}}}{\sqrt{2\pi z}} \left\{\chi_\nu \cos \ldots\right.$

should read: $bei_\nu z \sim \frac{e^{z/\sqrt{2}}}{\sqrt{2\pi z}} \left\{\chi_\nu(z) \cos \ldots\right.$

3 Equation for $\psi_\nu(z)$:

now reads : $\psi_\nu(z) = \frac{1}{2}\{\lambda_{\nu+1}(z) \ldots$

should read: $\psi_\nu(z) = \frac{1}{2}\{\lambda_{\nu+1}(z) \ldots$

4 Equation for ker_ν, z (two corrections):

now reads : $ker_\nu, z \sim -\sqrt{\left(\frac{\pi}{2z}\right) e^{-z/\sqrt{2}}} \left\{\psi_\nu^1(-z) \ldots\right.$

should read: $ker'_\nu\ z \sim -\sqrt{\left(\frac{\pi}{2z}\right) e^{-z/\sqrt{2}}} \left\{\psi_\nu(-z) \ldots\right.$

4 Equation for kei_ν, z:

now reads : $kei_\nu, z \sim \ldots$

should read: $kei'_\nu z \sim \ldots$

57 Omit entire text and replace with text on page 65.

65 Omit entire text and replace with text on page 57.

U.S. DEPARTMENT OF COMMERCE
WASHINGTON, D.C. 20230

OFFICIAL BUSINESS

POSTAGE AND FEES PAID
U.S. DEPARTMENT OF COMMERCE